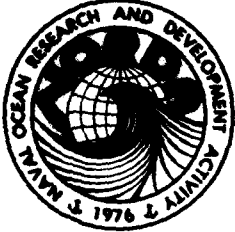MICROCOPY RESOLUTION TEST CHART
NATIONAL BUREAU OF STANDARDS-1963-A

UNCLASSIFIED

Naval Ocean Research
and Development Activity

NSTL Station, Mississippi 39529

Ocean Measurements Program

AD A137674

SUMMARY REPORT

OCEANOGRAPHIC MEASUREMENTS PROGRAM REVIEW

MARCH 1982

DTIC
ELECTE
FEB 8 1984

S   D

B

Ocean Programs Management Office

CONTENTS :

I. INTRODUCTION

The Ocean Measurements Program (OMP) is part of the Ocean Programs Management Office of NORDA and has been in operation since 1978. Sponsorship of the OMP is through the Chief of Naval Operations, Oceanographer of the Navy, OP-952D.

The purpose of the OMP is to provide quantitative descriptions of the upper ocean environment, ranging from vector and scalar mesoscale to microscale features. To achieve this purpose, the OMP is comprised of two complementary offices, Oceanographic Instrumentation Systems (OIS) and Oceanographic Techniques (OT), which work closely together. OIS is primarily concerned with the development of instrumentation to acquire the requisite ocean measurements, while OT is primarily concerned with design and verification of sampling and analysis techniques and with development of input to and verification of numerical models. The OMP emphasizes physical oceanographic upper ocean phenomena such as internal waves, vertical velocity shear, and upper ocean temperature, salinity, and density structure.

The annual OMP review was held on March 3 and 4, 1982, at the Naval Ocean Research and Development Activity (NORDA). The review, attended by 52 participants, served as a briefing for Naval program managers, Naval Oceanographic Office (NAVOCEANO) personnel who may use instrumentation and techniques developed under sponsorship of the OMP, and principal investigators and contractors funded by the OMP. The purpose of the annual review was to summarize past, present, and future work in a format that would facilitate communication among participants and provide an overview of the entire OMP and its applications.

This report is a summary of presentations by OMP principal investigators and contractors. Because it is intended for open distribution to review participants and to others who are involved with the OMP, it is unclassified. Any classified discussions at the review are not included in the report. Project summaries in this report were prepared by OMP personnel and contractors from material provided by the principal investigators and contractors. Several presentations were shortened or edited. The purpose of these summaries is to briefly present work sponsored by the OMP without extensive technical detail. The project summaries should not be considered scientific papers and should not be referenced without contacting the appropriate principal investigator or contractor. In most cases, published papers and/or reports are available to more completely describe the summarized work. This report is organized into two sections corresponding to the two parts of the OMP. Oceanographic Instrumentation Systems (OIS) projects are described in the first section, and Oceanographic Techniques (OT) projects are described in the second section.

II.   PROJECT SUMMARIES

        A.   OCEANOGRAPHIC INSTRUMENTATION SYSTEMS

ADVANCED MICROSTRUCTURE PROFILER

Michael Gregg
University of Washington
Applied Physics Laboratory
Seattle, Washington 98105

Abstract

A prototype Advanced Microstructure Profiler (AMP) was completed, operationally tested in local waters, and extensively used during a recent Johns Hopkins University Applied Physics Laboratory cruise. Overall instrument performance is suitable for good scientific measurements in the open ocean but several instrument modifications need to be made to optimize performance. These modifications involve utilization of an improved winch system, reduction of analog to digital conversion noise, reduction of mechanical vibration noise affecting shear measurements, and improvement of pressure seals to prevent flooding through sensor ports. These modifications are being made and additional at-sea experience with the AMP is being acquired during 1982. Future work planned for 1983 includes incorporation of a higher speed minicomputer system with the AMP, design improvements to make the AMP more suitable for operational use by NORDA and NAVOCEANO, and design improvements to reduce the cost and maintenance of electronic circuit boards for operational units. The capability of the AMP is considered proven and ongoing and future work is aimed toward development of an AMP design that is suitable for routine use.

BACKGROUND

During 1981 the initial sensor suite and data gathering system for the prototype Advanced Microstructure Profiler (AMP) was completed and the unit was operationally tested in local waters (Lake Washington and Puget Sound). This initial system used an HP 9845 desk-top computer system for data recording and for limited data processing to provide "quick-look" plots of raw sensor outputs following each operation.

The sensor suite as tested included: two accelerometers (one horizontal, one vertical); two thermistors (one for temperature gradient and one for temperature); a thin film temperature probe; two shear foil horizontal velocity gradient probes; and a pressure gauge. Also tested but not yet a permanent member of the sensor suite was a hydro-resistance anemometer for measuring velocity fluctuations along the longitudinal axis of the AMP. Incoming data is recorded on floppy disks using an HP 9845 computer. The sensors and sample rates are given in Table 1.

A second AMP unit, designated AMP II, was constructed to serve as a back-up to the possible loss of AMP I during a recent Johns Hopkins University Applied Physics Laboratory cruise. On this cruise, AMP I served as a major instrument platform for obtaining oceanographic background measurements and approximately 600 disks of oceanographic data were obtained.

Figures 1, 2, and 3 show examples of data. Most drops show a wobble in vertical acceleration ZA and horizontal acceleration XA at the beginning of the drop, which becomes increasingly damped with increasing depth. The wobble does not seem to affect the noise levels of high frequency data channels. The plots are decimated to compress the data from a drop onto a single page. This results in some misleading aspects to particular channels, e.g., often the low-pass channels appear much more "steppy" than they appear in

either analog or in detailed digital plots. Another difficulty is that the high sample rates of the velocity channels result in an undue emphasis on the high-frequency noise. Consequently, the unprocessed velocity data do not appear as intermittent in intensity as is actually the case.

The fiber-optic cable withstood some rather severe abuse without incurring a total cable separation, although on several occasions the inner fiber-optic fractured, causing loss of data transmission. In each instance, however, the fracture was found at a location where a sharp kink had been put in the cable through handling. These kinks generally occurred during cable payout from the winch when a turn was entrapped by other windings on the drum. A modification to the winch-lift-pole design will incorporate a traction pulley at the end of the pole to pull the cable off the drum under a slight tension. This modification should greatly reduce the kinking and fiber-optic fracturing problems previously encountered.

The overall performance of the instrument is now considered suitable for conducting good scientific measurements in the ocean. Efforts will continue, however, to further optimize the performance by reducing the A to D conversion noise levels, which are presently above the theoretically predicted values, by reducing mechanical vibration noise being picked up in the shear channels from the sensor protective struts, and by improving the pressure seal arrangement on the sensor probes to prevent flooding of the nose section through the sensor ports.

ONGOING WORK

Operational experience with AMP will be obtained during 1982 using the modified winch system with traction payout and a higher speed shipboard computer (PDP 11/34 or VAX) for data acquistion. Special bench tests will be conducted to locate the source of noise in the A to D converter and, based on the results of these tests, appropriate modifications will be made to reduce the A to D noise level. The sensor protective struts will be stiffened to move their resonance frequency above the frequency range of interest in the sensors. Back-up seals will be added in a new nose pressure bulkhead design for the sensor probes.

The winch unit will be modified in 1982 to incorporate line payout from a traction pulley at the end of the winch pole. If possible, a mechanical line-out indicator readable by the winch operator will be added as part of this modification. The deck-box is being modified to add a GPIB (IEEE 488) interface to enable the output from the AMP to be recorded on disk by a PDP 11/34, which will permit an increased data rate and uninterrupted recording during the longest anticipated AMP drops.

A field cruise using a Navy AGOR, the USNS DE STEIGUER, is scheduled to take place in October 1982 in the Pacific Ocean a few hundred miles off San Diego. A technical objective of this cruise is to develop techniques for working with the AMP from an AGOR-type ship. Scientific objectives are to study the relationship of vertical fine- and microstructure as measured by the AMP to internal wave fields determined from expendable current profiler (XCP) deployments, and to study the horizontal coherence of fine- and microstructure using AMP tow-yo's.

FUTURE WORK

Major tasks proposed for 1983 are to purchase a dedicated minicomputer and to develop the required software to use this computer with the AMP system, to put the AMP winch under computer control and add vehicle depth and line-out displays for the winch

6

operator, and to make design modifications to the AMP which will make production units more reliable and easier to operate.

Further vehicle development will be focused on making an instrument suitable for NORDA/NAVOCEANO to operate. This will involve mechanical design changes to facilitate opening and closing AMP pressure hull sections. In addition, the battery pack will be moved from its present location inside the main pressure hull to a separate pressure container external to the hull so that it can be replaced without opening the main pressure vessel. The electrical connector arrangement between sections of the AMP should be modified to eliminate the problem of cable pinching and wire breakage at the connectors, which sometimes occur when closing the AMP.

The possibility of replacing the wire-wrap circuit boards now used with printed circuits will be investigated. It is not clear that the same packing density can be obtained with printed circuits and consideration will have to be given to increasing the length of the AMP to permit full replacement. If printed circuits can be used, the production cost of future units will be reduced due to the minimal time required to debug PC boards compared to wire-wrap boards.

221-1

AMP - SENSORS AND SAMPLE RATES

CHANNEL	SENSOR	SAMPLES PER SECOND
TC	DISA COLD FILM	1181*
TH	FAST TIP THERMISTOR	394
TL	FAST TIP THERMISTOR	394
CN	N. BROWN CONDUCTIVITY	394
VX	X LIFT VELOCITY	788
VY	Y LIFT VELOCITY	788
VW	? W VELOCITY	1181*
PR	SETRA CAPACITANCE PRESSURE	394
XA	SETRA CAPACITANCE ACCELEROMETER ALIGNED HORIZONTALLY	394
ZA	MILDOON PEIZO-ELECTRIC ACCELEROMETER ALIGNED VERTICALLY	394
ENGINEERING	POWER, ETC., 10 CHANNELS @	39.4
	TOTAL WORDS/SEC	5515**

*BECAUSE OF PRESENT RECORDING RATE LIMITATIONS WITH HP-9845 ONLY ONE HIGH RATE CHANNEL (TC OR VW) CAN BE ENABLED AT ANY ONE TIME.

**SAMPLES PER SECOND CAN BE INCREASED TO 8777 WORDS/SECOND WITH PDP 11/34 OR PDP 11/44 SYSTEMS.

TABLE 1. LIST OF AMP SENSORS AND SAMPLE RATES.

PLOT RANGES
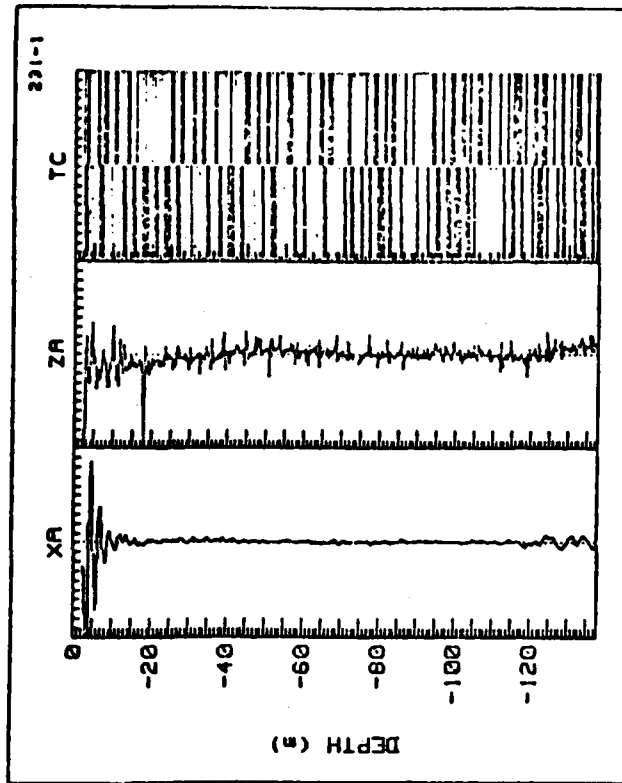
CHANNEL	MINIMUM	MAXIMUM	MEAN
XA	-3.40E+00	3.40E+00	3.71E-01
ZA	-2.30E+00	2.30E+00	-1.18E+00
TC	-3.20E+00	3.20E+00	-1.17E-01
DEPTH	0.0	137.98	

PLOT FROM FILES   0231   0232

DRO DATE/TIME   03 JAN 1982 2035(CHT)
PLOT DATE/TIME 03 JAN 1982 2053(CHT)

FIGURE 1. "QUICK LOOK" PLOTS OF HORIZONTAL ACCELERATION XA, VERTICAL ACCELERATION ZA, AND COLD FILM TEMPERATURE TC (COLD FILM TEMPERATURE NOT CONNECTED ON THIS DROP). UNITS ARE VOLTS REFERENCED TO MEAN VOLTAGE.

8

FIGURE 3. "QUICK LOOK" PLOTS OF CONDUCTIVITY CN, LOW-PASS TEMPERATURE TL, AND DROP SPEED DS. UNITS ARE VOLTS REFERENCED TO MEAN VOLTAGE.

FIGURE 2. "QUICK LOOK" PLOTS OF TEMPERATURE GRADIENT TH AND VELOCITY GRADIENTS VX AND VY (SENSITIVE AXIS IN X AND Y DIRECTIONS RESPECTIVELY). UNITS ARE VOLTS REFERENCED TO MEAN VOLTAGE.

9

HORIZONTAL CURRENT PROFILER

Thomas B. Sanford
Applied Physics Laboratory
University of Washington
Seattle, Washington 98105

Abstract

Instrumentation work for the OMP has shifted from the successfully developed expendable temperature and velocity profiler to development of horizontal current profilers that can measure horizontal variability of currents when towed from a ship. The objective is to measure spatial scales on the order of 1 m with a velocity resolution on the order of 1 cm/s. Because towed bodies equipped with current meters and acoustic Doppler techniques are unlikely to meet this objective, instrumentation that measures natural electric currents generated by water motion is being developed. This instrumentation will represent an improvement over the standard types of GEK systems that have been available for a number of years. Instrumentation under development will measure both velocity fluctuations and vorticity associated with water motion.

BACKGROUND

The feasibility of producing a towed current meter or shear meter suitable for rapid deployment and rapid towing is being evaluated. Figure 1 illustrates such a towed system. The goals are to minimize or eliminate interference from the motion of the towed platform, thereby reducing to some degree the sophistication and constraints of such a towed body, and to achieve as high a velocity sensitivity as possible, at the same time maintaining 1 meter vertical and horizontal resolution.

Abundant vertical profiler data are available showing extensive variability in the vertical direction, but much less information is available in the horizontal direction. One, perhaps the only, currently available system that gives relatively small horizontal resolution uses motionally induced signals. Figure 2 shows observations along a 4000 km tow using a GEK that is a prototype of the instrumentation being developed in this program. One remarkable aspect of these data is that the horizontal shear spectrum, the gradient of horizontal velocity in the horizontal direction, has most of its variance at the smallest horizontal scales, rather than in the large mesoscale eddies that are so noticeable in the velocity field.

TECHNIQUES

Various techniques could be used for measuring small scale horizontal variability. One possibility is to tow a current meter on a body and attempt to measure the motion of the body and the ocean currents relative to the body. This approach has been used to provide qualitative information, but lacks the ability to measure accurately flows with velocity scales less than 1 cm/sec. Clearly, vehicle motion dominates in this measurement. For example, an uncertainty of a few tens of meters in the position or drift of the towed body over tens of minutes represents several cm/s bias. Another measurement approach would be to utilize acoustic Doppler techniques, for example, from a ship. However, if velocity variations in the range of a few meters and at resolutions of less than 1 cm/s are to be measured, it is unlikely that acoustic Doppler systems would be capable of such performance, at least in the foreseeable future.

FUTURE WORK

Natural electric currents generated by water motion will be used for small scale horizontal flow measurements. Since electric currents exist in the absence of measurement platforms and have perfectly linear and instantaneous responses, it is possible to obtain observations of the flow and its variations independent of small platform excursions or velocity fluctuations. Two complementary approaches are being considered. One, a current transformer, is capable of measuring the velocity fluctuations at 1 meter resolutions, while the other, a vorticity meter, automatically and instantaneously senses the vorticity or swirl of the velocity field. These two observations complement each other and will be considered as one system. Design and testing of different fluid switches or salt bridge valves which will be needed in the construction of the vorticity meter are under way. The valves, which change the conductances of the electrical circuit, are used to open and close the passage between the electrodes and between one electrode and the sea. Design of a switch that operates reliably and nearly instantaneously requires evaluation of several unique switch approaches which are shown in Figure 3. The expectation is that a version of the vorticity meter suitable for evaluation will be produced for in-water tests this summer.

POWER SUPPLIES
VALVE CONTROLLER
&
RECORDER

DECK EQUIPMENT

SPOOL

8 CONDUCTOR PLAIT-
ED POLYPROPYLENE
ROPE

0-250M

VALVES

Ag-AgCl
ELECTRODES

ELECTRONICS
PRESS TRANSDUCER
& BATTERIES

OIL FILLED

TOWED UNIT

.5M

SEAWATER FILLED TUBE

~10-30M
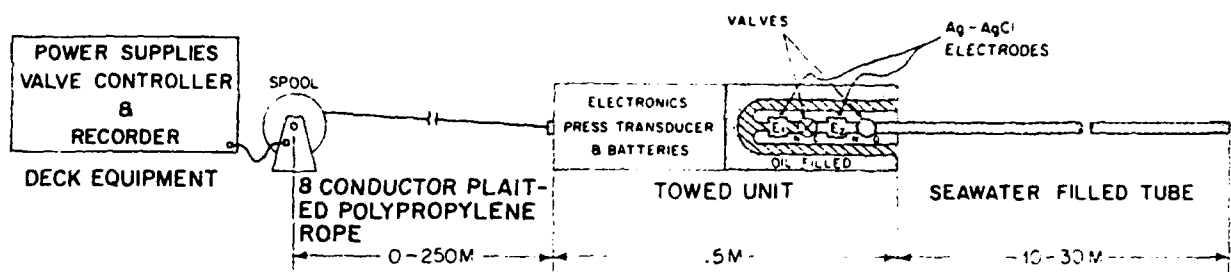
FIGURE 1. SCHEMATIC OF TOWED METER SYSTEM.
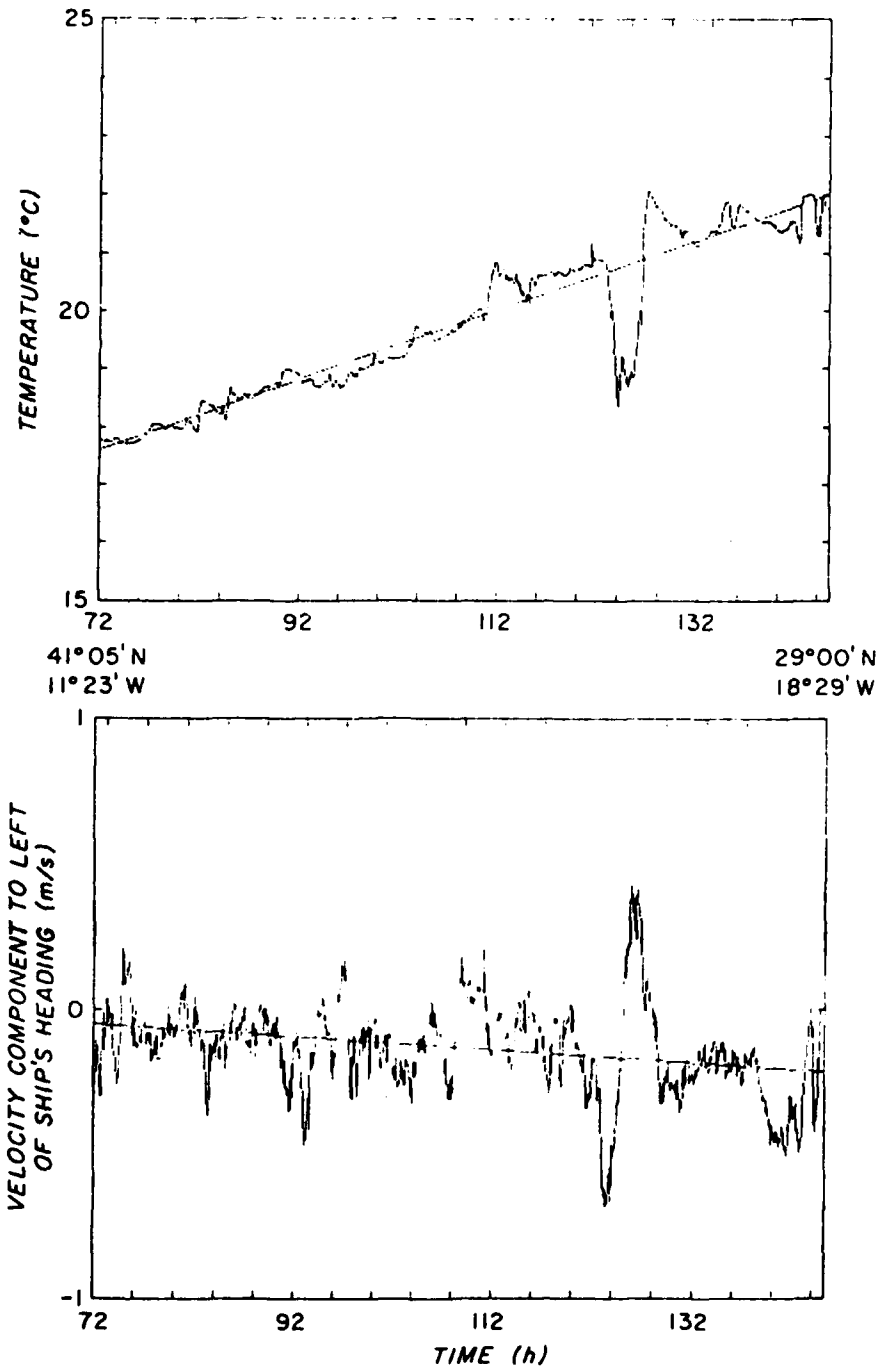
FIGURE 2. GEK SPEEDS AND SURFACE TEMPERATURE BETWEEN CAPE FINISTERRE, SPAIN, AND THE CANARY ISLANDS. THE DASHED LINES REPRESENT THE LEAST-SQUARES FIT OF THE DATA TO A SPATIAL MEAN AND TREND.

14

SWITCH APPROACHES

PINCHED TUBE   HYDRAULIC

FLEXIBLE
TUBE

IMMISCIBLE
NON-CONDUCTING
PUMP   FLUID

PLUNGER   ROTARY   ROTARY
                 CYLINDER   DISK

SOLID
SURFACE

PLAN VIEW   END VIEW

FIGURE 3. DIFFERENT SWITCH APPROACHES UNDER EVALUATION FOR VORTICITY METER.

ACOUSTIC SHEAR PROFILING

Robert H. Hill
Oceans Dynamics Branch
Environmental Sciences Division
Naval Research Laboratory
Washington, D.C.   20375

Abstract

Two types of acoustic systems, Doppler sonars and correlation sonars, are being investigated to measure vertical shear in the upper ocean from moving surface vessels. Additional field work with an Ametek/Straza Janus configured advanced Doppler sonar and a General Electric correlation sonar is planned. One potential advantage of the correlation sonar over the Doppler sonar is separation of trade-offs between spatial and velocity resolutions.

APPROACH

Work is underway to provide a technique for rapidly sampling vertical shear in upper ocean layers. This project is directed to the study of two types of high frequency backscattering sonars employed on surface vessels.

The first type uses Doppler shift information obtained with an array of narrow acoustic beams. Figure 1 is a schematic of the Doppler shear profiler. Field experience has been gained with an interim profiler of this type which, although lacking sufficient hardware fle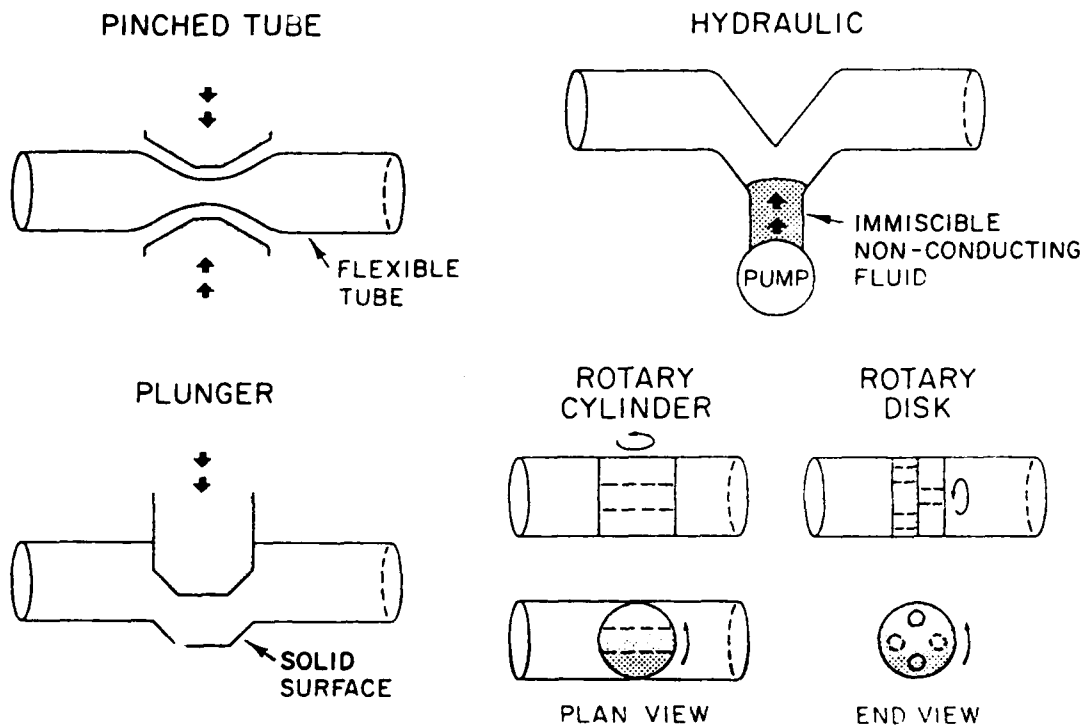xibility, has demonstrated the efficacy of this type of measurement. Major technical issues include attaining adequate measurement depth range and improving signal processing techniques to overcome the inherent trade-offs between spatial resolution and velocity estimation precision.

An advanced Doppler profiler, manufactured by Ametek/Straza, which will provide the desired operating flexibility and should offer the potential for improved signal processing, is being procured. Present plans are to prepare this system and execute a field evaluation experiment during an NRL cruise aboard the USNS HAYES in July 1982.

The second type of sonar being studied uses cross-correlations, across a spatial array, of backscattered signals resulting from a pair of identical transmitted pulses. This system is illustrated in Figure 2. Potential advantages of this technique, relative to the Doppler approach, include better geometry for vertical profiling and separation of the tight trade-off between spatial resolution and precision of velocity estimates. Major technical issues include uncertainty about pulse decorrelation times in the ocean and possible interference effects due to the simultaneous use of two pulses in the water column.

This study includes an at-sea evaluation of the Janus configured Doppler sonar and the correlation sonar to investigate common problem areas such as platform motions and the nature of scatterers. A prototype correlation sonar processing system has been offered by the General Electric Company. An experiment to clarify major technical issues was designed, a special acoustic array was prepared, other supporting systems were interfaced, and a field experiment was attempted in July 1981. Malfunctions in contractors' electronics hardware and, possibly, signal processing techniques precluded acquisition of reliable data with which to evaluate the correlation concept. New means

17

for completing this experiment will be determined to provide a relative assessment of the different approaches to meeting shear profiling requirements.

FUTURE WORK

During FY 82 plans for the advanced Doppler shear profiler include incorporating a 120 KHz capability into the system and preparing the system for experimental use. This will entail both mechanical installation and installation of the system control/data processing software. Experimental evaluation is planned for July 1982 and will include an investigation of the most feasible approach to platform motion problems as well as determining whether signal processing can provide the required resolution. Correlation sonar technical issues related to shear profiling will be resolved and the relative performance of Doppler and correlation techniques will be assessed.
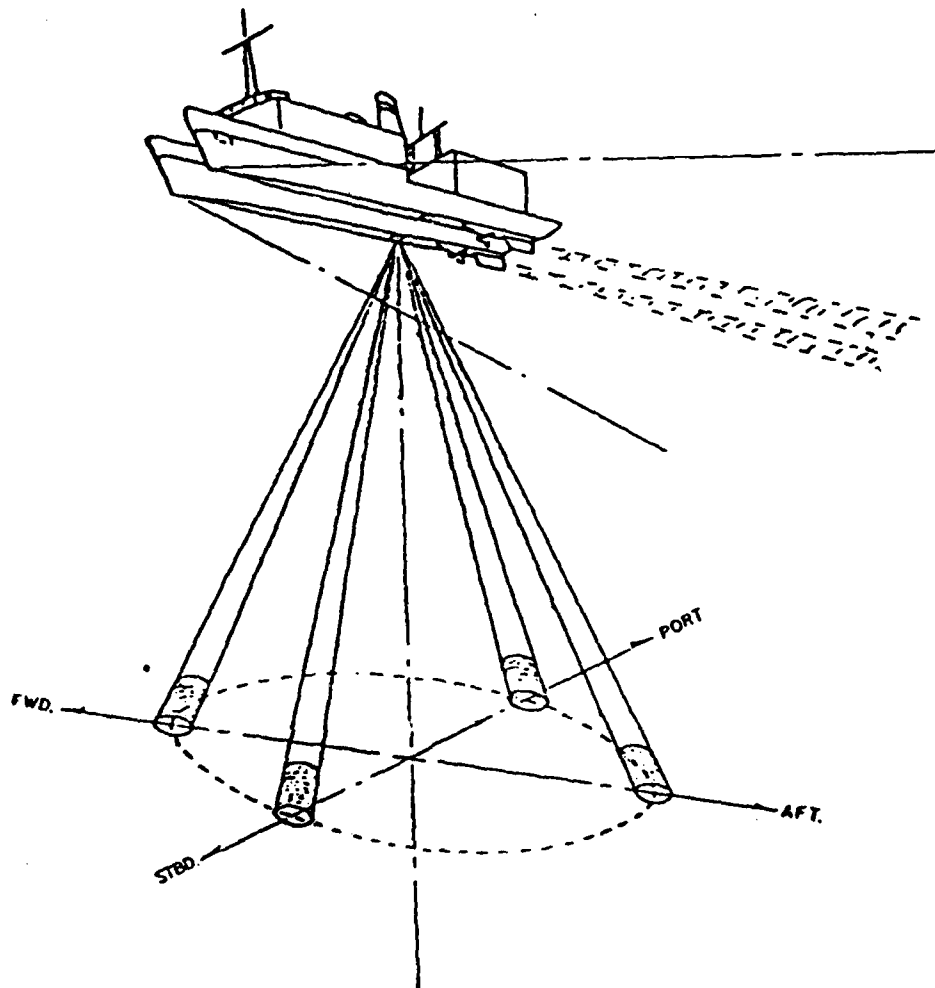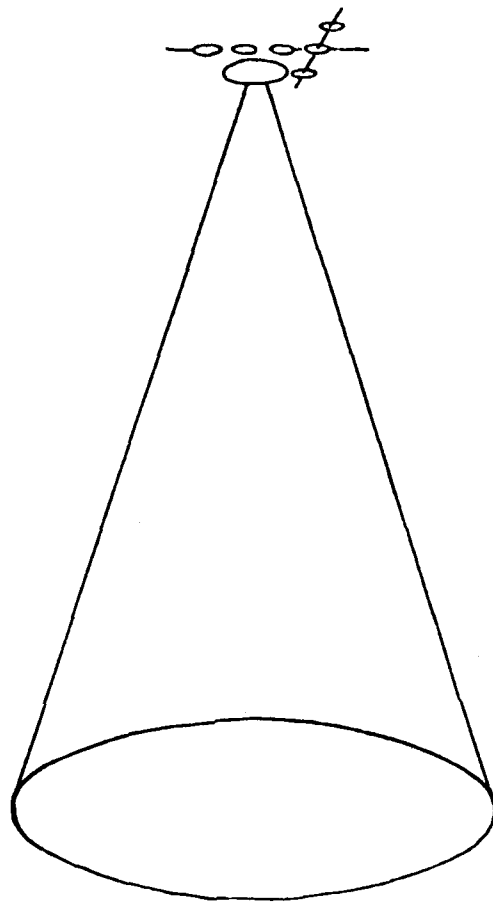
FIGURE 1. SCHEMATIC DIAGRAM OF DOPPLER SHEAR PROFILER BEAM ARRAY ABOARD USNS HAYES.

CORRELATION SONAR

FIGURE 2. SCHEMATIC DIAGRAM OF A POSSIBLE CORRELATION SONAR SHEAR PROFILER WITH RECEIVERS IN A "T" ARRAY.

FALL SPEEDS OF EXPENDABLES

Albert W. Green
Physical Oceanography Branch
Naval Ocean Research and Development Activity
NSTL Station, Mississippi 39529

Abstract

Mathematical equations were developed to describe fall rates of expendable probes as a function of probe physical characteristics, probe launch initial conditions, and oceanic properties, primarily viscosity. Solutions to these equations allowed determination of fall rate error sources and resulted in recommendations for procedures that can improve accuracies of measurements by expendable probes. The solutions may also provide a means to improve future designs of expendable probes.

BACKGROUND

Shipboard and airborne expendable ocean profilers are being increasingly used because of their improved performance and reliability. Expendables commonly used for ocean survey work do not include pressure sensors for direct depth estimates but rather depend on empirical relationships for these estimates. A study was undertaken to find methods of improving fall rates and depth-time relationships of expendables by identifying quantitative ambient and probe parameters that determine probe fall speeds. Control of critical parameters could lead to refinement of time-depth relationships and improved accuracies in vertical profile measurements so that these probes could provide precise and accurate measurements of fine scale variability and internal waves. Results are particularly applicable to expendable bathythermographs and current profilers (XBTs and XCPs).

A model was developed to estimate the bulk force balance on a vertically falling body with changes in mass and drag coefficient that were proportional to depth. Loss of wire results in changes in mass as well as changes in buoyancy forces acting on the probe, while the drag coefficient varies with depth as a result of increasing water viscosity caused by the decrease in temperature with depth. Integration of the force balance equation with simple linear assumptions of drag coefficient and mass variation with depth yields a depth-time relationship that incorporates the critical probe parameters as coefficients in the fall rate equation. The results given in Figure 1 show that the nominal terminal velocity of the probe is dependent upon its drag coefficient, mass, cross-sectional area, and ambient water density.

ERROR SOURCES

Dynamic depth error sources result from uncertainties in initial post-impact speed variations just after probe entry into the water, lack of sufficient control of drag coefficient variations due to probe body imperfections, and mass variations due to production variations. Other dynamic error sources include variations in the boundary layer and in the weight of the probe. These variations may result from geometric imperfections in the probe body or gyroscopic effects induced by probe rotation. Ambient effects on dynamic depth error include vertical velocities associated with internal gravity waves, vertical shear in the currents, and uncompensated changes in kinematic viscosity with depth. Magnitudes of selected dynamic error sources are listed in Table 1.

Some experimental errors could be eliminated by systematic experiment controls. Selection and calibration of thermistors for temperature estimates is of first importance in controlling experimental errors. Most thermistors currently in use are accurate to about $\pm 0.1^\circ C$, which could be a critical error for some applications. Multi-point calibration of thermistors with accompanying calibration curves for each unit, or lot, would provide a good quantitative basis for intercomparisons between CTD profiles and expendables. The exact starting time of the probe fall is also a significant error source for XCPs, particularly since there is presently no clear fall initiation signal. This is expected to be remedied in later production models. Another error source which can be controlled to some extent in normal deployment procedures is the height of the probe above the surface. Entry speed variations caused by varying fall time between launcher and the sea surface can contribute on the order of ± 2 m in depth error. The horizontal and temporal variations in temperature profiles make it difficult to make intercomparisons between standard shipboard profiling systems (CTDs) and the expendables to 1 m or less.

CONCLUSIONS

Refinements of manufacturing controls and experimental methods could reduce the cumulative normal error for depth versus time for a given probe to the level of $\pm 1\%$, which is approximately a factor of two better than the manufacturer's current specifications. Refinements beyond this point are possible, but perhaps impractical. Improvement in the error statistics could be accomplished by the following procedures:

1) Measure the mass and air and sea water displacement for each probe.
2) Calibrate probe thermistors at three temperatures to ± 10 millidegrees.
3) Employ a high speed analog digital conversion system with accurate clock and 13- to 14-bit resolution of probe voltage.
4) Maintain near-constant entry altitude and speed.
5) Make near-coincident space-time profiles with calibrated CTDs at regular intervals.
6) Assure that probe body geometry and surface features are consistent from probe to probe.

An experiment to evaluate the effects of these dynamic and experimental effects would provide an accurate assessment of measurement errors caused by variations in probe fall rate and an estimate of cost benefits of the refinements.

Bulk Force Balance
(dimensional form)

$$\frac{dw}{dt} = \frac{1}{2} \frac{\rho_w(z)c_D(z)}{M(z)} A\,W^2 - g\left(1 - \frac{M_w(z)}{M(z)}\right)$$

"(z)" indicates variation with depth

In the simplified analytical model it is assumed that:

$$\Delta\rho_w(z) = 0 \ , \ \Delta M_w(z) = 0$$

$$c_D = c_D(1-\delta z) \ , \ \delta <<< 1 \ , \ z \leq 0$$

$$M(z) = M_o(1+\alpha z) \ , \ \alpha << 1 \ , \ z \leq 0$$

$$(1-\delta z)(1+\alpha z)^{-1} \approx [1+(\delta+\alpha)z]^{-1} = (1+\eta z)^{-1}$$

FIGURE 1. BULK FORCE BALANCE ON A VERTICALLY FALLING BODY WITH DEPTH-DEPENDENT CHANGES IN MASS AND DRAG COEFFICIENT.

ERROR SOURCES	EXTREME	NORM	REFINED
DRAG COEFFICIENT	±3%	±1%	±0.5%
BUOYANCY	±2%	±.5%	±0.2%
INTERNAL WAVES	±0.8%	±0.2%	±0.2%
INITIAL POST-IMPACT SPEED	±0.3% -0.1%	±0.2% -0.1%	±0.1%
CUMULATIVE ERROR	+6.1% -5.8%	+1.9% -1.8%	±1%

TABLE 1. DYNAMIC ERROR SOURCES FOR TYPICAL APPLICATIONS.

THE DEVELOPMENT OF AN AIR-LAUNCHED
EXPENDABLE SOUND VELOCIMETER (AXSV)

Richard Bixby
Sippican Ocean Systems, Inc.
P.O. Box 139
Marion, Massachusetts 02738

Abstract

An Air Launched Expendable Sound Velocimeter (AXSV) which utilizes some hardware components from Air Launched Expendable Bathythermographs (AXBTs) and surface ship launched Expendable Sound Velocimeters (XSVs) is being developed. Laboratory tests, drop rate tests in tanks, over-the-side launches, and a limited number of air launches have proved the feasibility of the general design. Additional tests are needed to make minor improvements and to improve reliability. Once overall system performance is proven, limited production runs can begin.

BACKGROUND

During the past year Sippican has generated and tested a design for an Air Launched Expendable Sound Velocimeter (AXSV) which utilizes hardware from both the Air Launched Expendable Bathythermograph (AXBT) and the surface ship launched Expendable Sound Velocimeter (XSV). The intent of this program was to use standard production hardware where possible to reduce development time and cost. In addition, if the high volume production hardware for the AXBT could be available for the AXSV production, the cost of the AXSV could be reduced significantly. Figure 1 shows the AXSV design which was developed during this program.

Four major tests were conducted to develop the AXSV hardware and to demonstrate system feasibility. Tests included a probe drop rate test at the Underwater Weapons tank at the Naval Surface Weapons Center (NSWC), an over-the-side deployment test in local waters to check the probe and surface electronics system performance, and two air launch tests at the Sonobuoy Quality Assurance Facility in St. Croix to check the complete buoy performance.

BUOY OPERATION

The AXSV measures 36 inches long by 4.75 inches in diameter and weighs 13 pounds prior to air launch. Figure 2 shows an exploded view of the unit. The AXSV can be launched from a number of Navy ASW aircraft over a wide range of launch altitudes and speeds. Standard sonobuoy receivers such as the AN/ARR-52 and -72 are used to receive and demodulate the AXSV RF signal and the output frequency can then be displayed on an AQA-7 processor or into a MK-9 Digital XBT/XSV system.

Operation of the AXSV begins when the buoy is launched from the aircraft. The buoy housing floods after water impact and the seawater battery is activated. A fixed time delay of 33 seconds later, the probe falls free from the surface assembly. At this time, the audio output of the signal conditioner is switched to the transmitter and the depth vs sound velocity trace begins. The speed of sound in the water is proportional to the probe output frequency according to the following expression:

$$V = \frac{(.052)(3.281)}{(1/128f) - 2.35 \times 10^{-7}} \qquad (1)$$

where V is the speed of sound in meters/sec and f is the output frequency of the probe. The depth of the probe is determined by the time from release according to the following expression:

$$D = 1.500 + 6.10758t - .000260t^2 \qquad (2)$$

where D is the depth of the probe in feet and t is the time from release in seconds. At the end of the probe drop the transmitter shuts down and the surface unit scuttles.

TEST PROGRAM

The baseline design shown in Figure 1 is the result of a design and development program which began in December 1980. Included in this development was an extensive test program of both the AXSV and AXBT hardware to refine the designs generated, to collect performance data, and to develop confidence in the system's overall performance.

The first test in this sequence was the probe drop rate test conducted at NSWC. In this test both the new AXBT and AXSV probes were tested. During the next several months there were a series of air drop tests to develop the air launch/buoy separation system for both the AXBT and AXSV. In September three complete AXSVs were deployed over-the-side at Newport, RI, in about 1200 feet of water, to verify the results of the electrical systems testing conducted in the Sippican engineering lab. This was a complete electrical systems test and all three systems worked without any problems.

A final air launch test was planned for early November 1981 at the Sonobuoy Quality Assurance Facility in St. Croix. Problems in the assembly of these units associated with the weight of the probe nose breaking the probe release wire reduced the number of units at this test to five. Five additional units were to be tested at a later date. Overall, this test showed that this design concept, while needing additonal testing, was feasible. Another test was scheduled for December and then postponed until February 1982.

Five AXSVs were manufactured for the final air drop. The nose weight had been reduced and some of the production tooling was available to aid in assembly. This test was also conducted at the Sonobuoy Quality Assurance Facility and the units were launched from a P-3 aircraft traveling at 250 knots at 300 feet altitude. This test again showed the general design feasibility, although product reliability still needs improvement prior to a production run.

FUTURE WORK

The primary objective of this program was to develop an air launchable expendable sound velocimeter compatible with standard sonobuoy launch platforms and receivers. Befor this product goes into production it is recommended that additional

testing be conducted. First, in order to verify the probe drop rate which has been developed by extending the AXBT and XSV data, it is recommended that an additional drop rate test be conducted either at the NWSC underwater weapons tank or at sea for over-the-side comparison drops at sea with a known standard. Second, in order to improve the system's reliability, it is recommended that two additional air drop tests be conducted. In the first one the probe would not be allowed to deploy. After water impact the unit would be recovered for a simulated deployment at Sippican. In this way any defective probe could be analyzed for the cause of the defect and the design modified as required. Sippican will fund this test with internal development money and the test will be conducted by the end of March. After this test is completed, additional units should be manufactured and tested to demonstrate overall system performance. Once these two steps are taken, the AXSV should be ready for limited production runs.

1. Release Plate
2. Tab
3. Cover
4. Backup Ring
5. Electronics Board
6. Sea Water Battery
7. Electronics Housing
8. Seakeeping Spool
9. Inflation System
10. Probe Spool
11. Dereeling Guide
12. Probe Afterbody
13. Probe Nose
14. Probe Electronics
15. Bulkhead
16. Rubber Bumper
17. Preload Spring
18. Buoy Housing
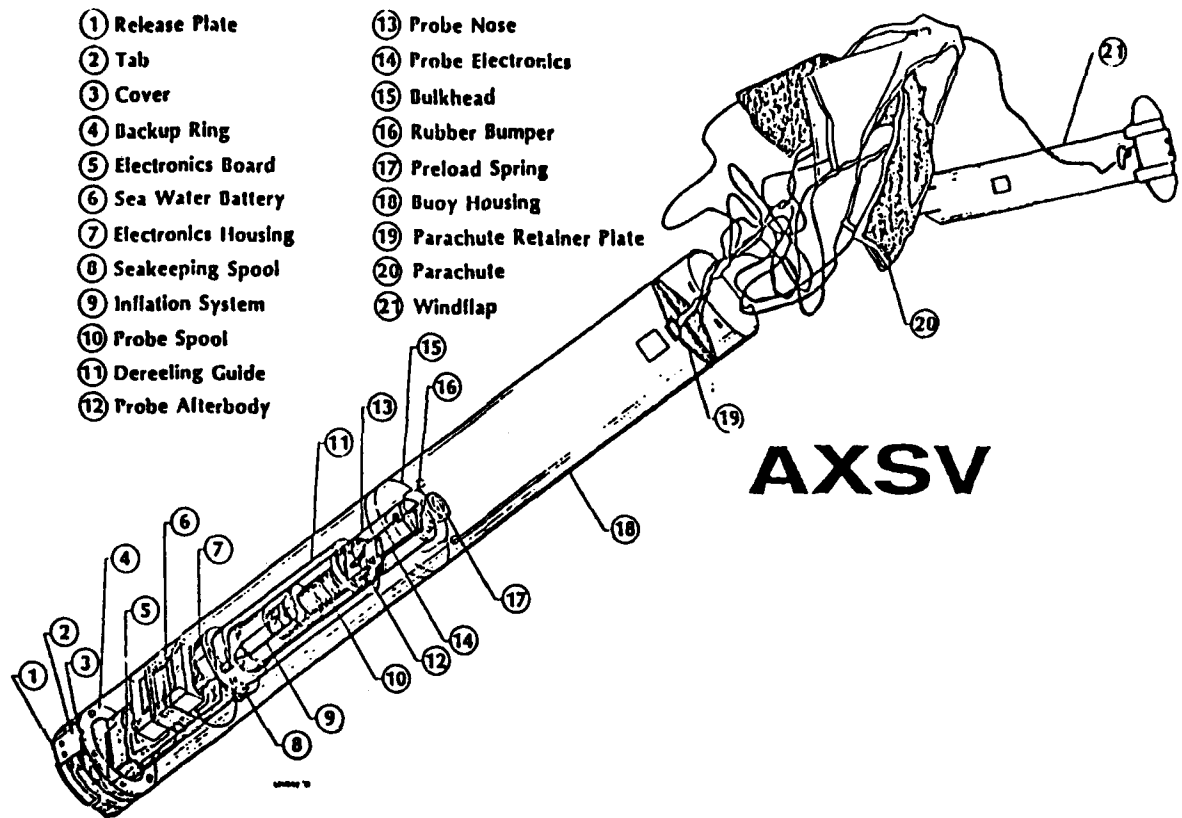19. Parachute Retainer Plate
20. Parachute
21. Windflap

AXSV

FIGURE 1.   DESIGN OF THE AIR LAUNCHED EXPENDABLE SOUND VELOCIMETER (AXSV).

28

AXSV
air launched expendable sound velocimeter

1 Release Plate
2 Backup Tab
3 Buoy Housing
4 Preload Spring
5 Parachute Retainer Plate
6 Parachute
7 Windflap
8 Cover
9 Float Bag

10 Electronics Cover
11 Electronics Housing
12 Bag Seal
13 Sea Water Battery
14 Backup Ring
15 Electronics Board
16 Inflation System
17 "O" Ring
18 Seakeeping Spool
19 Probe Spool
20 Probe Electronics
21 Probe Afterbody
22 Probe Nose
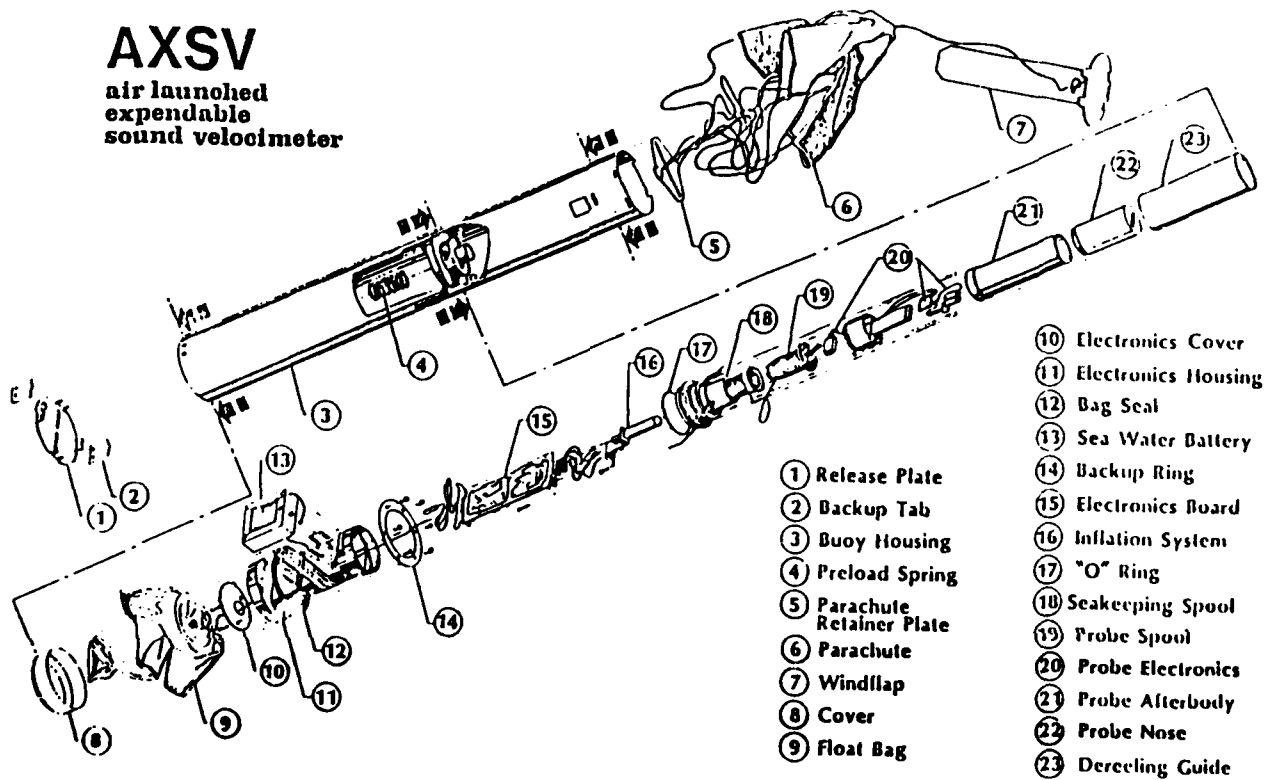**23** Dereeling Guide

FIGURE 2. EXPLODED VIEW OF THE AXSV.

INTELLIGENT DATA SELECTION SYSTEM

Randy Holland
Ron Miles
Naval Ocean Research and Development Activity
NSTL Station, Mississippi 39529

Abstract

Oceanographic phenomena, particularly upper ocean phenomena, are extremely variable and are measured by many types of sensors with different characteristics. In order to optimally collect data for each phenomenon of interest and to optimally summarize data so that remote measurements can be made over long time periods, an intelligent measurement system is needed. The general features of such a system have been determined and work is proceeding toward development of a system prototype.

BACKGROUND

Most oceanographic data, especially for higher frequency events, are not now collected in a time correlated form, nor are the data collection rates optimized for all events of interest. In addition, data storage for remote systems is often inefficient since fixed rate sampling often results in the recording of large amounts of nearly identical data. Lastly, non-idealized sensor outputs and effects of significantly different time constants cannot now be corrected at the source, thereby contaminating the recorded data.

The Intelligent Data Selection System (IDSS) offers the potential for removing most if not all of the aforementioned data collection limitations. The IDSS will be an adaptive data acquisition system having the ability to optimally acquire oceanographic data events of interest and store/transmit this data in compacted form. Additionally, the computing power of IDSS can be used to linearize sensor outputs and possibly to deconvolve sensor response time differences. The IDSS will permit the user, through software, to make data collection decisions as if the user were actually on scene. Operational requirements of IDSS are that it be of a size and weight that allow easy handling and deployment from an AGOR or smaller vessel, that it be capable of being deployed for a duration of 3 to 12 months, and that no field adjustment or setup be required. In addition, the system must be highly reliable and easily repairable.

DATA HANDLING

The IDSS will consist of a high speed input module which captures all environmental data of interest and temporarily stores it in scratch pad memory. A data categorization module will next analyze the scratch pad memory contents to decide which types of data are resident and the extent of each type. The data categories are presently being defined and will likely be similar to the following: Category I includes quasi-steady state data which show little if any trend and small low frequency excursions about the mean and which do not change substantially over long time periods. Category II includes trend data and/or low frequency fluctuations which represent relatively slowly changing events. Category III data consist of even higher frequency fluctuations and/or fast rates of change that can be described reasonably well by periodic functions. Category IV data are the highest frequency data captured and may also consist of nonperiodic transitions and transients which show medium to steep slopes.

After categorization, the data sets will be transferred to special data

processing/compaction modules. Only Categories I, II, and III are candidates for compaction. Category I data may be represented by single data points separated by long time periods. Category II data may be represented as statistical information or by means of a linear regression resulting in a slope and a variability band. Category III data may be represented spectrally, possibly by fast Fourier transforms. Category IV data may require total data capture at various sampling rates to preserve the complex nature of the data. Each special data processing/compaction module will process the data and summarize it in accordance with its compaction program(s). Compaction techniques being considered include histograms (frequency distributions), range information, statistical reductions, regressions, slope determinations, spectral analysis, and FFT analysis.

Once compaction has been completed, the data will be merged together, with appropriate timing information, in a composite data set for storage on board or transmission to some distant receiver site. Figure 1 is a schematic diagram of the IDSS design concept. Because of the modular nature of IDSS, additional processors can be added as needed to implement additional data processing/compaction techniques or to linearize and/or deconvolve sensor raw data streams.

DEVELOPMENT CONSIDERATIONS

Of primary concern in the development of IDSS is its operational reliability. The requisite complexity of a system like IDSS often means greatly reduced reliability and increased difficulty with maintenance. Considerable efforts are being expended to include reliability/maintainability in the basic design. Additionally, the applicability of fault-tolerant designs is being carefully considered.

Questions which must be considered in the development of IDSS are: How is information content altered as a result of compaction? What is the potential reliability for such a complex system? Will the system be "friendly" to the researcher and repair technician? What will it take to deploy and recover? And how long can it stay on station?

SUMMARY

In summary, the IDSS will offer, when completed, a tool for remote unattended ocean data collection that permits the researcher to implement the kinds of data collection decisions that would be made by the researcher if on scene. The primary benefits consist of significantly more useful data per collection effort and potentially much longer time on station. These benefits may result in a substantial increase in the quantity of usuable data per dollar spent on data collection. Secondary benefits include the ability to collect time correlated data sets and to linearize and deconvolve (time skew) sensor data streams.

FUTURE WORK

The development schedule for the IDSS calls for concept design and trade-off analysis to be carried out during FY82 and to be completed in early FY83. Signal processing and compaction analysis is to be completed by the end of FY82. Prototype system design will take place in FY83 and prototype system construction will begin in mid FY83 and be completed in mid FY84. Laboratory testing of the prototype system will be completed in early FY85 and at-sea prototype testing will take place throughout FY85.
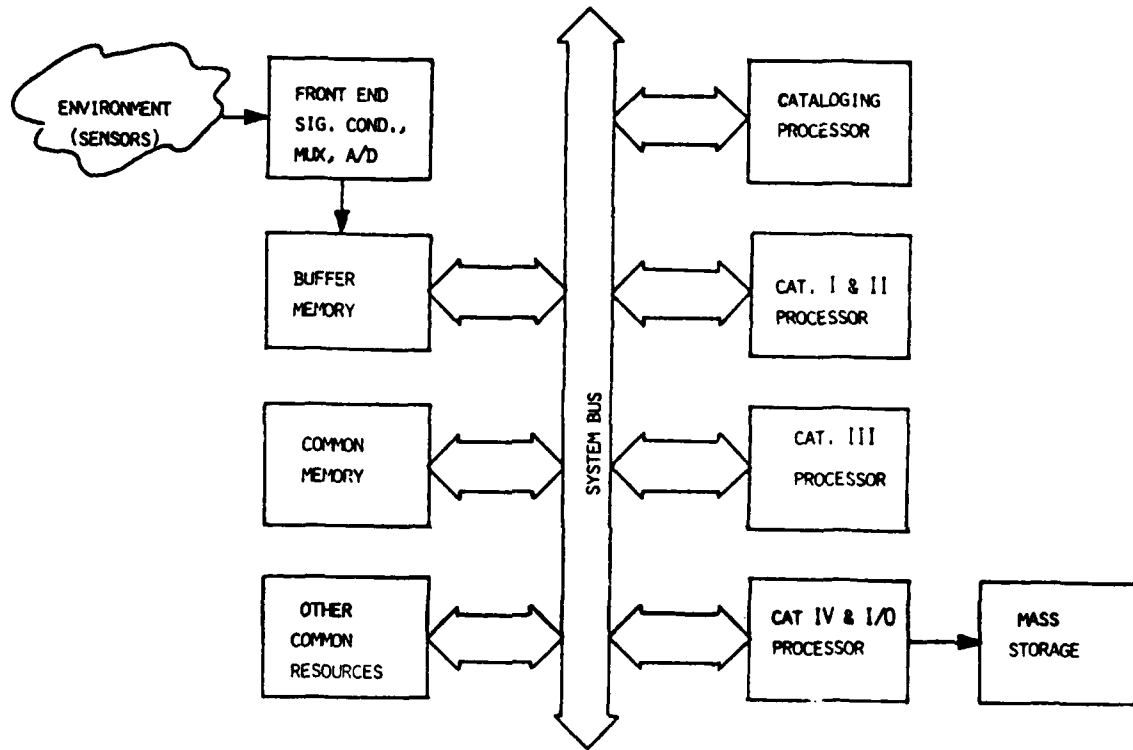
IDSS DESIGN CONCEPT

FIGURE 1. SCHEMATIC OF IDSS DESIGN CONCEPT.

BIOLUMINESCENCE DATA AND DETECTORS

Jon R. Losee
Naval Ocean Systems Center
San Diego, California   92152

Abstract

At-sea measurements of bioluminescence were made at several locations since 1979 using both submersible and onboard photometer systems.   High resolution time series data, wavelength spectra, and vertical bioluminescence profiles were obtained.   New submersible instrumentation is being developed to operate to 200 meters depth and a new onboard system is being developed to operate from an underway ship.

BACKGROUND

The Naval Ocean Systems Center (NOSC) has been making bioluminescence measurements since 1979 in such diverse ocean areas as the Beaufort Sea, the North Atlantic, the Norwegian Sea, and the Sea of Cortez.   NOSC instrumentation is based on nuclear fast counting techniques.   In situ measurements are made using fast electronics and very sensitive single photon counting techniques.   Measurements show ultraviolet (wavelengths shorter than 400 nm) marine bioluminescence and indicate that the spectral region 440-360 nm does not correlate to the major component centered at 480 nm.

PRESENT INSTRUMENTATION

NOSC instrumentation is based on observation of bioluminescence generated by the turbulence of flowing seawater in a viewing chamber.   Two types of detectors are used for measurements.   One is a submersible photometer deployable to 100 m, shown in Figure 1.   The second, shown in Figure 2, is an onboard system which pulls water from the ship's sea chest for underway measurements.   An additional lab system, shown in Figure 3, is used to measure isolated organisms obtained from plankton samples.

All detectors use RCA 8575 photomultipliers (PMTs) in single photon count mode. Average intensities of signal pulses from the PMTs are determined by 100 sec counts obtained by Ortec scalers.   High time resolution data, such as the example in Figure 4, are obtained by collecting the pulses into time bins ranging from 10 μsec to 1 sec, which are switch selectable on two Davidson multi-channel analysers.   Normally 10 msec bins are used.   The analysers are used synchronously with a 1023 bin capacity.   These data are recorded in 1023 channel blocks on digital magnetic tape.

Narrow band (10 nm) optical spectra are generated at depth by remotely turning a filter wheel in the submersible detector.   Figure 5 shows sample color spectra for the Beaufort and Norwegian Seas.   Figure 6 is a similar figure for a location in the north Pacific Ocean.   Depth profiles of bioluminescence intensity using discrete and continuous measurements compare well, as shown in Figure 7 for the north Pacific Ocean.

NEW INSTRUMENTATION

New instrumentation includes a submersible photometer deployable to 200 m and an onboard system which pulls water from the ship's sea chest for continuous underway measurements.   Figure 8 illustrates the submersible system.   The basic detector design, shown in the lower part of Figure 8, is the same for these two measurement systems.   Both

detectors use four RCA 8575 PMTs in the single photon count mode, each with a different optical filter. Data from each tube is combined in 10 msec time bins and these data are converted to a digital format using an 8085 microprocessor based system. For the submersible detector, depth and temperature sensors are also included. For the onboard system, temperature, salinity, and flow rate sensors are included. A PDP-11 mini-computer system is used to read, analyze, and display the data.
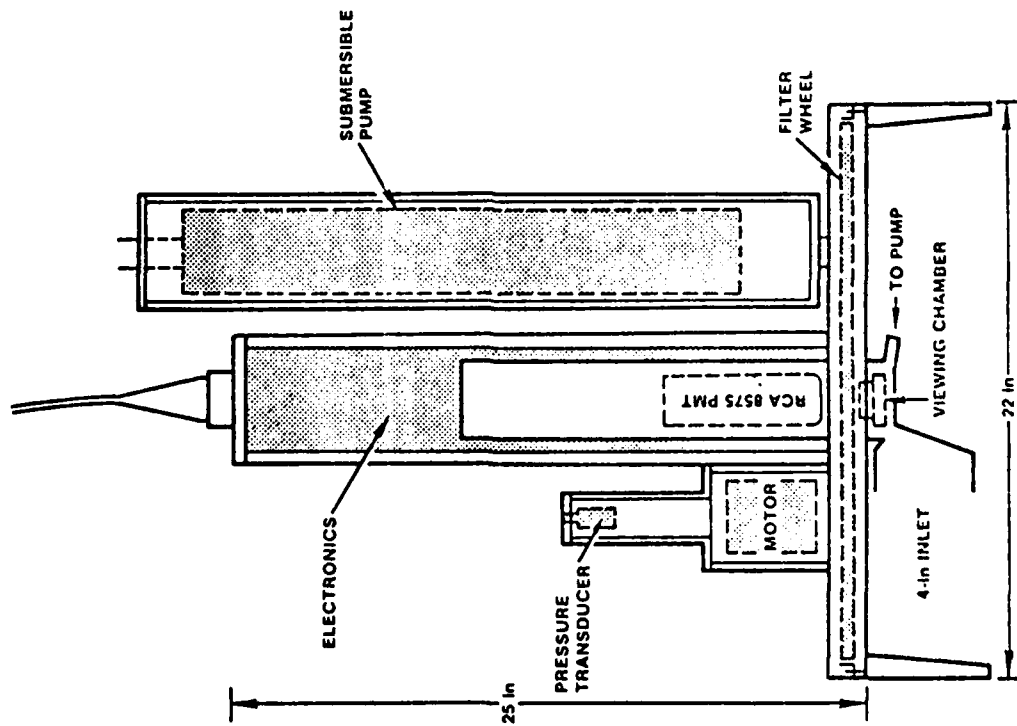
FIGURE 2. NOSC ON-BOARD BIOLUMINESCENCE DETECTOR

FIGURE 1. NOSC SUBMERSIBLE BIOLUMINESCENCE DETECTOR. THIS DETECTOR IS DEPLOYABLE TO 100 METERS.

FIGURE 3.   NOSC LABORATORY PLANKTON TEST CHAMBER.
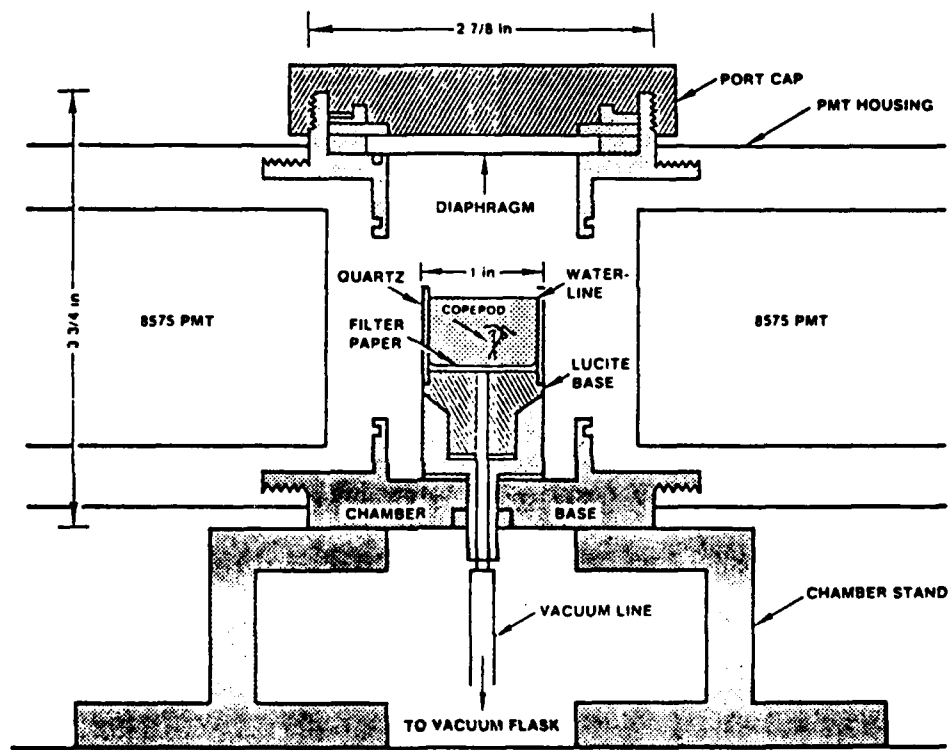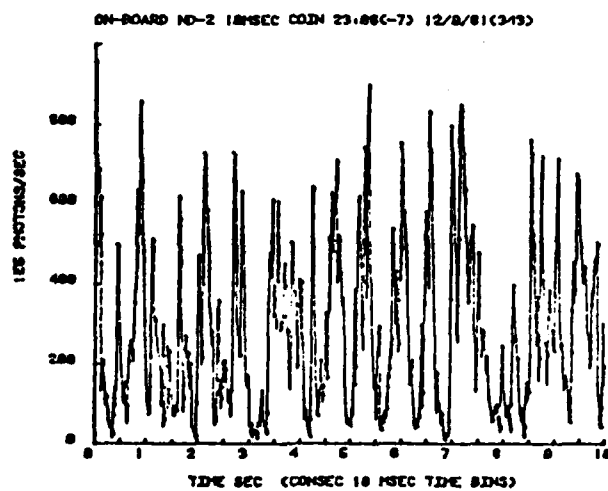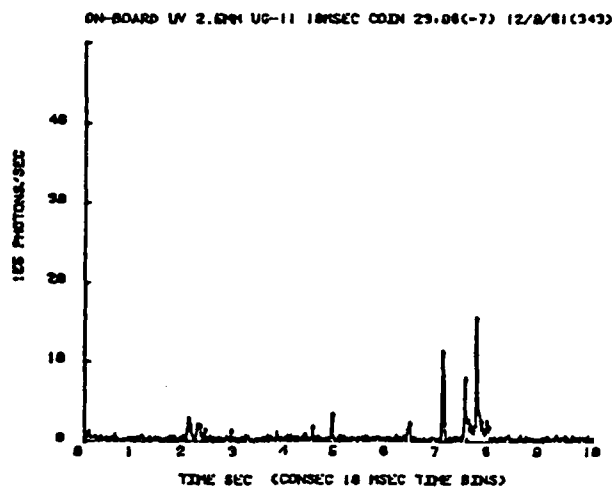
FIGURE 4. HIGH TIME RESOLUTION SYNCHRONOUS BIOLUMINESCENCE DATA WITH ULTRAVIOLET (TOP) AND BROAD BAND (BOTTOM) FILTERING.
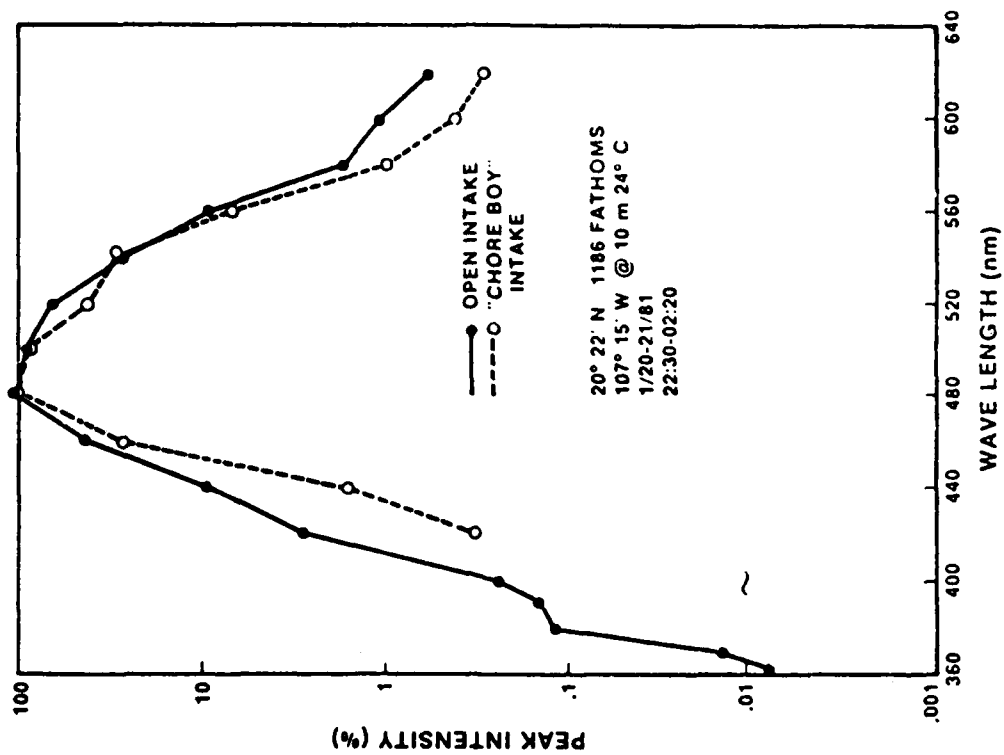
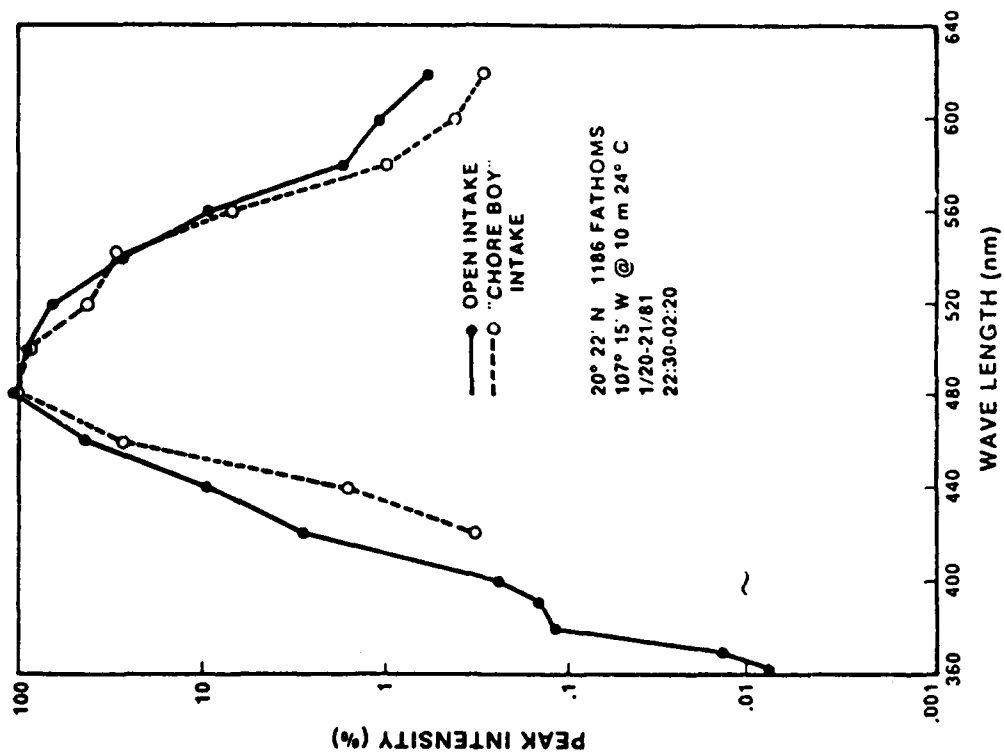FIGURE 6. BIOLUMINESCENT COLOR SPECTRA FOR NORTH PACIFIC OCEAN.

FIGURE 5. BIOLUMINESCENT COLOR SPECTRA FOR BEAUFORT AND NORWEGIAN SEAS.

40

STA# 11 23 48.74 N, 112 29.33 W D#8.3K/MIN 80:36(-8) 12/14/81(348)

BIOLUMINESCENCE INTENSITY(PMT K COUNTS/SEC)

STA# 11 23 48.74 N, 112 29.33 W 80:51-82:48(-8) 12/14/81(348)

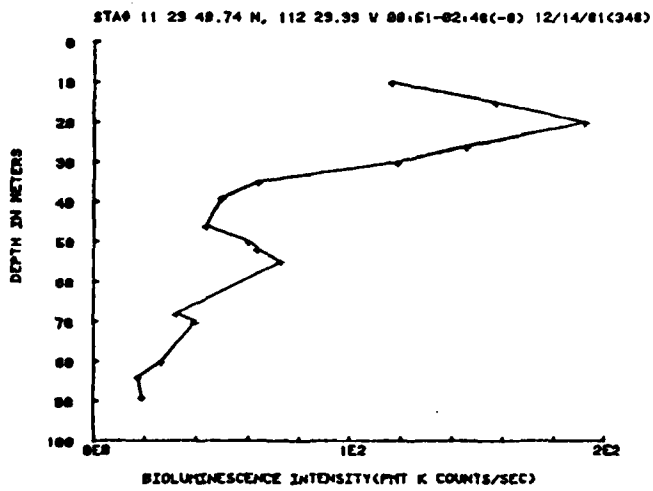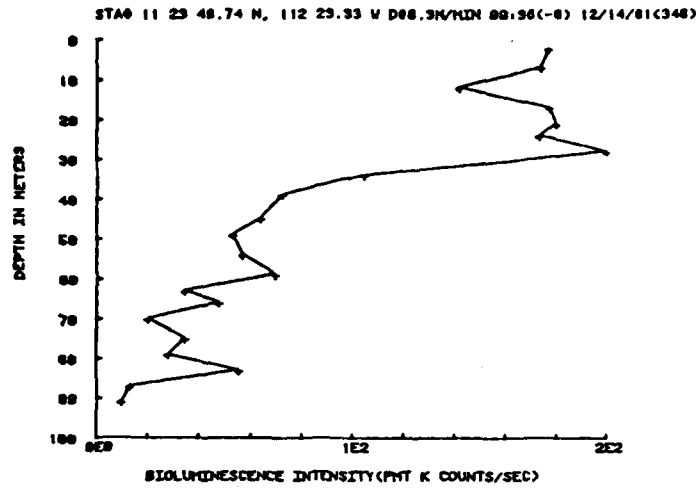BIOLUMINESCENCE INTENSITY(PMT K COUNTS/SEC)

FIGURE 7. BIOLUMINESCENCE BROAD BAND INTENSITY AS A FUNCTION OF DEPTH. CONTINUOUS DATA IS SHOWN IN THE TOP FIGURE, DISCRETE DATA IN THE BOTTOM FIGURE.
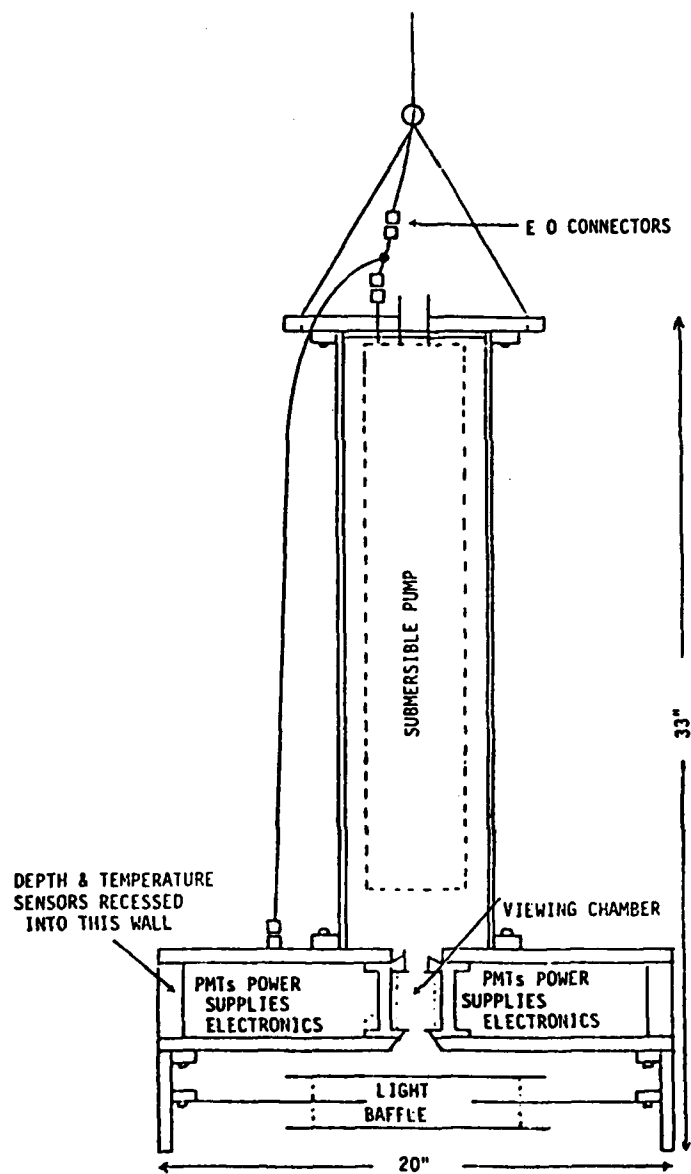
41

FIGURE 8. NEW SUBMERSIBLE BIOLUMINESCENCE DETECTOR, DEPLOYABLE TO 200 METERS. THE NEW ON-BOARD SYSTEM USES THE SAME DETECTOR DESIGN SHOWN IN THE LOWER PORTION OF THIS FIGURE.

CURRENT MEASUREMENT TECHNOLOGY HANDBOOK

Edward C. Gough
Planning Systems Incorporated
1700 Old Spanish Trail
Slidell, Louisiana 70458

SUMMARY

The Oceanographic Instrumentation Systems (OIS) project of the Ocean Measurement Program (OMP) at NORDA manages the development of advanced oceanographic sensors, instrument packaging, deployment schemes, and measurement systems for various U.S. Navy programs. OIS routinely collects pertinent information from technical literature, manufacturers, individual investigators and others, and assesses this information for its potential impact on present or future OIS projects. Some of this information is being compiled into an Oceanographic Instrumentation Handbook which, in addition to serving internal OIS needs, will be available to other Navy and academic users. Because of its involvement in the development of advanced shear and velocity profilers, OIS is preparing a handbook of current measurement technology as a low cost prototype of such a product. Planning Systems Incorporated produced this handbook, which will be updated as needed to account for new technology and new points of view.

The purpose of the Current Measurement Technology Handbook is to assess existing current measurement technology and capability, to provide OIS with information for investment and other management decisions, and to establish a controlled "data base" on one important phase of oceanographic instrumentation.

The handbook contains a chapter on measurement and instrumentation issues which discusses cosine response; fouling; accuracy, including steady flow, turbulence, and scale of flow; operations, including deployment, duration, and data capacity; and intercomparisons. Following this chapter, separate chapters discuss mechanical, acoustic, and electromagnetic current measurement technology. These chapters include discussions of the history of the individual technology, of its theory of observations, and cf presently available commercial systems. Following these chapters in the handbook are a chapter discussing emerging current measurement techniques, a chapter summarizing commercial current meters, and a chapter summarizing experimental current meters. The handbook concludes with a bibliography and a glossary.

II.   PROJECT SUMMARIES

       B.   OCEANOGRAPHIC TECHNIQUES

REPORT ON SUBSURFACE TEMPERATURE INVERSIONS
IN THE NORTH ATLANTIC AND THE NORTH PACIFIC
AND THEIR RELATIONSHIP TO STABILITY PROFILES

William J. Emery
Department of Oceanography
University of British Columbia
Vancouver, B.C., Canada VGT 1W5
(Presented by R. Hollman)

Abstract

Investigation of temperature minima that occur in much of the high latitude North Pacific and parts of the eastern North Atlantic has continued. NAVOCEANO air launched expendable bathythermograph (AXBT) data have been used to examine features of the temperature minima in the eastern North Atlantic. Parameterization of minima in terms of depth, magnitude, and vertical extent has proven useful for objective interpretations. Both investigation of CTD profiles and computer simulation studies are being used to determine characteristics of salinity adjustments that accompany establishment of temperature minima.

BACKGROUND

Historical hydrographic and CTD data indicate an omnipresent subsurface temperature minimum in much of the high latitude North Pacific and in portions of the eastern North Atlantic. The cold temperature inversion forms as a residual of winter water colder than both the water below it and that in the overlying upper layer, which is heated in spring and summer. Whether this process occurs locally or at some distant location from which the cold water has been advected is not yet known.

OBSERVATIONS

Data from a single site such as ocean weather station PAPA (50°N, 149°W) is not sufficient to indicate the dominance of either local formation or advection from a distant source. In Figure 1, for instance, a mean annual time series from station PAPA suggests that both mechanisms may operate at different times. In the series of temperature profiles a small minimum develops in May apparently as a residual of winter-spring cooling combined with early summer warming. This locally formed inversion is present and strengthens through June, July and August but is gone by September. In November a much stronger, but narrower, temperature minimum appears which persists into February. This is probably a result of the advection of much colder water into the region from another formation area so that the resulting sharp temperature minimum is not a consequence of local cooling. This series suggests that over a representative yearly cycle both local formation and advection may be contributing to the presence of a cold temperature inversion.

Both of these temperature minima are stabilized by an adjustment of the vertical salinity gradient, which is most obvious in the difference between the October and November salinity profiles. These changes are fairly subtle, however, and it is difficult to distinguish a profile with a temperature minimum by its corresponding salinity profile alone. The complexity of the relationship between salinity and temperature, in the presence of a temperature minimum, is emphasized by selected individual temperature-salinity (TS) curves shown in Figure 2. Here three different TS curves from weather

station PAPA are presented along with the mean TS curve from all available data. It is readily apparent that none of the individual curves even comes close to the mean, which must be regarded as a somewhat artificial quantity resulting from the averaging of widely different TS curves.

The temperature inversion in each of the individual TS curves is revealed by an inflection point at which the TS curve is multi-valued so that each temperature is associated with more than one salinity. Differences in the shape and location of the individual inflection points alter this set of values for each curve, so no single TS curve can be used to choose a salinity value which will match an observed temperature profile containing a subsurface minimum. Since a salinity input is required to compute stability for a dichothermal temperature profile, it is necessary to understand the mechanism by which a salinity profile adjusts to balance the temperature inversion and to maintain a stable density profile.

Changes in the shape of the TS curve inflections shown in Figure 2 are related to changes in the shape and nature of the temperature minimum itself. Figure 1 illustrates the marked differences between the late spring temperature minimum and that found in the fall-winter. Thus a first step in understanding the salinity profile adjustment is to parameterize the temperature inversion itself.

DATA ANALYSIS

Cold temperature inversions are parameterized in terms of depth (D), magnitude (M) and extent (E), as illustrated in Figure 3. Maps of these quantities are expected to differentiate areas where the minimum was formed locally from those where it had entered a region by advection. In addition, these parameter maps will be useful in tracing advective features back to their source regions.

AXBT data from the eastern North Atlantic collected by NAVOCEANO were used in an analysis of subsurface temperature inversions. The analysis was restricted to inversions with the largest magnitude (M) for each profile. Maps of D, M, and E were prepared for each of four seasons. Maps for spring (March-April) are shown in Figure 4. Only a relatively small percentage (~25%) of all the AXBT drops in this period exhibited sharp enough temperature minima to qualify for this study. Small temperature scale ($\Delta t < 0.2^{\circ}C$) inversions (both maxima and minima) were considered as instrument noise and thus excluded from examination. The inversion was deepest north of Iceland and near $50^{\circ}N$, $25^{\circ}W$ as shown in Figure 4a. Although these two regions appear to be quite separate, a few inversions were observed between them. Most minima, however, were located north of Iceland in the southern portion of the Denmark Strait. It is interesting to note that in this region the strongest features, shown in Figure 4b, are found away from the Icelandic coast and more in the center of the Strait. Investigation of how the vertical salinity gradient changes in response to a temperature inversion to maintain a stable density profile was approached from two directions. First, the limited number of quality CTD observations available were examined to provide high quality estimates of the vertical temperature, salinity and density profiles. In most cases the water column was found to be stably, if weakly, stratified. In the second approach, a computer program was developed to compute the salinity profiles corresponding to input profiles of density and temperature. Thus, for a specified stable stratification, temperature profiles displaying minima with various values of D, M and E can be input to find corresponding salinity profiles. Some common adjustments of the salinity structure in response to the temperature inversions are expected to be identified by this approach. For example, a marked shift in the salinity gradient has been found to be a typical adjustment. Analysis of the inversion parameters outlined above is proving valuable in characterizing the primary modes of variability so

48

that a limited selection of candidate temperature profiles can be examined.

FUTURE WORK

CTD data from the NAVOCEANO cruises in the Northeast Atlantic will be examined in an effort to better establish the relationship between temperature minimum, salinity and stability. A limited quantity of historical CTD data will be included in the study.

The parameterization of temperature minima using historical ship XBT data yields results surprisingly different from results obtained from NAVOCEANO AXBT data. This may be a result of a broader definition of the individual season for AXBT analysis. A reliable "climatology" of the inversion parameters would be useful for comparison with individual AXBT surveys.

These analysis techniques will be used to study the temperature minimum in the North Pacific, which is expected to be a stronger and and more widespread feature. Ongoing NAVOCEANO AXBT flights should again provide data for the mapping of D, M, and E. A larger amount of historical CTD data should prove valuable in evaluating upcoming NAVOCEANO shipboard measurements.
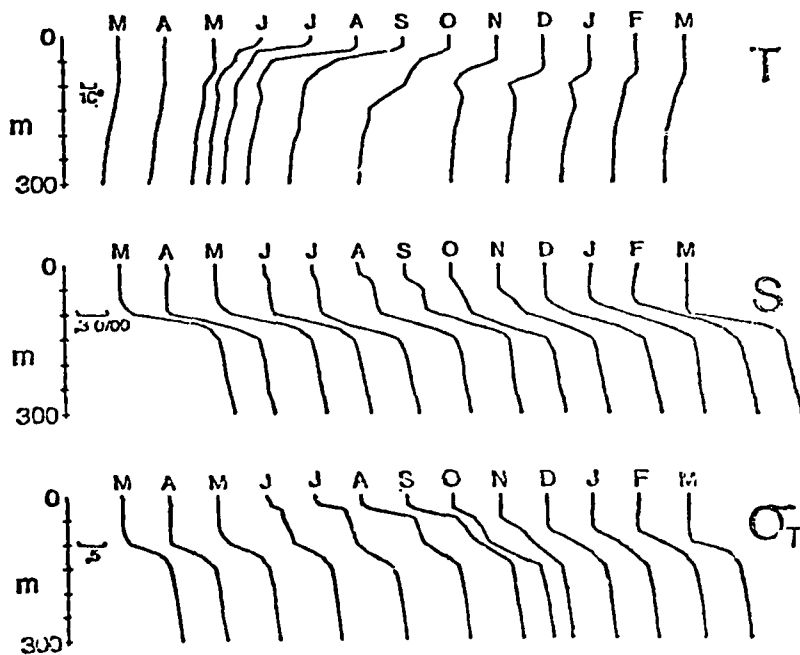
FIGURE 1. MEAN ANNUAL TIME SERIES OF TEMPERATURE (T), SALINITY (S), AND DENSITY (σ_t) PROFILES AT WEATHER STATION PAPA (50°N, 149°W). PROFILES ARE MONTHLY ANNUAL MEANS BASED ON DATA FROM 1964 TO 1978.

FIGURE 3. PARAMETERIZATION OF A COLD WATER TEMPERATURE INVERSION IN TERMS OF DEPTH (D), MAGNITUDE (M), AND EXTENT (E). TEMPERATURE PROFILE IS FROM THE EASTERN NORTH PACIFIC.
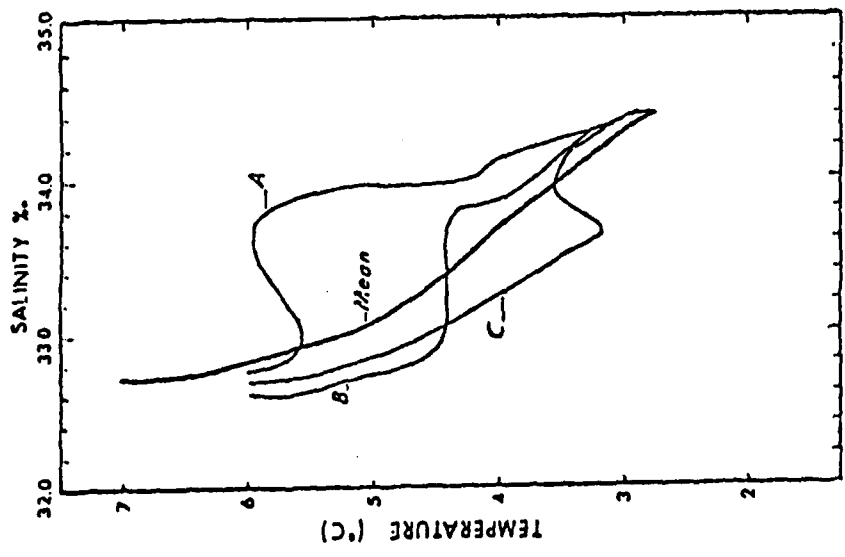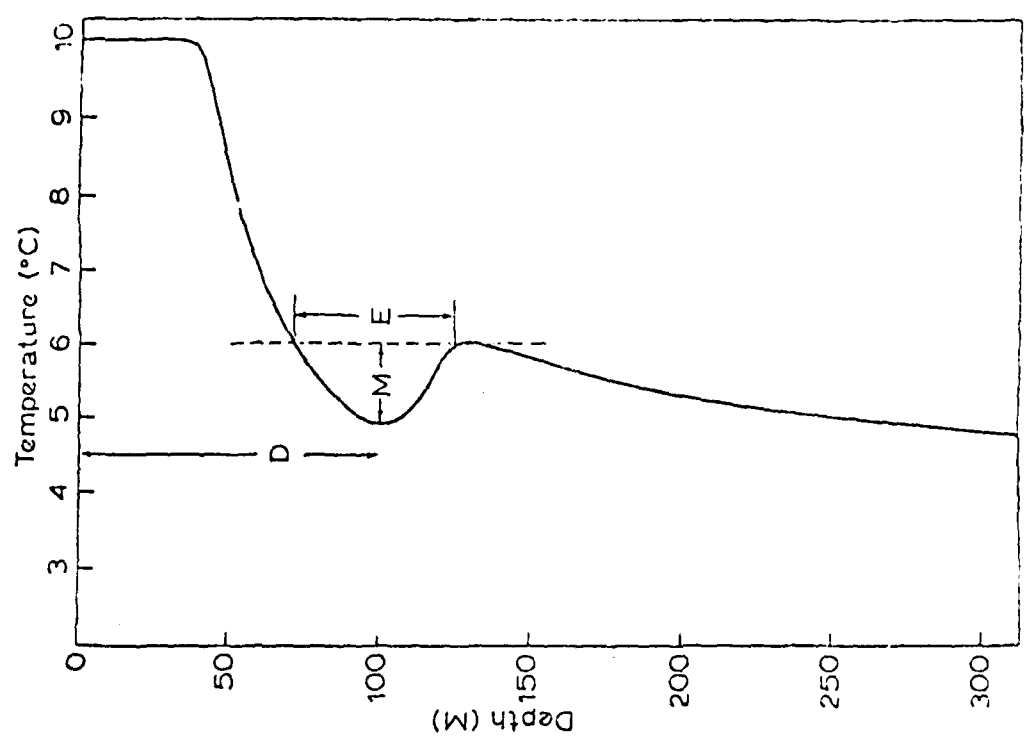

FIGURE 2. THREE INDIVIDUAL TEMPERATURE-SALINITY CURVES AND THE LONG TERM ANNUAL MEAN AT OCEAN WEATHER STATION PAPA. THERMAL INVERSION APPEARS AS AN INFLECTION IN CURVES A, B, AND C.

51

a. DEPTH OF TEMPERATURE INVERSION.
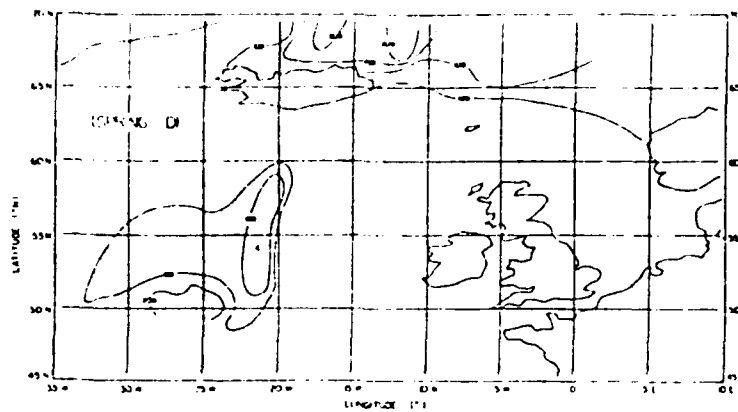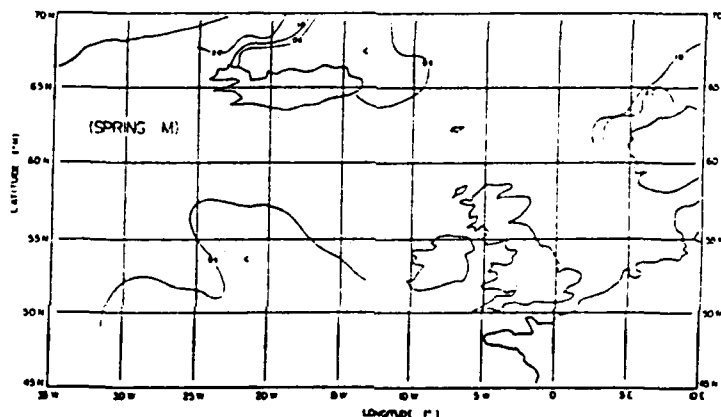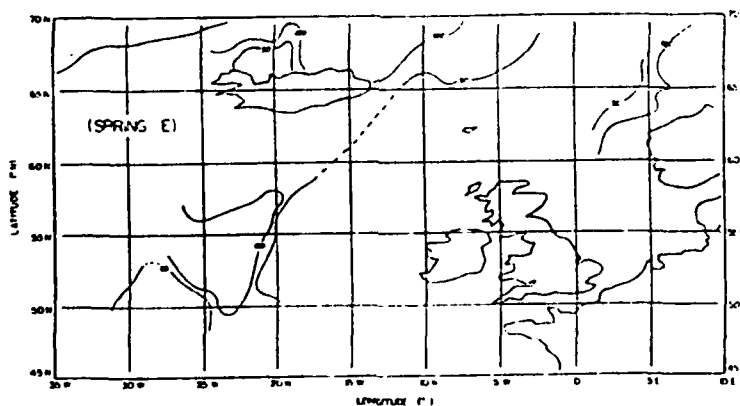

b. MAGNITUDE OF TEMPERATURE INVERSION.

c. EXTENT OF TEMPERATURE INVERSION.

FIGURE 4. MAPS OF TEMPERATURE INVERSION PARAMETERIZED QUANTITES DEPTH (D), MAGNITUDE (M), AND EXTENT (E) FOR SPRING SEASON (MARCH-APRIL) IN THE NORTH ATLANTIC.

SUPPORT OF THE OCEAN MEASUREMENTS PROGRAM

A.W. Green
D.A. Burns
Z.R. Hallock
K.D. Saunders
Naval Ocean Research and Development Activity
NSTL Station, Mississippi 39529

Abstract

Several aspects of NORDA Physical Oceanography Branch work for the Ocean Measurement Program (OMP) are presented. Four self-contained sections describe additional results from the Acoustically Tracked Oceanographic Mooring Experiment (ATOM), analysis of XCP and CTD data from the Norwegian Sea, assessment of fine structure variability, and a mooring motion workshop sponsored by NORDA in 1981.

INTRODUCTION

During the past year the Physical Oceanography Branch of NORDA has been involved in analysis of data obtained in the Acoustically Tracked Oceanographic Mooring (ATOM) experiment, in processing and analysing expendable current profiler (XCP) and conductivity-temperature-depth (CTD) data collected in the Norwegian Sea during the fall of 1980, and in developing analytic and display methods for assessing fine structure variability in the upper ocean. These three areas are briefly discussed here. In addition, a summary is included of a workshop on mooring motion that was convened in July 1981 by the Physical Oceanography Branch.

I. ATOM EXPERIMENT

BACKGROUND

The ATOM experiment was designed to investigate upper ocean variability in the high frequency, high wavenumber (HFHWN) range of internal gravity waves. Corrections to the three-dimensional mooring trajectory during the experiment were made for vertical excursions that occurred as deep currents depressed the mooring below the original design depth. The high density of current meters on the upper part of the mooring provided an opportunity to obtain estimates of current shear over long periods of time and to examine the variability of shear in relation to low frequency events.

RESULTS

Results of the ATOM experiment indicate that additional design modifications would significantly decrease horizontal and vertical motions of a mooring of this type, even under extreme current shear conditions. The mean high frequency internal wave variance was found to decrease slightly with distance below the pycnocline. Significant short-term variations in the high frequency background are adverse to the mean trend. Sub-pycnocline inertial band energy levels are positively correlated with local wind variations. The cross-correlation of band-passed rectified power levels of inertial band and local wind speed were positive and significant. Low frequency fluctuation intensity in the inertial-semidiurnal tidal band showed no discernable correlation with variations of high frequency internal wave activity. Modulation of the vertical shear by inertial

currents did not produce expected spontaneous fluctuations of high frequency energy, even when inertial shear was most intense. Generally, high frequency band current fluctuations (greater than 1 cph) are not coherent at vertical scales greater than 7 m. The high frequency band temperature fluctuations were found to be highly coherent at separations of 35 meters and greater. Mooring motions at frequencies less than about 3 cph showed no significant effects on horizontal current measurements but do affect unmeasured changes in current meter orientation. Vertical motions of the current meter array superimposed on a background of large mean shear or mean temperature gradient may create nonlinear effects, which will appear as peaks of the superharmonics of the vertical oscillation frequency. Mooring motions as recorded by acoustic travel time and Doppler tracking systems generally are at least two orders of magnitude smaller than the observed horizontal currents in each frequency band up to 1 cph. The baseline of system noise for the acoustic tracking systems coincides with the frequency domain in which the noise levels caused by variations in the orientations of the meters become significant.

Analysis of the azimuthal motions of the current meters shows that variations in azimuthal orientation introduce errors in shear computations and apparent velocities. Magnitudes of these errors are comparable to, if not greater than, those introduced by noise in the acoustic tracking system. This type of error can be removed by measurement of current meter attitude with respect to the flow at each velocity realization. Using calibration data for each current meter, the azimuthal response can be deconvolved from the velocity record, and the velocity errors can be reduced by a factor of 5 to 10. The magnitude of these errors was about 2% to 8% in the extremes, but these errors are significant in shear measurements. General application of this procedure requires calibration of each current meter and a time consuming, detailed analysis of each current record. Four current meters in the ATOM mooring were calibrated accurately enough to use the measured azimuthal response for removal of orientation error. The orientation-induced errors were significant but appear to have no effect on the shape of the spectral slope in the current meter fluctuation records. The most noticeable effect is in estimates of relative shear at high frequencies and small vertical separations.

The ATOM mooring would have had less horizontal and vertical displacement had the upper 500 m of the mooring, including the main subsurface flotation, hard-hat glass ball floats, current meters and ancillary mooring displacement measurement systems, been streamlined. High frequency, high wavenumber fluctuations did not create high frequency mooring oscillations nor were the high frequency fluctuations coherent enough to induce significant mooring motions.

In future measurement programs in which accurate long-term measurements of current shear are required, it is imperative that the current meters receive pre- and post-deployment calibrations of azimuthal response. The azimuthal response characteristics of each meter should be applied to the data analysis process to remove orientation errors.

Intense, rare HFHWN events occur but are not entirely understood. One such event appeared to have a duration of approximately 90 minutes during which the local shear observed on five current meters increased by an order of magnitude and temperature gradients were extremely variable, even reversing sign in some cases. The rather weak stratification and strong shear probably precipitated stratified shear instabilities during these events.

The ATOM experiment also included expendable current profiler (XCP) and CTD data for estimating bulk Richardson numbers. Significant errors in XCP temperatures and depth/time relationships limit the vertical resolution of Richardson numbers. The electromagnetic field in the vicinity of a CTD may interfere with XCP performance. Such

54

interference was observed in two cases in which the XCP apparently passed within a few meters of the CTD profiler, although there was generally no indication that the CTD nor the local ship's magnetic field influence were significant to XCP measurements when there was 40-50 meter separation between the XCP and the disturbing object.

II. NORWEGIAN SEA CURRENT SHEAR OBSERVATIONS

BACKGROUND

Measurements in the vicinity of the subpolar front in the Norwegian Sea and the Iceland-Faeroe Gap were obtained using XCPs and CTDs. Inertial modulation of currents in this area were expected to be very intense. In addition, records of geomagnetic variability were obtained during the experiment to examine effects of geomagnetic variability on the XCP system. These data will also be used to determine the feasibility of estimating profiles of stability and bulk Richardson number from XCP and CTD profiles that are near-coincident in space-time. As expected, fine structure variability within the front was greater than that in the North Atlantic waters to the south.

RESULTS

No strong inertial period variations were found in the XCP profiles. The low intensity of the inertial shear is probably due to the relatively weak vertical stratification in the frontal zone, which does not support the high vertical wavenumber inertial oscillations that are observed in more strongly stratified regions in the lower latitudes.

Two strong geomagnetic events occurred in the vicinity of the experiment with time scales of hours, which are considerably greater than the time scale of XCP profiles. These events appeared to have no high frequency components that affected the performance of the XCP profilers, although an absolute velocity offset by some temporally dependent factor not directly measurable probably occurred as a result of these events.

Because of weather and operation schedules, few XCP and CTD coincident profiles were made. Comparison of temperature profiles between the two instruments showed significant errors, some of which could be attributed to a single calibration temperature offset in the XCP, although higher order temperature errors were also present. Velocity profiles from the XCPs were used to compute bulk shear, and CTD profiles from nearby stations were used to compute Brunt-Väisälä profiles. These data were merged in plots of bulk Richardson number and logarithmic plots of shear squared and Brunt-Väisälä frequency squared. This representation appears to give a good estimate of apparent bulk dynamic stability for the water column, and is also useful in sorting the dynamic stability data according to reasonable error criteria.

III. FINE STRUCTURE VARIABILITY

BACKGROUND

Fine structure variability can be classified and described in terms of deviations from background variables relative to mean isopycnal surfaces. This investigation was designed to develop analytical tools for examining larger numbers of CTD profiles and to provide a means of differentiating types of intrusive, double diffusive processes and internal wave straining. A large quantity of CTD data has been obtained from instruments in the rapid vertical profiling (yo-yo) mode, and display and analysis schemes emphasizing

55

variability are being developed for analysis of these data. During a CTD yo-yo sequence, the relative displacement caused by ship drift and current motion provides a small scale vertical slice representation of variability over a few kilometers.

RESULTS

Representations for the high frequency, high wavenumber variability that would allow rapid and accurate interpretation of the types of dynamical regimes that could be encountered are being investigated. The most successful representation to date is based upon a two-dimensional display of sea water property anomalies referred to isopycnals. This method allows the display of large quantities of data with magnification of critical parameters such as horizontal changes of salinity or temperature, presence of double diffusive processes, and horizontal intrusions of differing water types along isopycnal surfaces. These displays aided in isolating events that could not otherwise be easily discerned from standard profile plot sequences. The algorithms and methods developed can be directly implemented on high speed, large minicomputers that will be used on future survey ships. Methods of further improving the use and display of fine scale variability extracted from CTD yo-yo profiles are being investigated.

Near the subpolar front there is evidence of cold fresh water sinking below warm salty water and the development of conditions for double diffusive instabilities such as salt fingers. The presence of salt finger instabilities would drastically increase the intensity of microscale variability. In contrast, Sargasso Sea regions are virtually devoid of intrusive anomalies, except at the bottom of the surface mixed layer. Differences between the subpolar frontal region and the Sargasso Sea are significant when considering variations in high frequency, high wavenumber variability in the upper ocean.

IV. MOORING MOTION WORKSHOP

SUMMARY

A workshop to discuss the effects of mooring motion on current measurements sponsored by the Physical Oceanography Branch in July 1981 was attended by 25 participants from 15 institutions. Discussions focused on mooring dynamics, signal contamination and sensor-mooring interactions, measurements of mooring motion, and methods for reducing measurement noise. Although considerable effort has been expended on developing dynamical models of mooring motion, evaluation of the results of these models is incomplete. Effects of mooring motion signal contamination were discussed and it was concluded that each mooring should contain at least one presssure recorder for estimating vertical excursions of the mooring. These vertical excursions are a source of significant error since the instruments may be subject to large vertical gradients of the measured variables (T, V, S). The combination of vertical fluctuations and large background vertical gradients of velocity or scalar fields produces spurious harmonics of the vertical fluctuation frequency. Methods for reducing measurement noise were discussed and it was concluded that at least the upper segments of moorings should be streamlined to limit drag and reduce wind vibrations, and that the vertical/azimuthal responses of the meters should be incorporated in analyses that require estimates of shear or low-level HFHWN motions.

OVERVIEW OF SAI WORK

Richard B. Lambert, Jr.
Science Applications, Inc.
1710 Goodridge Drive
P.O. Box 1303
McLean, Virginia   22102

Abstract

SAI work for the OMP began early in fiscal year 1979.   A brief review of this work is presented and a complete list of SAI reports for the OMP is provided.   Principal accomplishments during the past year are given in another paper by D. Rubenstein.

PREVIOUS WORK

SAI began participation in the OMP by providing technical assistance for planning purposes.   However, most work has involved scientific projects that can be divided into two broad categories: numerical/analytical modeling of the upper ocean, and analysis of existing data, including data available in historical archives.   The principal objectives have been to develop general descriptions of the upper ocean which will improve the effectiveness of the operational navy, and to guide and improve the experiment design and data analysis techniques used by NAVOCEANO.

Work began with assessments (reviews) of both existing models and existing data to identify what was available and usable as well as what was missing and needed.   These assessments led SAI to focus on the ocean shear field as an area with very limited data and of immediate importance to Navy programs.   A large number of technical reports have been completed.

Modeling reports are listed in Table 1.   The principal contribution is the Review of Ocean Models which focuses specifically on upper ocean features of prime importance to the OMP.   It includes reviews of large-scale ocean circulation models, frontal generation and structure models, upper ocean models (mixing layer, air-sea interaction, etc.), and internal wave models.   Initial efforts at shear modeling focused on internal wave spectral models and statistical pictures of vertical profile data.   Some of these results were presented at the last OMP review, and this work has since been completed.   In the past year emphasis has shifted to characterization of time variability of shear, particularly near inertial frequencies.

Completed analysis reports are listed in Table 2.   Existing data available for upper ocean descriptions were reviewed, focusing on shear, internal waves, and fine structure.   As a result of this review, initial technical efforts focused on the ocean shear field.   Available vertical profile data were used in an attempt to assess the variability from one oceanographic regime to another.   Emphasis was placed on shear distribution for project number 0652 and on Richardson number distribution for project number 0393. Primary results are contained in the following reports: Spatial Distribution of Vertical Shear, Some Methods of Calculating Ri (Richardson Number), and Observed Spatial Variations in Ri.   There is substantial evidence that the mean square shear is directly related to local stratification.   Hypotheses that a universal distribution of Richardson number exists were not confirmed, although values tend to cluster about unity.   The manner by which Richardson number is calculated is important; some aspects of this are described in the report, Some Methods of Calculating Ri.   Table 2 shows that work has

moved toward time series characteristics during the past year.

In summary, SAI has completed or is preparing a number of reports relating to numerical/analytical modeling and data analysis. It is important to note that the work has really emphasized shear and that modeling and analysis are two related approaches toward a better understanding of shear.

TABLE 1. TECHNICAL CONTRIBUTIONS ON MODELING

TITLE (AUTHOR)   OMP DISTRIBUTION DATE

I. PROJECT 0849--Technical assistance, model review, and internal wave
    shear

        1. Report on JASIN Data Display
        Meeting (Lambert)   May   1979

        2. Mooring Dynamics Experiment:
        Plan Review Summary (Lambert)   June   1979

        3. Modeling of Internal Wave
        Induced Shear (Grabowski)   March 1980

        4. Characterization of Shear
        and Richardson Number
        (Grabowski and Hebenstreit)   July   1980

        5. Vertical Shear Modeling
        and Analysis (Grabowski
        and Hebenstreit)   Nov   1980

        6. Review of Ocean Models
        (Grabowski and Hebenstreit)   Jan   1981

II. PROJECT 0084--Shear Modeling

        1. Statistical Modeling of
        Shear in the Upper Ocean
        (Hebenstreit and Grabowski)   March 1981

        2. Models of Near-Inertial Vertical
        Shear (Rubenstein)   Nov   1981

        3. Dynamical Model of Wind-Induced
        Near-Inertial Motions (Rubenstein)   Nov   1981

        4. Near-Inertial Motions: A Preliminary
        Model-Data Comparison (Rubenstein)
        (see 0075)   Jan   1982

III. PROJECT 501--Shear Modeling

        1. Work just begining (Rubenstein)

TABLE 2. TECHNICAL CONTRIBUTIONS ON ANALYSIS

TITLE (AUTHOR)   OMP DISTRIBUTION DATE

I. PROJECT 0652--Reviews of Upper Ocean Measurements and Vertical
    Profile Analysis (Shear)

        1. Vertical Shear (Conference)
        (Lambert)   March   1980

        2. Recent Internal Wave Observations
        (Conference) (Rubenstein, Grabowski,
        Lambert and Kirwan)   March   1981

        3. Fine and Microstructure (Conference)
        (Rubenstein, Lambert and Newman)   May   1981

        4. Data Report--SCIMP and YVETTE
        (Lambert, Evans and Hendricks)   July   1980

        5. Comparison of Vertical Profilers
        (Rubenstein, Newman and Lambert)   Sept   1980

        6. Spatial Distribution of Vertical
        Shear (Patterson, Newman, Rubenstein
        and Lambert)   March   1981

II. PROJECT 0393--Vertical Profile Analysis (Richardson Number)

        1. Shear Data Descriptions
        (Lambert and Patterson)   Aug   1980

        2. Some Methods of Calculating Ri
        (Newman, Patterson and Lambert)   Apr   1981

        3. Observed Spatial Variations in Ri
        (Patterson, Newman and Lambert)   Apr   1981

        4. Vertical Shear and Ri in the Upper
        Ocean (Lambert, Newman and Patterson)   May   1981

III. PROJECT 0075--Vertical Profiles and Low Frequency Time Series

        1. Estimates of YVETTE Measurement Error
        (Newman, Molinelli, and Paterson)

        2. Cross Coherence of N^2 and S^2
        (Rubenstein and Newman)

60

3. Analysis of Shear From Current Meters
(Rubenstein and Newman)   June   1981

4. Interpretation of Shear Time Series
From Pollard (1970) Current Meter Array
(Rubenstein and Newman)   Feb   1982

5. Near Inertial Motions: A Preliminary
Model-Data Comparison (Rubenstein)
(see 0084)   Jan   1982

6. Final Report on MILE Current Meter
Analysis (Rubenstein and Newman)   March   1982

IV. PROJECT 502--Review of Turbulence

1. Work Just Beginning (Kirwan)

NEAR-INERTIAL SHEAR:
DYNAMIC AND STATISTICAL MODELING

David M. Rubenstein
Fred C. Newman
Science Applications, Inc.
1710 Goodridge Drive
P.O. Box 1303
McLean, Virginia 22102

Abstract

Work described here has concentrated on the description of vertical shear, particularly near inertial frequencies. A linearized dynamic model was developed to examine shear caused by internal wave response to wind forcing. A statistical model has been investigated to relate mean square shear to Väisälä frequency and to the vertical separation used for the calculations. The successful comparison with current meter data enables vertical scales of shear in the seasonal thermocline to be obtained. A statistical approach is also being used to describe the probability distribution of shear. Comparisons of the dynamic model have been made to current meter data from Site D. Additional comparisons and eddy diffusivity adjustments will be based on Site D and MILE current meter data.

BACKGROUND

The importance of vertical shear, defined as the vertical derivative of horizontal velocity, to Navy programs has been described in a number of documents. Recent focus has been on shear over a vertical spatial scale range of one meter to a few tens of meters, and a time scale of order one inertial period. A significant portion of the total shear in the thermocline is in the near-inertial frequency range. Clockwise rotary frequency spectra of shear, illustrated in Figure 1, show sharp peaks at the inertial frequency.

APPROACH

Two approaches have been taken to study near-inertial shear. The first approach was deterministic, in which a dynamic model of internal wave response to wind forcing was derived. The second approach was statistical, in which an empirical prediction of S^2 as a function of N^2 and vertical separation Δz was constructed.

The dynamic model is based on the three-dimensional equations of motion, with Boussinesq and hydrostatic approximations, in a constant f-plane. The x-coordinate is in the direction of propagation of the wind stress field. Induced motions are assumed to be weak, such that $U \ll f/k$, where U is a horizontal velocity scale of the internal wave field, and k is a horizontal wavenumber scale of the wind field. The equations are linear and assumed to be homogeneous in the y-direction. A Fourier transform of the equations is performed in the x-direction. Vertical dependence is expressed as a Tchebyshev polynomial expansion since convergence properties in a non-periodic domain, especially in the surface boundary layer, are much better than those of a Fourier expansion, and the equations are stepped forward in time numerically. The wind stress field, generally of the form $\tau(x,t)$, is applied as a forcing mechanism at the upper boundary. Eddy diffusivity and Väisälä frequency profiles are projected onto Tchebyshev expansions, and serve to simulate dissipation and stratification.

A number of validations were performed against numerical solutions, including forcing stress functions applied to an unstratified fluid, as shown in Figure 2. The open circles include a v-component drift. This drift has been subtracted out to obtain the closed circles. Also, an impulsive stress was applied to a uniformly stratified fluid, as shown in Figure 3. In this case the numerical results, in agreement with the analytic solution, show that the response of vertical velocity to an impulsive wind stress evolves in vertical modes, with the first two modes becoming strongest. The response along a dispersion curve increases with frequency.

Shear response from the model results was compared to the gain function computed from current meter data at Woods Hole Site D, using more realistic profiles of Väisälä frequency and eddy diffusivity. The results, shown in Figure 4, show qualitative agreement; for better quantitative agreement, it is necessary to fine tune the shape of the eddy diffusivity profile.

The second approach has essentially been the development of a statistical model of mean square shear, S^2. An idealized version of the composite shear spectrum of Gargett et al. (Journal of Oceanography, v. 11, pp 1258-1271, 1981.) was assumed and was used to derive an expression of S^2 as a function of N^2 and vertical separation Δz. For large Δz S^2 asymptotically becomes proportional to $N^2/\Delta z$. Results from this model are compared to values of S^2 calculated from the MILE data set and are in good agreement, as shown in Figure 5.

In general $\overline{S^2}$ is proportional to $\overline{N^2}$, but within the seasonal thermocline both quantities rapidly vary with depth so that vertical shear profilers cannot measure statistically reliable spectra in the seasonal thermocline. However, the statistical model allows the shear spectra obtained from deep vertical profiles to be related to current meter-derived $\overline{S^2}$ as a function of N^2 and Δz. Thus the range of validity of the Gargett et al. composite spectrum can be extended into the seasonal thermocline.

This statistical approach also allows the description of the probability distribution of shear. In the short term, probability distributions of shear components $\Delta u/\Delta z$ and $\Delta v/\Delta z$ are dominated by the bimodal distribution associated with inertial oscillations. The amplitude of inertially oscillating shear varies in time so that in the long term, over several inertial periods, the bimodal distributions tend to smear out and approach a Gaussian distribution, as illustrated in Figure 6. Using the model for S^2 described above, the variance of the individual shear components was estimated and used to parameterize a Gaussian distribution which agrees well, based on the Kolmogorov goodness-of-fit test, with 19-day observations of shear distribtution.

FUTURE WORK

The shape of the eddy diffusivity profile will be fine-tuned on the basis of gain computed from the Site D data, and the results compared with the gain computed from the MILE current meters. This should provide an estimate of the universality of the eddy diffusivity. More realistic wind stress fields will also be used and it should be possible to incorporate a bottom boundary with a radiative rather than a reflective boundary condition, in order to better model a deep ocean. The dissipation of inertial oscillations in the mixed layer through the generation and propagation of low frequency internal waves into the thermocline will be studied.

Eddy diffusivity in the model represents a statistically averaged value, although in reality dissipation is strongly dependent on Richardson number. A nonlinear model of dissipation may yield a better understanding of the interaction between the wind-forced

wave field and the background "global" internal wave field. By incorporating stochastic bottom boundary forcing with statistics comparable to the Garrett and Munk "universal" spectral model, the development of a saturated wave field and interactions with fluctuating wind-induced motions could be investigated.
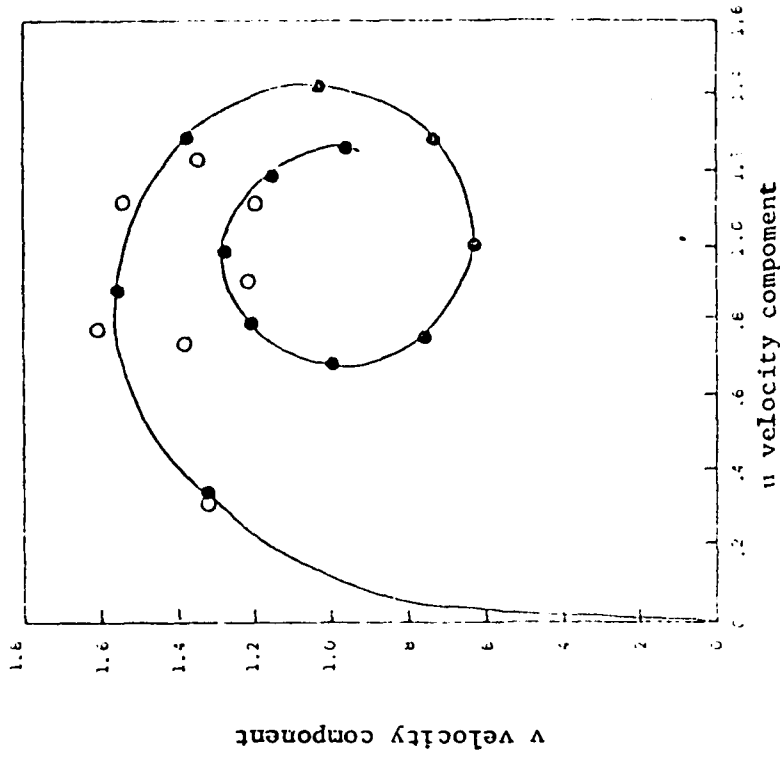
FIGURE 2. COMPARISON BETWEEN ANALYTIC (SOLID CURVE) AND NUMERICAL (CIRCLES) SOLUTIONS. THE TOTAL SURFACE CURRENT (OPEN CIRCLES) BEGINS TO DIVERGE FROM THE ANALYTIC SOLUTION AFTER ABOUT 1/2 INERTIAL PERIOD. THE SURFACE CURRENT MINUS THE BOTTOM (DRIFT) CURRENT (SOLID CIRCLES) AGREES EXACTLY WITH THE ANALYTICAL SOLUTION. THE V VELOCITY COMPONENT IS IN THE DIRECTION OF WIND STRESS PROPAGATION.
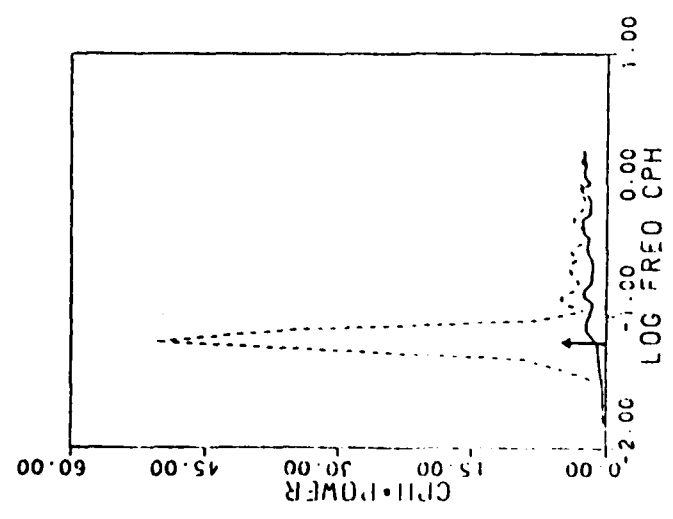
FIGURE 1. VELOCITY SHEAR ROTARY SPECTRA. CLOCKWISE SPECTRUM IS SHOWN BY DASHED LINE, COUNTERCLOCKWISE SPECTRUM BY SOLID LINE. NOTE THE SHARP PEAK AT THE INERTIAL FREQUENCY, INDICATED BY THE ARROW, IN THE CLOCKWISE SPECTRUM.

FIGURE 4. COMPARISON BETWEEN OBSERVED (SOLID LINE) AND MODELED (DASHED LINE) GAIN FUNCTIONS BETWEEN 12 AND 32 METERS. GAIN IS DEFINED AS THE AMPLITUDE OF THE RATIO OF THE CROSS-SPECTRUM OF WIND-STRESS AND SHEAR TO THE AUTO-SPECTRUM OF WIND STRESS. EDDY DIFFUSIVITY PROFILE FOR CASE B HAS THE SAME SHAPE BUT TWICE THE MAGNITUDE OF CASE A.

FIGURE 3. RELATIVE AMPLITUDE RESONSE, AT 18 m BELOW THE SURFACE, OF w^* VELOCITY COMPONENT TO AN IMPULSIVE FORCING FUNCTION FOR UNIFORM STRATIFICATION AND EDDY DIFFUSIVITY PROFILES. CHANNEL DEPTH IS 100 m. DASHED CURVES SHOW THE DISPERSION RELATIONS FOR THE LOWEST THREE VERTICAL MODES.

67

FIGURE 6. PROBABILITY DISTRIBUTION OF NORMALIZED HORIZONTAL SHEAR $\Delta u / \Delta z$. OBSERVED DISTRIBUTION SHOWS BIMODAL CHARACTERISTICS ASSOCIATED WITH INERTIAL OSCILLATIONS. OVER SEVERAL INERTIAL PERIODS THE OBSERVED DISTRIBUTIONS WILL TEND TO APPROACH THE THEORETICAL GAUSSIAN DISTRIBUTION.

FIGURE 5. COMPARISON OF MODEL CALCULATIONS OF MEAN SQUARE SHEAR S^2 TO OBSERVATIONS FROM THE MILE DATA SET.

FINE STRUCTURE NEAR A FRONT: DATA ANALYSIS

C.M. Gordon
Physical Oceanography Branch
Naval Research Laboratory
Washington, D.C. 20375
(Presented by R. Mied)

Abstract

Time series of Lagrangian drogue and CTD observations have been made near an ocean front. These data are being analyzed to characterize hydrographic fine structure, to investigate its space-time evolution, and to distinguish front-related intrusive features in the fine structure. Flow in a major intrusive feature near the front differs from flow above and below the feature.

MEASUREMENTS

During the period of October 5-8, 1979, NRL Code 4340 conducted a series of XBT, CTD and Lagrangian drogue measurements at a location approximately 80 miles west of Bermuda ($32^{\circ}00'N$; $65^{\circ}40'W$). The XBT survey at the site indicated the presence of an ocean front, characterized by a $1^{\circ}C$ change in mixed-layer temperature. Figure 1 shows the location of the experiment and the mixed layer temperatures. The dashed line indicates the location of the front. Preliminary CTD profiles, as shown in Figure 2, indicate salinity reversals suggestive of intrusions or interleavings often associated with frontal systems. An experiment was carried out to obtain information on the current flow and space-time evolution of the T-S fine structure in the neighborhood of the front.

The vertical distribution of current was measured by following six drogues deployed at depths of 6, 21, 52, 95, 139 and 257 m. The drogues were tracked for approximately one day and sequentially located using LORAN-C. Figure 3 is a plot of drogue sightings and probable trajectories. Current speeds ranged from about 30 cm/sec in the mixed layer to about 10 cm/sec below 139 m. At this site the mixed layer moved as a slab in a way consistent with a wind-driven drift current. The flow below 95 m was fairly uniform. The most striking result of the measurements was that flow in the major intrusive feature was quite different from flow in the water masses above and below it. That is, the direction of drogue #4 was opposite to that of the other drogues during a considerable part of its trajectory. Figure 4 shows drogue separation as a function of time for several drogue pairs. Current shears in the depth intervals between drogues varied from 1.4×10^{-4} to 8.5×10^{-3} sec^{-1} and for the most part were attributable to changes in current direction rather than current speed. Currents at 6, 52 and 139 meters were monitored less frequently during the time series of CTD profiles.

Eighty-five CTD casts between the surface and 300 m depth were obtained over a period of 62 hours. Because of the vertical current shear there is some space-time ambiguity in interpretation of the time series of CTD profiles. In order to minimize this difficulty the ship position was maintained between the drogues at 52 and 139 m during most of the measurements. The CTD data treatment thus far has concentrated on reduction of the data volume by averaging over appropriate depth intervals, computation of normalized vertical gradients of T and S, and evaluation of the magnitude and period of vertical ship motion and its effect on the apparent T and S gradients.

FUTURE WORK

Future planned data processing includes estimating internal wave amplitudes from vertical excursions of isotherms and characterizing the temporal evolution of specific features in the fine structure in order to separate structure associated with water mass mixing from internal wave related effects.
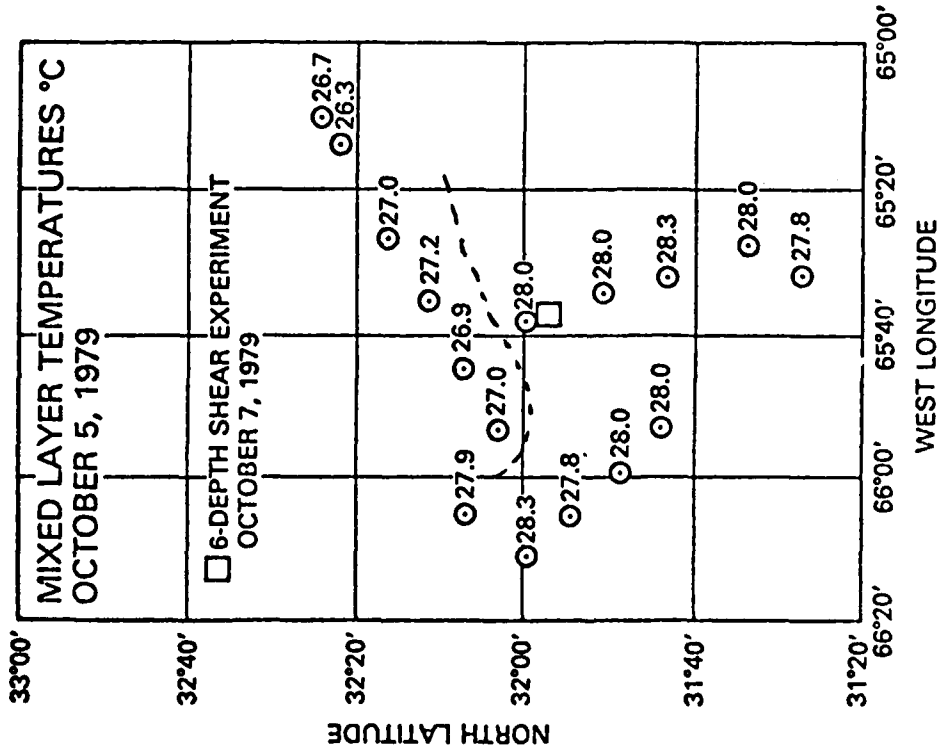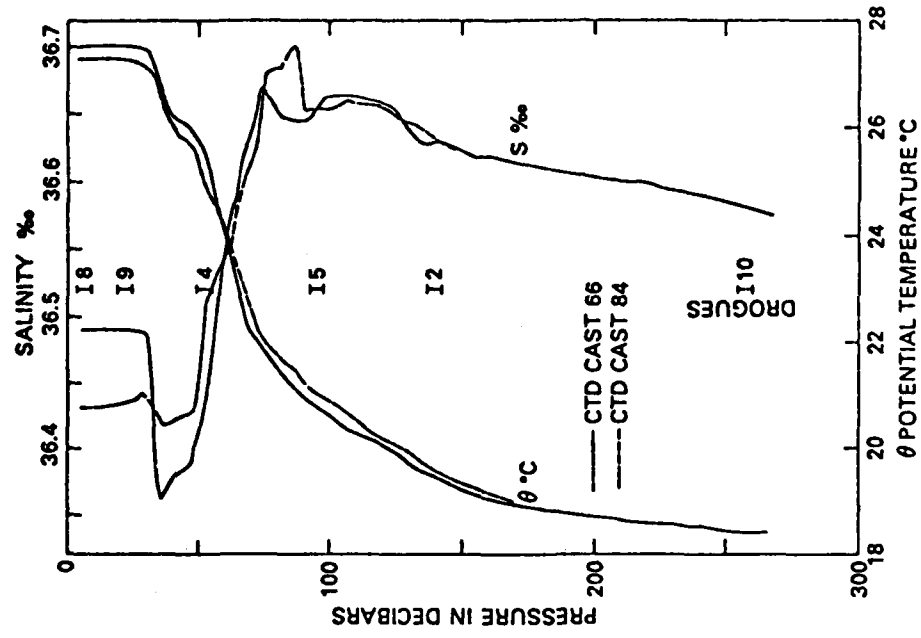
FIGURE 2. PRELIMINARY CTD PROFILES. THE SALINITY REVERSAL SHOWN IN THESE PROFILES SUGGESTS THE PRESENCE OF A FRONTAL SYSTEM.
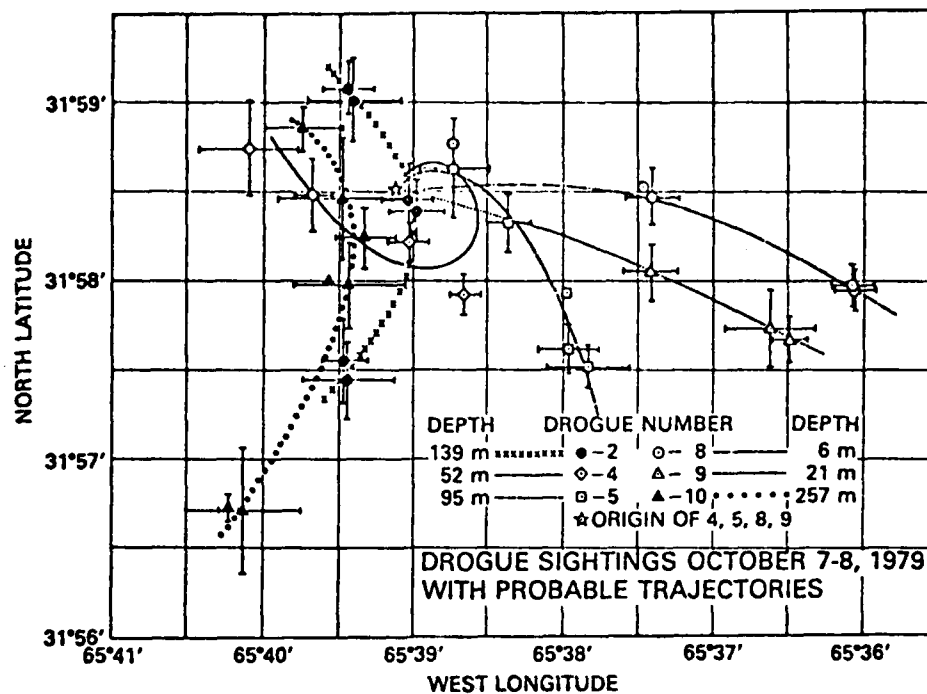

FIGURE 1. LOCATION OF THE EXPERIMENT. DASHED LINE INDICATES POSTION OF THE FRONT. CIRCLES INDICATE XBT DROPS. MIXED LAYER TEMPERATURE AT XBT SITES IS ALSO GIVEN.

FIGURE 3. DROGUE SIGHTINGS AND PROBABLE TRAJECTORIES DURING THE SHEAR EXPERIMENT.
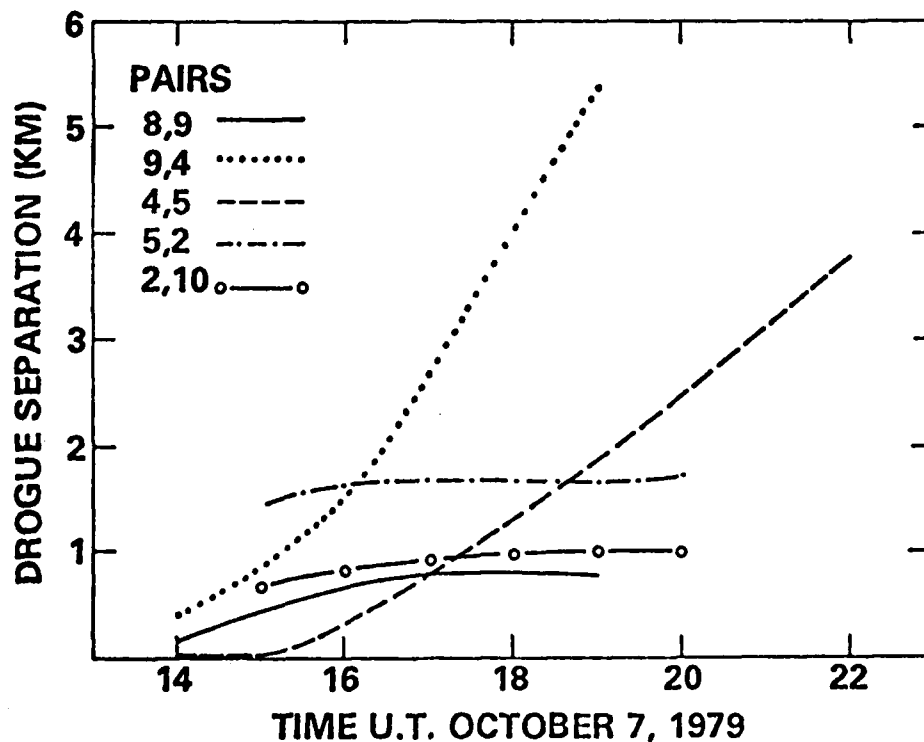
FIGURE 4. DROGUE SEPARATION AS A FUNCTION OF TIME. THE SLOPES OF THESE CURVES GIVE CURRENT SHEAR.

THE CORRELATION BETWEEN TEMPERATURE FINE STRUCTURE
AND MESOSCALE SHEAR

Richard P. Mied
Naval Research Laboratory
Washington, D. C. 20375

Abstract

The goal of the work described here is to measure, understand, and quantitatively model the correlation of vertical mesoscale shear with dropped temperature fine structure variance. The June 1979 USNS LYNCH XBT data set for the FREDDEX eddy was examined. Mesoscale shear in each of two "synoptic" eddy views was calculated and examined for correlation with the variance of the dropped spectrum of temperature fine structure. In view of the large number (382 and 177 for the two eddy views, respectively) of drops, the two correlation coefficients of order -0.3 are deemed significant, indicating a weak decrease of variance with increasing vertical shear.

BACKGROUND

Oceanic temperature fluctuations with vertical length scales of tens of meters to kilometers and time scales of minutes to hours are investigated. In the most general sense, fine structure is believed to be a manifestation of internal waves and lateral intrusions. A vertical length scale range from 1 m to 100 m is of most interest in this context. Although the intensity of the dropped internal wave displacement spectrum varies with the stability frequency, it is difficult to generalize for lateral intrusions. Moreover, the variation of the level of fluctuation of the fine structure is unknown in space and time.

APPROACH

The June 1979 LYNCH cruise was conducted in the Sargasso Sea to densely sample a Gulf Stream ring, the FREDDEX eddy, by traversing it many times in many directions. A collection of these traverses forms one of two snapshots of the eddy. Figure 1 shows the first such snapshot. The LYNCH data set was analyzed for vertical mesoscale shear and dropped temperature fine structure variance. The shear was estimated from the thermal wind equation, using historical T-S data for the area to obtain density. The variance was calculated by detrending the data after fitting a cubic equation in depth to the temperature profile, calculating the fast Fourier transform, and summing for the variance in the 1 m to 100 m wavelength range.

RESULTS

A linear regression of the variance upon the current shear, from the second synoptic picture shown in Figure 2, yields a correlation coefficient of -0.3 for 177 XBT drops. The data are quite scattered but indicate a weak tendency for fine structure variance to decrease with increasing vertical shear. The scatter probably arises from three sources: 1. Only mesoscale shear was examined and shear due to inertial waves was disregarded. 2. The calculation of shear was made from the thermal wind equation, rather than from the more accurate gradient wind equation. 3. XBT drops close in space but separated in time by three days differ, indicating that the data from which the shear is calculated may not be as synoptic as desired for these calculations.
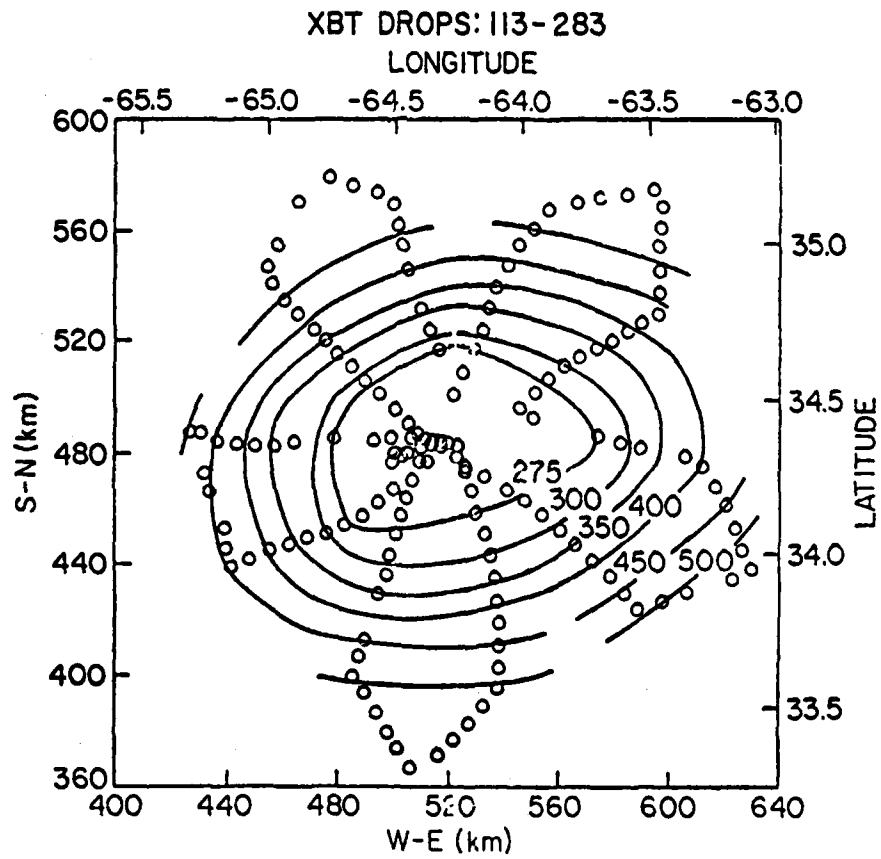
FIGURE 1. CONTOURS OF CONSTANT DEPTH (m) OF THE 15° ISOTHERMAL SURFACE FOR THE FIRST SYNOPTIC VIEW. OPEN CIRCLES INDICATE THE POSTIONS OF XBT DROPS.
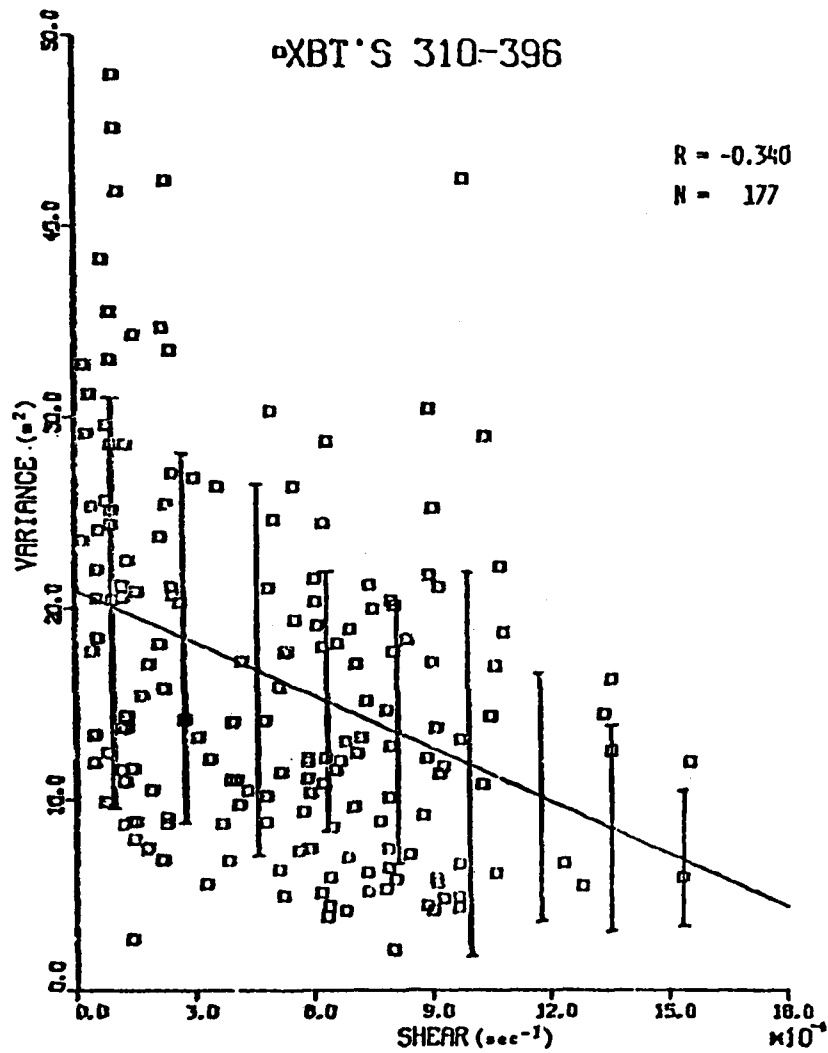
FIGURE 2. A LINEAR REGRESSION OF THE SCALED FINE STRUCTURE TEMPERATURE VARIANCE ($N \langle T'^2 \rangle /(d\overline{T}^2/dz)^2$) UPON THE SHEAR FOR THE SECOND EDDY SNAPSHOT INDICATES A WEAK DECREASE IN THE VARIANCE AS THE VERTICAL SHEAR IS INCREASED. THE ERROR BARS SHOW THE STANDARD DEVIATION OF THE DATA ABOUT THE FITTED LINE.

SIGNAL PROCESSING FOR COMPUTING SALINITY

John Ehrenberg
University of Washington
Seattle, Washington 98105

Abstract

Sensor responses introduce errors into calculations of salinity from temperature and conductivity measurements. These errors depend on the particular sensors used, the drop speed of the instrument, and the relative alignment of a pair of temperature and conductivity sensors. Digital filtering techniques for equalizing temperature and conductivity sensor outputs are being invesitgated.

BACKGROUND

The relationship between salinity, conductivity, and temperature is nonlinear, although in practice the relative changes in conductivity and temperature are small enough to allow the following linearized equation to be used for calculating salinity:

$$\Delta S(d) = \frac{\partial S}{\partial T} \Delta T(d) + \frac{\partial S}{\partial C} \Delta C(d) \tag{1}$$

where $\Delta S(d)$, $\Delta T(d)$ and $\Delta C(d)$ are the relative changes in salinity, temperature and conductivity, respectively. For typical ocean conditions,

$$\frac{\partial S}{\partial T} \approx - 10 \frac{\partial S}{\partial C} \tag{2}$$

which indicates the importance of temperature effects.

EFFECTS OF SENSOR RESPONSE ON MEASUREMENTS

It would be easy to measure S(d) using Equation (1) if $\Delta T(d)$ and $\Delta C(d)$ could be measured exactly. However, what is actually measured are temperature and conductivity as modified by the response of the sensors, so it is necessary to know the sensor response in order to determine what salinity value has actually been measured. Measurements of the transfer function of thermistors have been made using a plume tank, and the frequency of Neil Brown conductivity cells has been measured using a stratified tank constructed at the Applied Physics Laboratory of the Universtiy of Washington. Preliminary results show the following features of the frequency response curves for the sensors:

1) The temperature sensor response is not the same as that of the conductivity cell at any drop speed.

2) Both the individual response and the relative response of the sensors are speed dependent. At low drop speeds the thermistor has the highest cutoff frequency, whereas at high speeds the opposite is true.

3) The measured conductivity amplitude response contains nulls and is very noisy at

wavenumbers beyond the first null.

4)   The measured phase response is very sensitive to sensor alignment. As a result there will be some uncertainty in the measured phase response of both the conductivity and temperature sensors.

Differences in the responses of the two sensors can in some cases produce an incorrect salinity record when the measured temperature and conductivity are used in Equation (1), as was illustrated by the results of a simulation. The temperature sensor and conductivity cell were modeled by transfer functions that closely matched the preliminary sensor responses obtained using the plume tank and stratified tank. The input temperature signals used for the study were diffused steps with an adjustable step width. A typical input pulse is shown in Figure 1. The resulting computed salinity and density for a 1 m/s drop speed are shown in Figure 2. The responses of the sensors were most closely matched for this drop speed. These curves were obtained by adjusting the relative spatial location of the two sensors to produce a minimum spike in the computed salinity. The effect of a sensor misalignment is shown in Figure 3. These results are again for a 1 m/s drop speed. However, in this case, the relative locations of the sensors have been shifted by 1.5 cm. These results show that even when the amplitude responses nearly agree, phase shifts caused by displacement of one of the sensors can produce spiking in the computed salinity and density. The computed salinity for aligned and misaligned sensors at 0.2 m/s drop speed are shown in Figures 4 and 5, respectively. For this drop speed the amplitude responses of the two sensors differ considerably and there is spiking in the computed salinity for both aligned and misaligned sensors.

MODIFICATION OF SENSOR RESPONSES

In order to minimize the problem of conductivity and temperature sensor mismatch, one or both of the sensor frequency responses must be modified. The response of the temperature sensor and that of the conductivity cell need to be deconvolved (removed) from the measured temperature and conductivity sensor outputs. That is, if $x(t)$ is the sensor output with Fourier transorm $X(f)$, and $H(f)$ is the sensor transfer function, then the deconvolved output, $y(t)$, is given by

$$y(t) = F^{-1}\left(X(f) \, H^{-1}(f)\right) = F^{-1}\left(\frac{X(f) \, H^{*}(f)}{|H(f)|^{2}}\right) \tag{3}$$

where F^{-1} is the inverse Fourier transform operator. The deconvolution filter greatly enhances the low amplitude noisy portion of the spectrum of $X(t)$. Performing the operations in Equation (3) for real data will result in a $y(t)$ that is completely dominated by noise. For this reason, it would not be practical to try to flatten the response of the conductivity cell for wavenumbers near or beyond the location of the first null in the response.

Another possibility for equalizing the responses of the two sensors is to low pass filter the output of each sensor with a filter that has a corner frequency below those of either sensor. While this method will produce a matching frequency response for the two filtered sensors, it has some undesirable side effects. First, the filter corner frequency may have to be chosen so low that it will remove much of the higher frequency content in the temperature, conductivity and salinity records that may be of interest. Furthermore,

78

the low pass filter can in itself produce some undesirable outputs. When a signal with considerable high frequency energy is put into a low-pass filter, the low-pass filter output will "ring." The magnitude and characteristics of the ringing will depend on both the input signal and the filter. This effect is illustrated in Figures 6 and 7 which show the outputs of ideal (rectangular response) low-pass filters to an input step 5 cm wide.

Another problem that further complicates the deconvolution operation is that the sensor output signal level, and therefore the signal-to-noise ratio, can change by orders of magnitude in a single record. The processing method must therefore be designed for the worst case signal-to-noise ratio or adapt to changing signal and/or noise levels.

SUMMARY

Potential problems that may be encountered in computing salinity and density from temperature and conductivity sensor outputs and approaches to dealing with these problems have been identified and are listed below.

Potential Problems:

1. Inverse filter enhances high frequency noise (Maximum frequency of equalized response will depend on signal-to-noise ratio).

2. Temperature and conductivity response change with speed.

3. High frequency roll-off of equalizing filter can cause ringing in filter output. This will result in errors in the computed T-S diagrams and in the calculation of N^2.

Approaches to Potential Problems:

1. Continue simulation of typical and worst case situations to determine magnitude of the problem and sensitivity to response mismatches, phase and alignment uncertainties and high frequency roll-off characteristics of filters.

2. Design equalization filters for fixed speed and fixed signal-to-noise ratios.

3. Develop methods for modifying filters for varying drop speeds and signal-to-noise ratios.

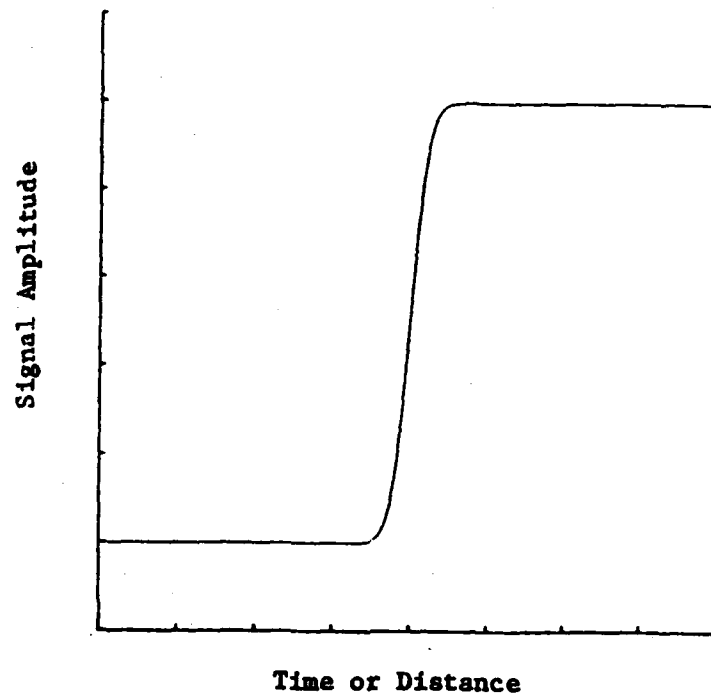4. Test filtering procedures on actual data.

FIGURE 1. TYPICAL TEMPERATURE AND CONDUCTIVITY INPUT SIGNAL FOR SIMULATION STUDY. THIS INPUT PULSE WAS USED FOR RESULTS SHOWN IN FIGURES 2-5.
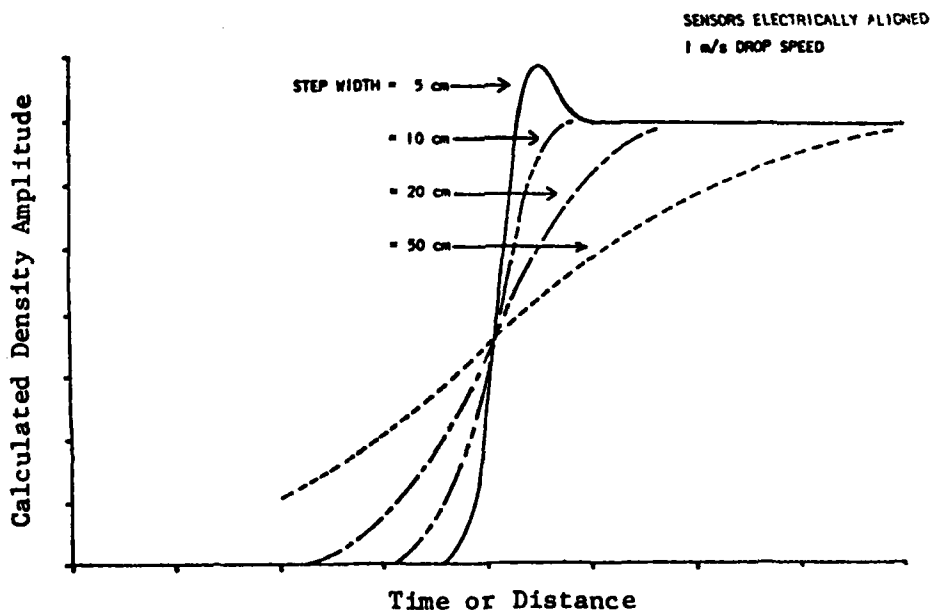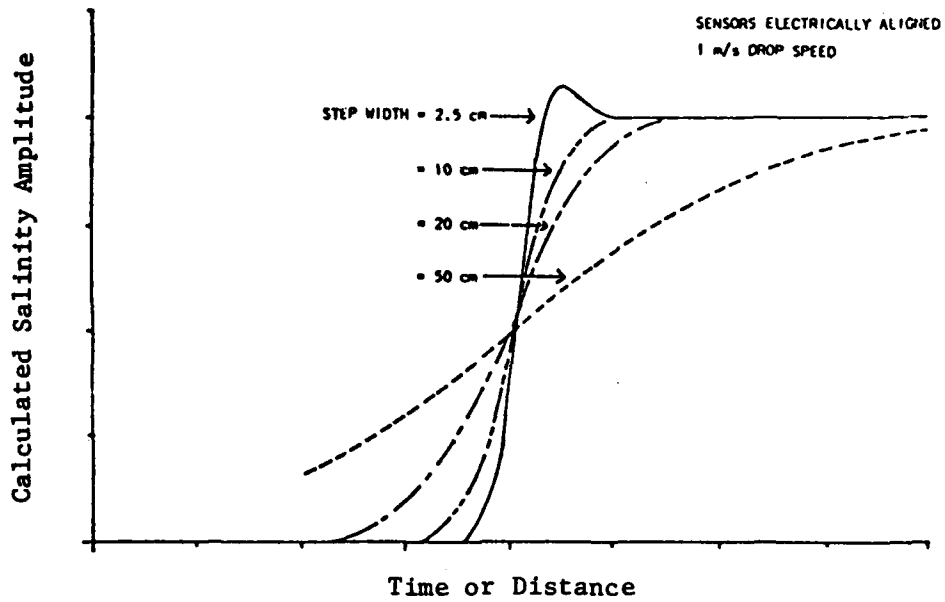
FIGURE 2. CALCULATED SALINITY (TOP) AND DENSITY (BOTTOM) FOR 1 m/sec DROP SPEED WITH SENSORS ALIGNED.
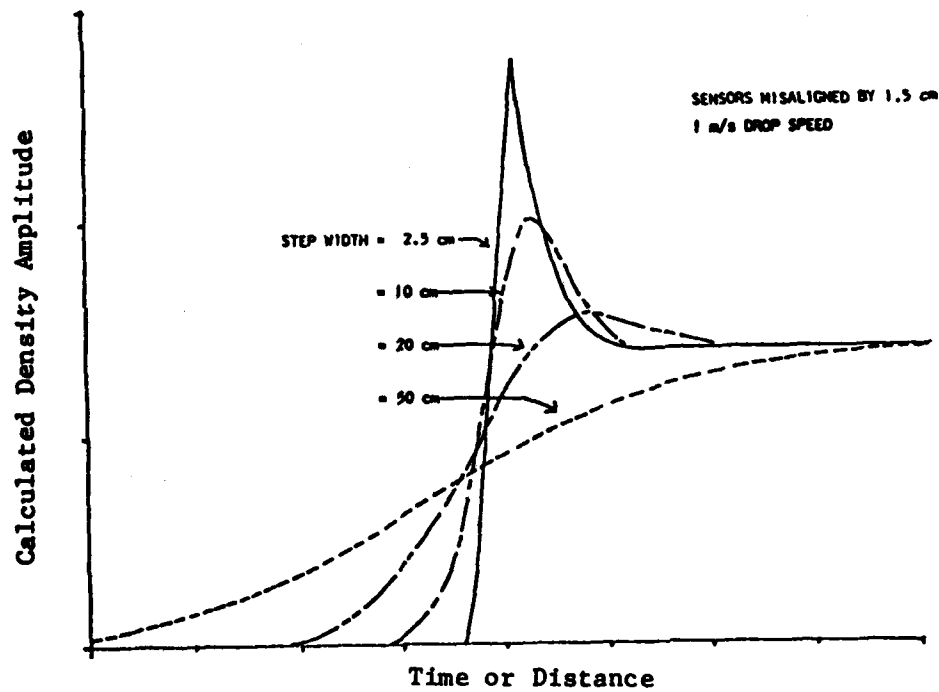
81

Top figure labels: SENSORS MISALIGNED BY 1.5 cm / 1 m/s DROP SPEED; STEP WIDTH = 5 cm, = 10 cm, = 20 cm, = 50 cm; Y-axis: Calculated Salinity Amplitude; X-axis: Time or Distance

Bottom figure labels: SENSORS MISALIGNED BY 1.5 cm / 1 m/s DROP SPEED; STEP WIDTH = 2.5 cm, = 10 cm, = 20 cm, = 50 cm; Y-axis: Calculated Density Amplitude; X-axis: Time or Distance
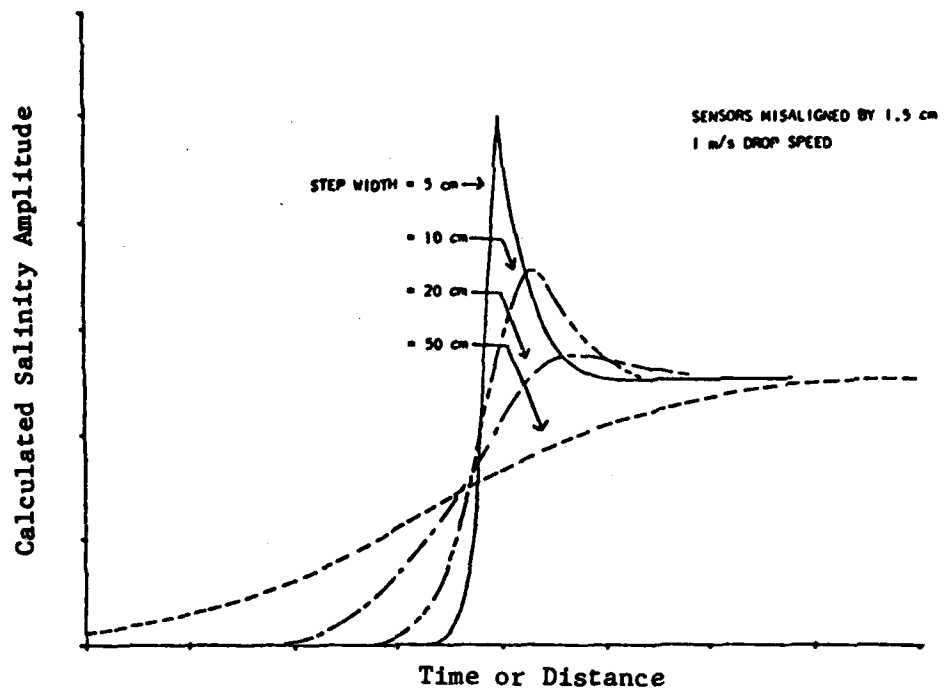
FIGURE 3. CALCULATED SALINITY (TOP) AND DENSITY (BOTTOM) FOR 1 m/sec DROP SPEED WITH SENSORS MISALIGNED BY 1.5 cm.

82
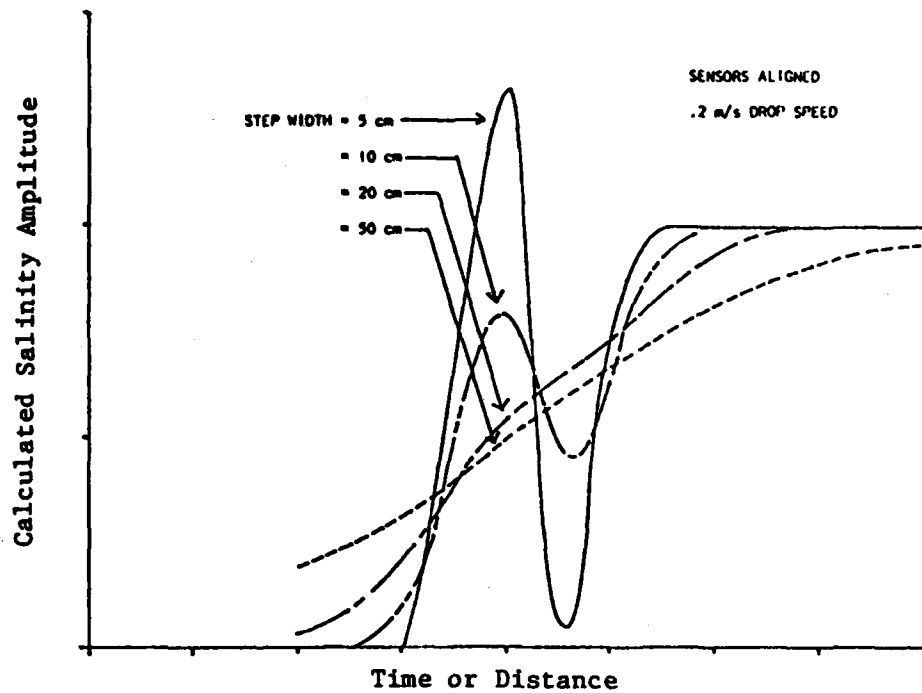
FIGURE 4. CALCULATED SALINITY FOR 0.2 m/sec DROP SPEED WITH SENSORS ALIGNED.
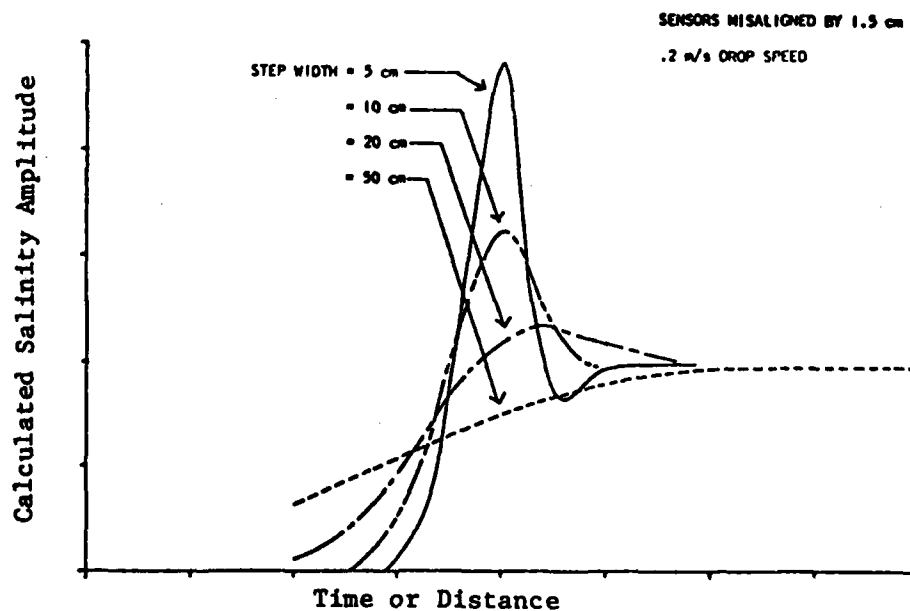
FIGURE 5. CALCULATED SALINITY FOR 0.2 m/sec DROP SPEED WITH SENSORS MISALIGNED BY 1.5 cm.

5 cm STEP WIDTH
1 m/s DROP SPEED
4.5 c/m FILTER CUTOFF
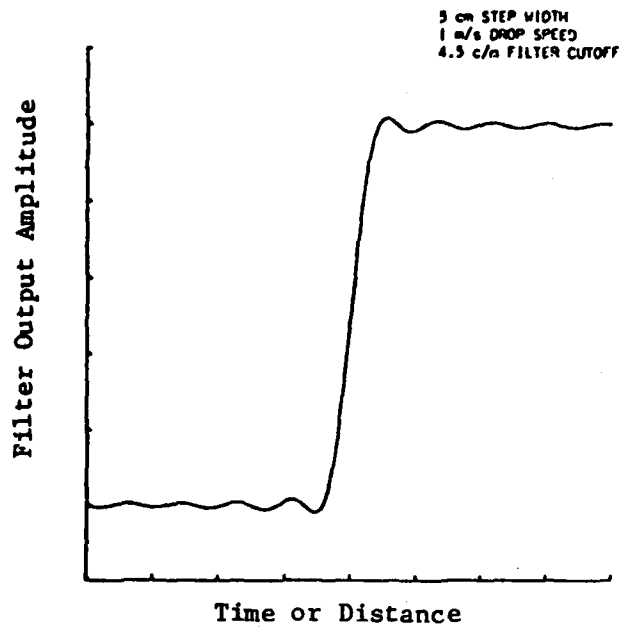
FIGURE 6. OUTPUT OF IDEAL RECTANGULAR RESPONSE LOW PASS FILTER WITH 4.5 c/m FILTER CUTOFF FOR AN INPUT WITH 5 cm STEP WIDTH AND 1 m/sec DROP SPEED. COMPARE TO FIGURE 1 AND NOTE RINGING EFFECT.
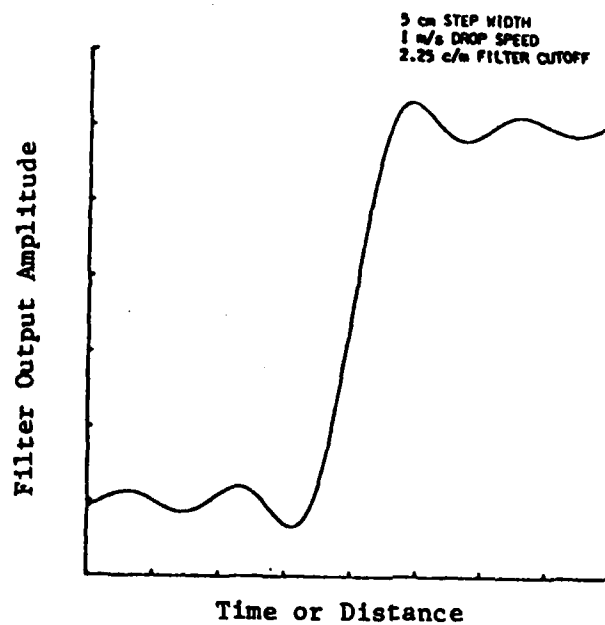

5 cm STEP WIDTH
1 m/s DROP SPEED
2.25 c/m FILTER CUTOFF

FIGURE 7. OUTPUT OF IDEAL RECTANGULAR RESPONSE LOW PASS FILTER WITH 2.25 c/m FILTER CUTOFF FOR AN INPUT WITH 5 cm STEP WIDTH AND 1 m/sec DROP SPEED. COMPARE TO FIGURE 1 AND NOTE RINGING EFFECT.

84

EXPENDABLE DISSIPATION PROFILER

Thomas R. Osborn
Rolf G. Lueck
Department of Oceanography
University of British Columbia
Vancouver, BC, Canada, V6T TW5

Abstract

Development has continued on the expendable dissipation profiler (XDP). The design has been successfully modifed to reduce vibrations associated with dereeling of the wire surface link from the XDP. With a working prototype developed, additional field tests are planned to compare XDP measurements to those made by such systems as the Camel II profiling sensor and by instrumentation on the Dolphin submarine. Data acquisition and logging functions are being combined into one module to ease XDP use, and on-board data processing techniques are being refined. Documentation and demonstration of XDP use will be provided to NAVOCEANO personnel for a North Pacific cruise in late 1982.

INTRODUCTION

Oceanic microstructure is studied in order to understand the role of turbulence in circulation and in the distribution of salt and heat in the oceans. An expendable instrument for measuring microstructure is desirable since it would be readily deployable even during severe weather conditions, profiles could be closely spaced horizontally to produce nearly simultaneous profile sections, instruments could be repeatedly deployed at a given site to produce time series of vertical dissipation profiles, and there would be no recovery problems. Such an expendable dissipation profiling instrument would be a unique tool for oceanographic studies. Vertical profiles of the local rate of turbulence dissipation give a quantitative measure of the local intensity of turbulence. Unlike temperature fluctuations, which are a combined measurement of the large scale temperature structure and the velocity field, velocity dissipation measurements can be directly related to local energetics. Thus the generation, decay, and spreading, as well as the spatial and temporal variation, of turbulence in the ocean can be studied.

INSTRUMENT DESIGN

Engineering sea tests of various prototype models of the expendable dissipation profiler (XDP) have been recently completed with satisfactory results. Several problems encountered in the development of this instrument have been resolved. Contamination of the shear signal by vibrations resulting from dereeling of the wire link was substantially reduced by placing a 1/2 inch thick disc of open cell foam between the tail-piece containing the wire spool and the remainder of the body. However, the subsequent sloppy coupling of the tail piece caused the instrument to wobble at 1 Hz with an unacceptably large amplitude of approximately 20°. Attempts to increase the stiffness of the coupling between the tail piece and the remainder of the body without also increasing the signal contamination caused by the dereeling of the wire failed. The standard Sippican wire spool that unwinds from its outside was replaced with a custom wound spool that unwinds from its inside, thus reducing rattling and torquing action generated as the wire spool unwraps. The spools are nested in foam and placed inside of a second rear mounted 5 inch extender that replaces the tapered tail piece normally found on XBTs. Drag stabilization

is provided by a one-half inch wide 3/8 inch thick band of foam glued around the rear of the extender that contains the spool.

The broad band noise of the XDP is between 10^{-7} to 10^{-6} watts/m^3, which compares favorably with Camel II noise level of 2×10^{-7} w/m^3, the lowest of any instrument in operation. The wobble of the instrument has been reduced to less than 1° at 3 Hz. All analog electronics to support the XDP have been constructed and successfully sea tested. These include the internal electronics of the profiler, the variable gain deck receiver, and the phase-locked loop demodulator. The electronics for digital data recording have been designed but have not yet been constructed or tested.

ONGOING WORK

With the development of a working prototype model of the XDP, ongoing work now entails evaluating, demonstrating, and documenting the capability of this instrument. Scientific evaluation of the instrument involves comparing XDP measurements with those of other turbulence measuring systems such as the Camel II and the Dolphin submarine. During a joint ship experiment with the USS DOLPHIN and the R/V ACANIA scheduled for April 1982 simultaneous horizontal and vertical profiles of turbulence will be measured. Twenty-five XDPs will also be deployed on each of two Warm Core Ring cruises in 1982 for comparison with Camel II measurements. In addition, simultaneous CTD-O_2 and velocity measurements will be made. This will be an opportunity to demonstrate how the XDP measurements can be integrated with other larger scale observations and to evaluate the instrument in direct comparison with other turbulence measurement systems.

Data acquisition and logging functions will be integrated. It is important to make the operation of the XDP system as simple and straightforward as possible in order to encourage acceptance and to reduce lost data. Analog components of the module have been built and tested. This module will facilitate the acquisition of the PM signal from the XDP, will output analog signals of shear and temperature, digitize the data into 14 bits, record/playback the data on a cassette tape recorder, and transmit/receive the data to/from any computer with a RS232 interface. Thus XDPs can be deployed at sea with only this module and any cassette tape recorder. The at-sea digitized data can later be transferred onto 9-track tapes in the laboratory.

Development of data processing techniques will continue through the coming year in order to obtain a technique which can be used at sea with a minimum of operator input. A new sea-going computer system based on a DEC LS1-11/23 computer with all software compatible with 11/34 computers is being installed and will be used to digitize all microstructure data. Processing of XDP data involves removal of approximately 0-5 meters of contaminated data from 450 meter profiles resulting primarily from collisions with plankton, with some contamination from signal drop out. These clean profiles are Fourier transformed and integrated to calculate the mean square shear $(\partial u/\partial z)^2$ from which the rate of kinetic energy dissipation is estimated using the turbulence equation $\epsilon = 7.5 \nu (\partial u/\partial z)^2$, where ν is kinematic viscosity.

FUTURE WORK

The XDP will be used on a NAVOCEANO cruise to the North Pacific in late 1982. Operating procedure and data processing will be demonstrated and some XDP measurements will be incorporated into the NAVOCEANO program. Documentation of the XDP system and its operation will be provided in advance of this cruise.

DATA ANALYSIS AND FIELD PROGRAMS

Thomas B. Sanford
Applied Physics Laboratory
University of Washington
1013 Northeast 40th Street
Seattle, Washington 98195

Abstract

Considerable expendable current profiler (XCP) data have been collected in the Norwegian Sea/Iceland Faroes Ridge area. Preliminary analysis of these data shows seasonal effects on shear and intrusions of water masses in the vicinity of the Polar Front. Because the performance of XCPs in the vicinity of the earth's magnetic equator is uncertain, an intercomparison experiment near the magnetic equator is planned with an independent profiler system, TOPS (Total Ocean Profiling System), that is not dependent on the vertical component of the earth's magnetic field.

TEMPERATURE AND VELOCITY IN THE NORWEGIAN SEA

Figure 1 shows locations of XCP data collected in the Norwegian Sea/Faroes Island area. Analysis of these data indicates seasonal variability in the velocity and shear fields. Data obtained on the October 1980 cruise, shown in Figure 2, exhibit larger values of velocity and shear than were observed in the same general area in May of the following year, shown in Figure 3. This difference is probably an effect of winter cooling and homogenization of the Norwegian Sea. The October observations were obtained while there was still an appreciable vertical temperature and, presumably, buoyancy gradient. The May data, on the other hand, were obtained after considerable winter cooling and mixing and exhibit a much more uniform temperature profile and subdued shear.

Another set of profiles was obtained across the Polar Front just north of the Iceland Faroes ridge. The front is clearly revealed in the velocity profiles. Approaching from the north, the front and the surface mixed layer deepen until the front is crossed and the mixed layer is quite thick. There is a general warming from north to south across the front. In this area a velocity shear of about a knot occurs over a few hundred meters. Slightly farther to the south is the Iceland Faroes ridge, and profiles across it reveal strong flows which seem to be tied to water temperature, as expected. Tongues, or intrusions, of warm water from the North Atlantic penetrate into the Norwegian Sea, while comparable structures of colder Norwegian Sea water overflow into the deep North Atlantic. Temperature and velocity profiles, shown in Figure 4, show evidence of these counterflows. The next stage of analysis is to compute statistics such as spectra and coherence between velocity and temperature and to produce a more comprehensive description of the data.

FUTURE WORK

Velocity profiles in the vicinity of the magnetic equator will be obtained using XCPs. Figure 5 shows the locations of the earth's magnetic poles and equator. This work is being performed in conjunction with Dr. Hayes of the Pacific Marine Environmental Laboratory of NOAA and will be carried out aboard the NOAA ship DISCOVERER. The performance of XCPs in the vicinity of the magnetic equator is uncertain as a result of the XCPs dependence upon the magnitude of the vertical component of the earth's magnetic field, which vanishes at the magnetic equator. Actual observations are needed to verify expectations of instrument performance. Intercomparison with the profiler system

TOPS against nearly simultaneous XCP drops will aid in evaluation of XCP performance. TOPS has a Neil Brown Instrument Systems acoustic current meter, together with an acoustic tracking system using bottom moored transponders. The magnetic equator at 95°W is approximately at 8°S. Observations will be made across a section from 3°N to 8°S, thereby assuring that the magnetic equator is occupied. The mean square velocity differences between these two profilers will be calculated as a measure of the performance of the XCP. The TOPS instrument should continue to function in the vicinity of the magnetic equator since it is dependent only on the horizontal component of the earth's magnetic field, which is used as a compass. From these data the utility or appropriateness of the XCP method in the vicinity of the magnetic equator will be assessed.
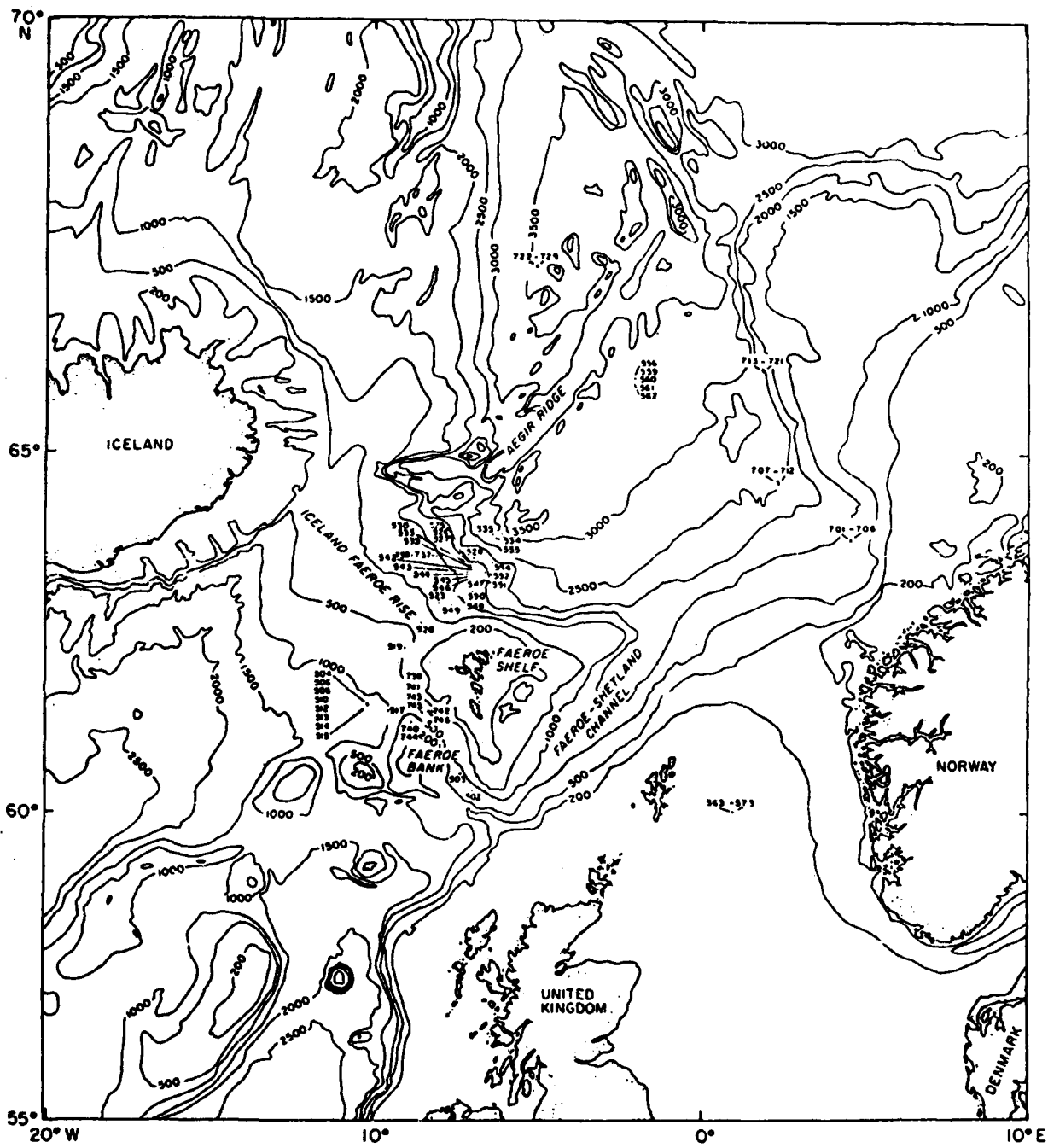
FIGURE 1. LOCATIONS OF XCP DATA COLLECTED IN NORWEGIAN SEA/FAROES ISLAND AREA.

TIME(hrs) (27 OCT 1980)

XTVP T-PROFILES (66°N,2°W)

TIME(hrs) (27 OCT 1980)

UNROTATED XTVP PROFILES (66°N,2°W)
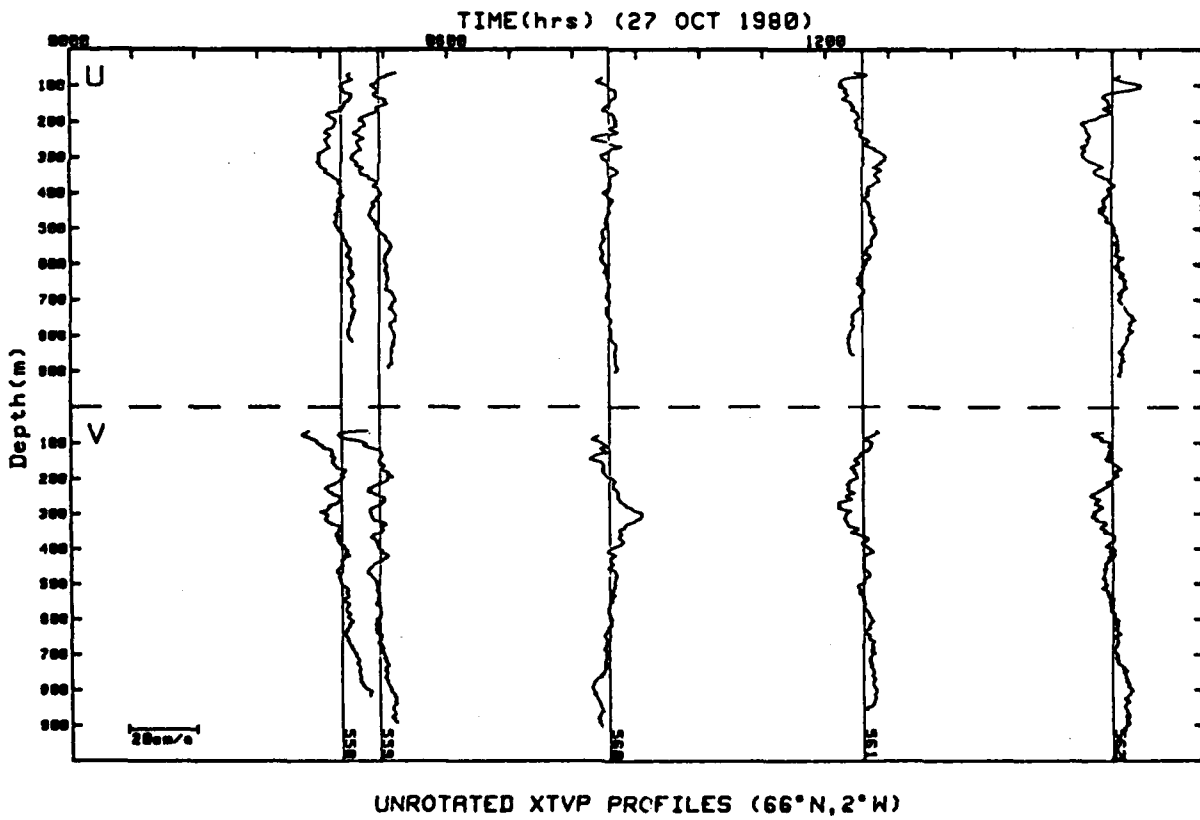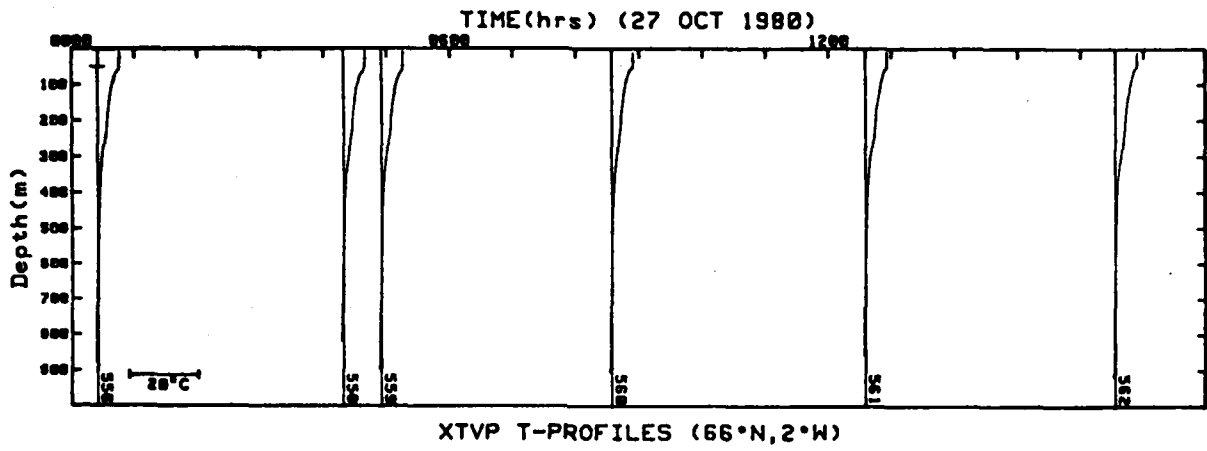
FIGURE 2. XCP (XTVP) DATA COLLECTED IN OCTOBER 1980.

TIME(hrs) (19 MAY 1981)

XTVP T-PROFILES (67°N,5°W)

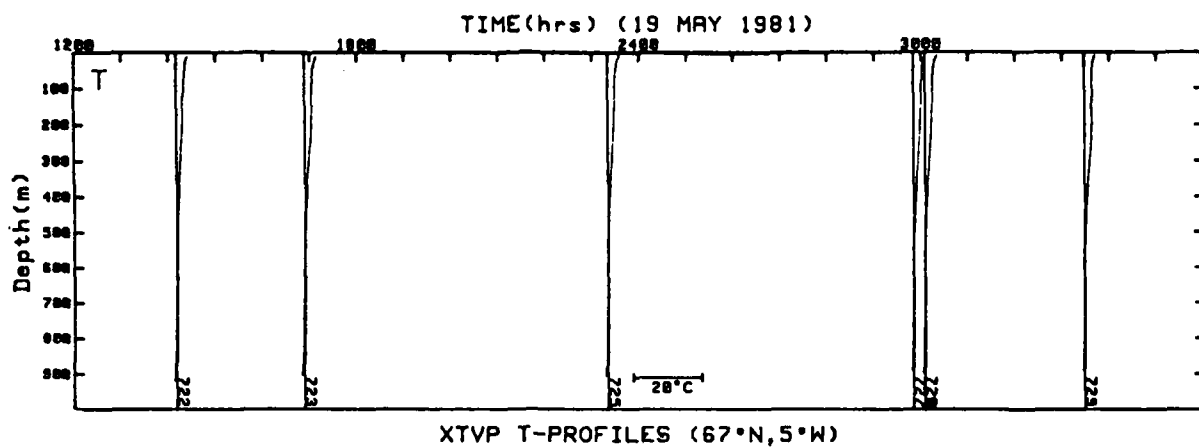TIME(hrs) (19 MAY 1981)

UNROTATED XTVP PROFILES (67°N,5°W)
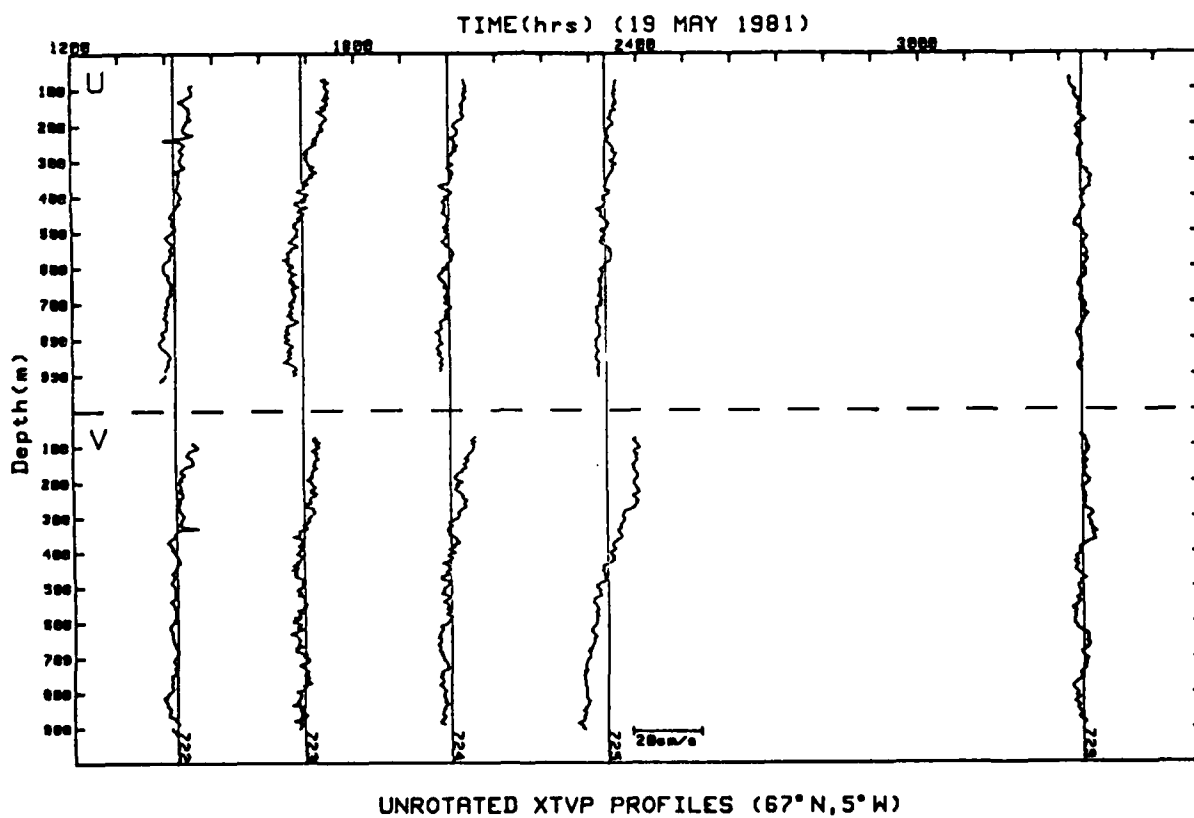
FIGURE 3. XCP (XTVP) DATA COLLECTED IN MAY 1981.

91
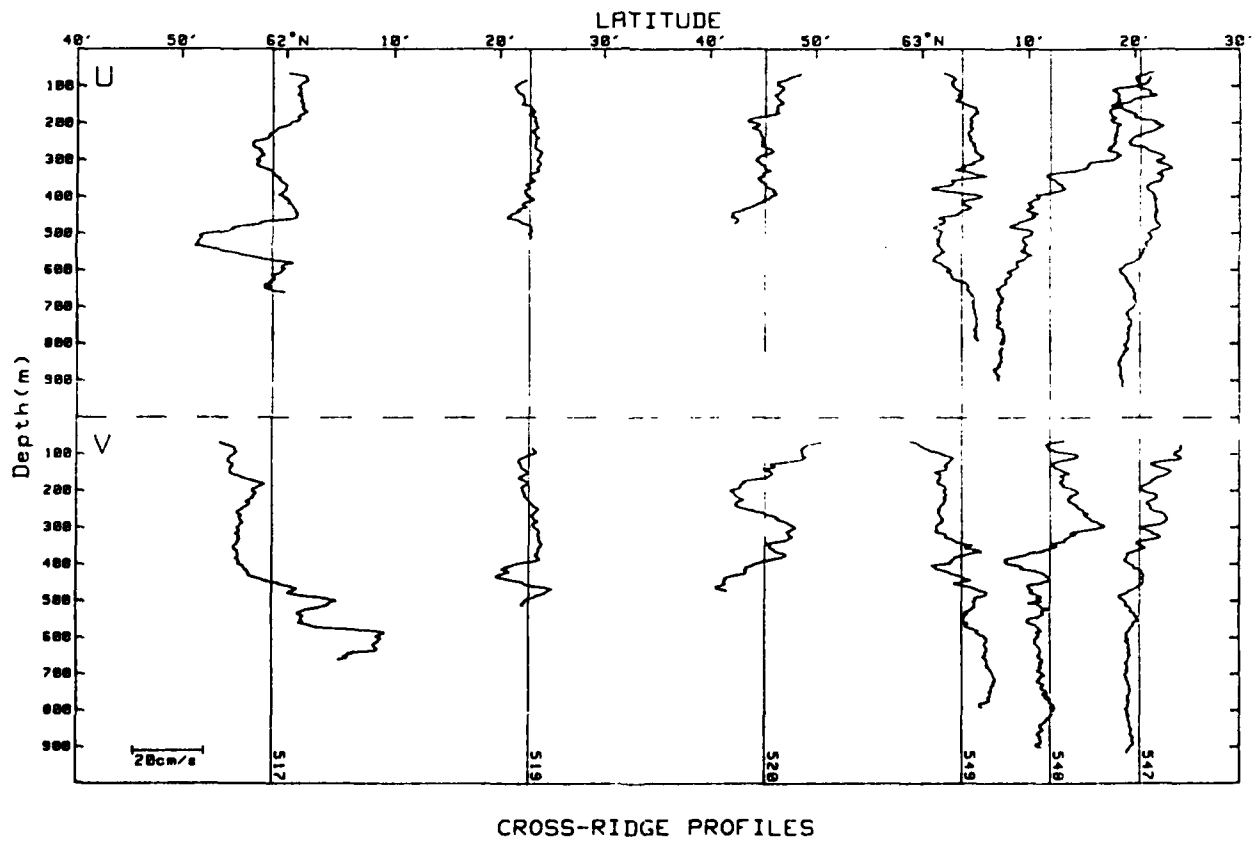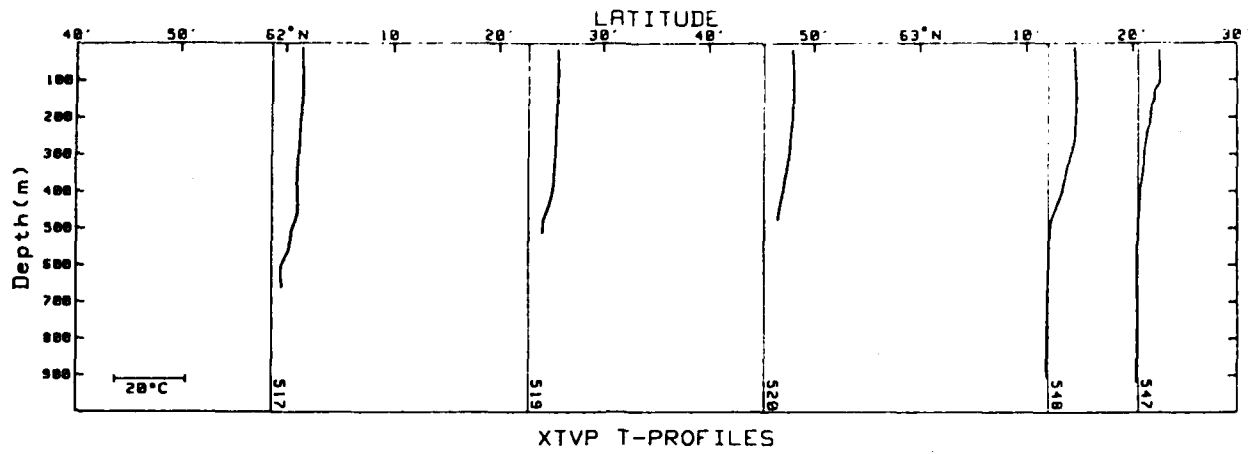
FIGURE 4. TEMPERATURE AND VELOCITY PROFILES ACROSS THE POLAR FRONT.
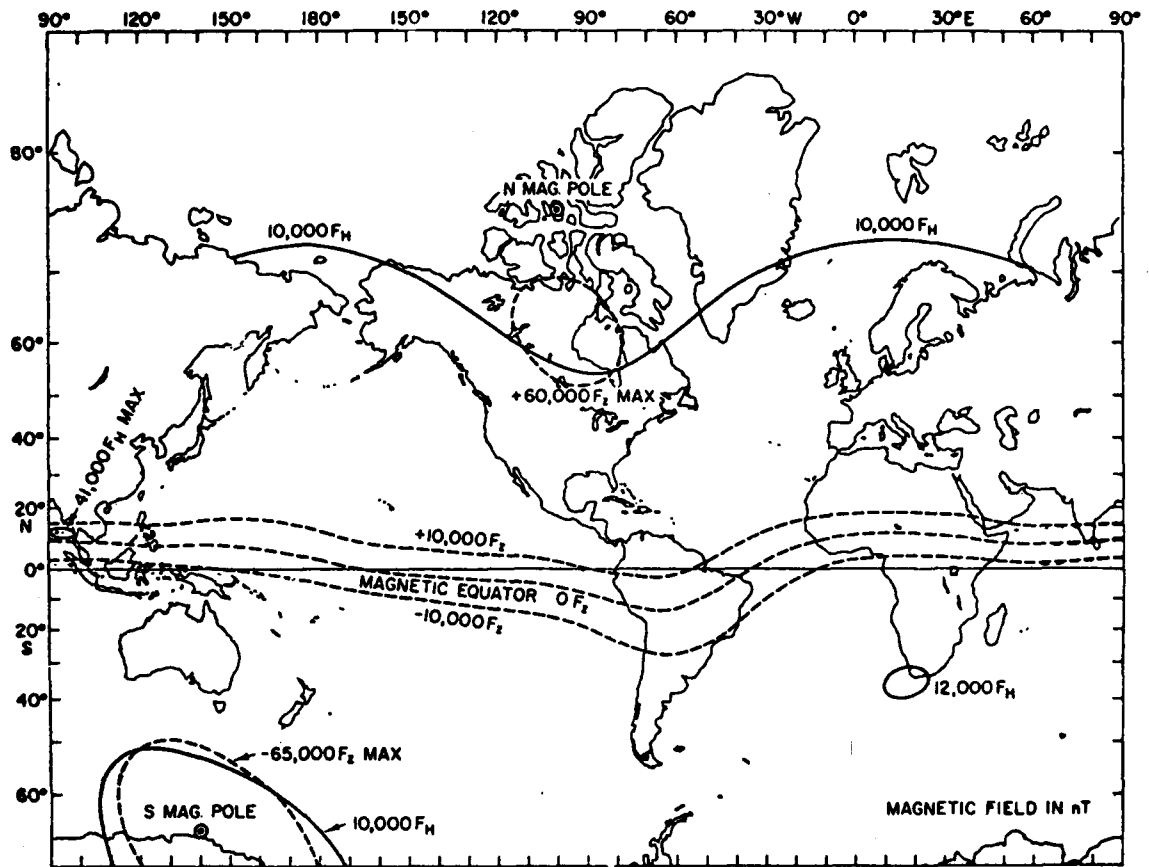
FIGURE 5. LOCATIONS OF EARTH'S MAGNETIC POLES AND EQUATOR.

UPPER OCEAN BACKGROUND PROGRAM

Robert Pinkel
Marine Physical Laboratory
Scripps Institution of Oceanography
University of California
San Diego, California 92152

Abstract

Analysis has continued for data collected with a system of four Doppler sonars from FLIP during May 1980. Representative forms of internal wave frequency-wave number spectra have been investigated and found to deviate in some aspects from the often used Garrett-Munk formulation. Additional work has included estimates of the Doppler sonar accuracy by comparison of two instruments, investigation of acoustic scattering from the turbulent wake of a towed plankton net, and preliminary work on transmitting coded Doppler system data.

BACKGROUND

The Marine Physical Laboratory (MPL) has been investigating small scale upper ocean background by means of a Doppler sonar measurement system used from the research platform FLIP. During 1980 MPL has been involved in analyzing data obtained during a major data collection effort undertaken in May 1980.

RESULTS

Figure 1 is an example of system current measurements to a depth of 700 m over a time period of approximately one week. This figure illustrates the system's capability to continuously monitor upper ocean current variability over extended time periods so that both spatial and temporal analyses can be performed. Additional examples were provided at the last OMP review.

The mean form of the internal wave spectrum has been analyzed. Two significant differences are noted between this estimate of the spectrum and the Garrett-Munk synthesized model. First, a ridge of energy at high wavenumber-low frequency, not predicted by Garrett-Munk, has been seen in previous and recent temperature profiling from FLIP. This low frequency spectral shoulder has a profound effect on the distribution of shear in the sea. Figure 2 is an example of a current frequency-wave number spectrum illustrating this finding. A second finding is that the continuum band of frequencies between tidal and approximately .5 cph seems to be dominated by the harmonics of the tidal and inertial frequencies. This suggests that the dominant non-linear interactions produce forced non-resonant waves, rather than the resonant (triad) offspring produced by weakly non-linear systems. As most internal wave theories have assumed the resonant triad interaction to be dominant, this finding needs to be further investigated.

In addition to the spectral analysis effort, progress during 1981 has been made in several areas. The accuracy of the MPL Doppler sonars has been quantified by comparing two instruments operated side by side. The RMS difference in velocity sensed by the sonars is of order 2-4 cm/sec after 30 sec of pulse-to-pulse averaging. Acoustic scattering from temperature microstructure in the wake of a towed plankton net has been investigated. A rough estimate of scattering level has been determined as a function of time after generation. Preliminary criteria for coded transmissions from Dopplar sonars

have been established.

FUTURE WORK

During 1982 analysis of the May 1980 data set will continue. Analysis tasks for the OMP include:

1) A comparison of data from the FLIP profiling CTD with that from the Doppler sonar. Linear theory suggests a relationship between the two types of data, yet the existence of the tidal harmonics casts doubt on some aspects of the theory. As NAVOCEANO survey vessels are equipped primarily with CTDs, the relationship between the output of this sensor and the measured shear should be investigated in detail.

2) A comparison of the near-surface internal wave spectrum with that from the deep sea. Most existing information on the internal wave field comes from well below the thermocline. The relationship between deep and near-surface measurements is still not well known. Both CTD and Doppler sonar information will be used in an attempt to clarify this picture.

3) A study of techniques to improve range and velocity resolution in Doppler sonar systems. To get the resolution required by the OMP, a new generation of Doppler sensors is required. The first attempts at adapting existing coded pulses produced promising results. Further exploration of possible Doppler codes will be performed.
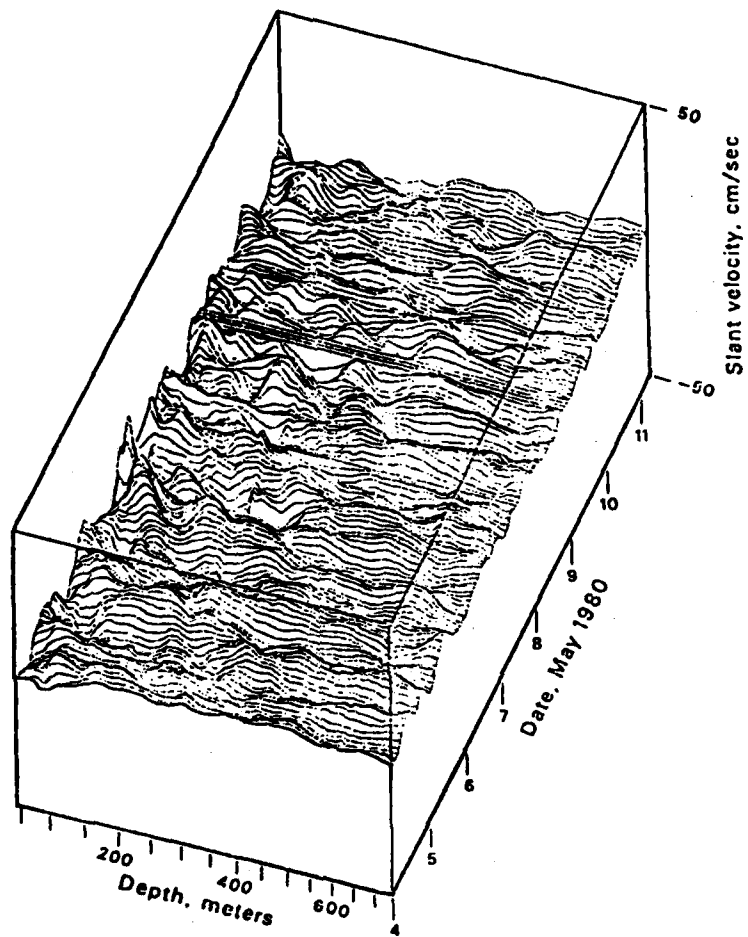
70 kHz VELOCITY PROFILE: 7 DAY RECORD

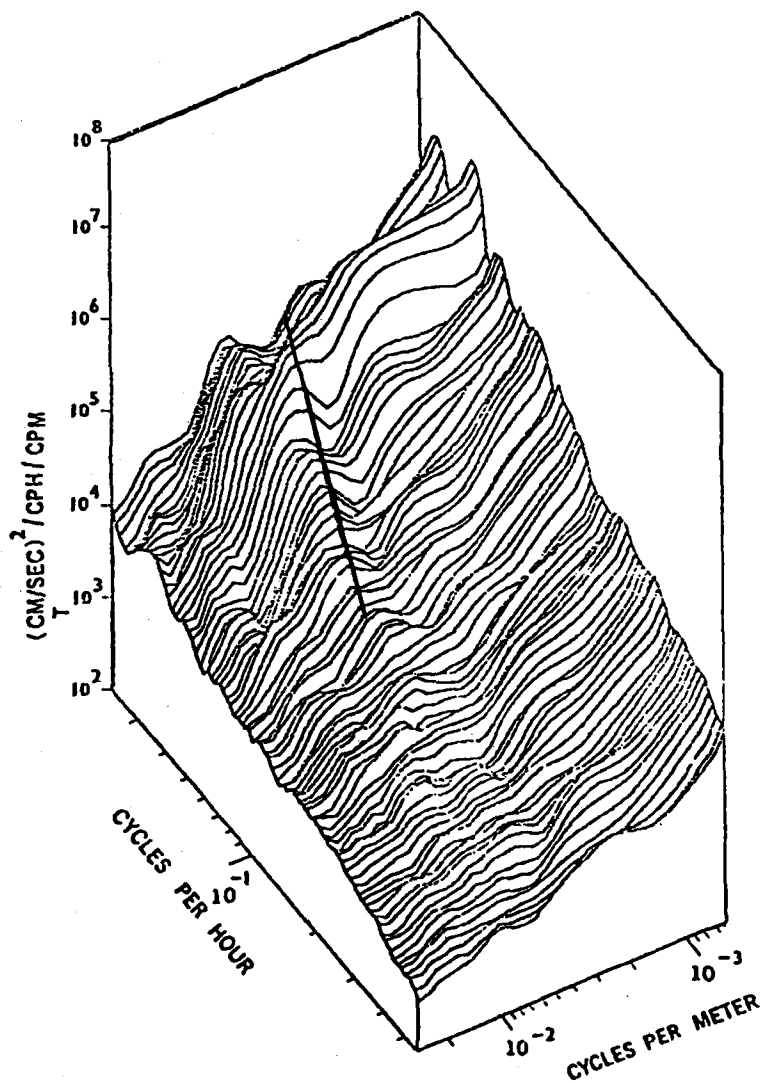**FIGURE 1.** **HOURLY VELOCITY PROFILES FROM 50 TO 750 m MEASURED DURING 4 TO 11 MAY 1980.**

FIGURE 2. A WAVENUMBER FREQUENCY SPECTRUM OF OCEANIC INTERNAL WAVES. ENERGY DENSITY IS GIVEN AS A FUNCTION OF FREQUENCY AND 45° SLANT WAVENUMBER. THE RIDGE OF ENHANCED LOW FREQUENCY HIGH WAVENUMBER ENERGY IS INDICATED BY THE SLANTING LINE.

ELIMINATION OF FINE STRUCTURE CONTAMINATION FROM TOWED SPECTRA
AND
INTERPRETATION OF CLOSELY SPACED XBT DATA

Michael Karweit
Department of Chemical Engineering
The Johns Hopkins University
Baltimore, Maryland 21218

Abstract

The work described here addresses two data analysis areas. One area concerns the development of a mathematical technique to remove fine structure contamination from internal wave measurements. This technique is shown to be suitable for use with NAVOCEANO instrumentation used in a porpoising mode. A second area develops techniques to interpret closely spaced XBT temperature profiles. These techniques involve a pattern recognition approach based on offset differences and stretching functions. Fifteen closely spaced NAVOCEANO XBT temperature profiles were used as a data set. Results indicate that use of measured temperatures without corrections may cause problems for interpretation of ocean dynamics or probe trajectories. The XBT analysis technique development is continuing with the goal of separating effects such as fall rate from real ocean effects.

I. A PROCEDURE FOR ELIMINATING FINE STRUCTURE CONTAMINATION FROM TOW SPECTRA USING THE NAVOCEANO TOWED CTD

BACKGROUND

Spatial characteristics of internal wave fields can be measured by a towed sensor which records temperature and conductivity. Internal waves are expected to vertically disturb surfaces of constant density so that a probe towed at a fixed depth will record density modulations proportional to internal wave displacements. With a single towed sensor not following a surface of constant density, the recorded data can be interpreted, and spatial characteristics of internal waves deduced, only if it is assumed that the local vertical density gradient is linear.

Although the vertical density gradient may be macroscopically linear, microscropically it is frequently "steppy," consisting of segments of uniform density separated by very thin regions of high density gradient. This steppiness is referred to as fine structure and has vertical length scales on the order of a meter. Spectra from towed sensors are contaminated by fine structure in a way that makes it difficult to extract that portion of the energy that is due to the internal wave field. An internal wave energy spectrum should follow a k^{-2} spectrum.

APPROACH

For a perfectly linear density profile, a straight line horizontal tow records fluctuations of density corresponding to the negative of the excursions of the isopleths so that a correct internal wave spectral form can be obtained. For a linear but steppy density profile, the density at a step is taken as the average of the densities of the adjacent layers. Figure 1 shows hypothetical data records from a probe moving

horizontally through an internal wave field for a smooth vertical profile and for a steppy profile with uniform steps.

Where the signal is flat, no information is being received. However, where the data record shows a discontinuity, the vertical excursion of the density profile is being registered. A reduced data set including only those points where the sensor passes through a step would perfectly reflect the displacement of the density field, although two potential problems with this are that there may not be enough data points to obtain the desired spatial characteristics of the internal wave field, and that the data points are unequally spaced.

The first problem may be dealt with by assuming that the internal wave field is wavenumber band limited and spatially periodic, an approximation that does not particularly distort spectral estimates. The spectral properties of the internal wave field can then be obtained from N independent observations, and, if the data set contains at least this quantity of data, the entire internal wave displacement character can be reconstructed. If not enough data are recorded to satisfy the N criterion, the probe may be vertically oscillated in order to find any discontinuities. If the depth of the sensor is monitored, the oscillation trajectory can be removed from the data record.

A simple numerical experiment illustrates the above technique. For a band-limited internal wave field, the vertical excursion at an instant of time is

$$\zeta(x) = \sum_{k=1}^{N} \frac{1}{k} \cos(2\pi kx + \phi) \tag{1}$$

where x is horizontal distance and ϕ is an arbitrary phase. The vertical displacement $\zeta(x)$ will have an energy spectrum of k^{-2} for wavenumbers 1 to N and zero for $k > N$. Suppose that the undisturbed density profile is $\rho(z) = \rho_0 + cz$ where z is depth and c is the constant gradient. If this horizontally uniform field is vertically displaced by the internal wave field $\zeta(x)$, the density field will be

$$\bar{\rho}(x,z) = \rho_0 + c(z - \zeta(x)) \tag{2}$$

The recorded signal from a probe sampling along x at $z = z^*$ would be

$$\bar{\rho}(x,z^*) = \rho_0 + cz^* - c\sum_{k=1}^{N} \frac{1}{k} \cos(2\pi kx + \phi) \tag{3}$$

This is the data set analogous to that which would be obtained from a horizontally towed sensor.

To emulate a macroscopically linear, but steppy, density profile, it is assumed that the steps are of equal size with a step in density $\Delta\rho$. A recorded signal from this field could be

$$\tilde{p}_s(x,z^*) = \Delta\rho \; integer \left[\tilde{p}(x,z^*)/\Delta\rho \right] \tag{4}$$

Figure 1 in fact shows sample data from $\tilde{p}(x,z^*)$ and $\tilde{p}_s(x,z^*)$ for c = 1 and $\Delta\rho$= 1.

For the particular case of 512 sample points in period X, with N = 60, so that the maximum wavenumber is well below the Nyquist limit, a standard fast Fourier transform on $\tilde{p}_s(x,z^*)$ yields the spectrum plotted in Figure 2. What should occur is a straight line with slope -2 from 0.0 (log of wavenumber 1) to 1.78 (log of wavenumber 60), and a negative infinity everywhere else. What actually occurs because of the fine structure problem is a k^{-2} spectrum extending with some noise beyond 1.78.

A new data set, significantly smaller than 512 and at nonuniform intervals, is obtained by including only those points where the sensor passes through a step so that every data point in the new set is an accurate reflection of the displaced density field. Because of the nonuniform data spacing, a matrix inversion is necessary to carry out the Fourier transform on these data. If the amplitude scale of the internal wave field, say Z_w, is small compared to the thickness of the uniform density layers, that is, if $Z_w/(c/\Delta\rho)$ is small, there will not be enough independent data points in the reduced set to resolve the band of wavenumbers. This problem could be solved by intentionally causing the probe to intersect more discontinuities by vertical porpoising. If the probe takes on a vertical oscillation z_p = a $cos(2\pi k_p x)$ where k_p = 25, the signal will be slightly modified from Equation (4) to become

$$\tilde{p}_p(x,z^*) = \Delta\rho \; integer \left[\left[\tilde{p}(x,z^*) - c \; z_p(x) \right]/\Delta\rho \right] \tag{5}$$

If $\tilde{p}_p(x,z^*)$ is Fourier transformed, the result, shown in Figure 3, clearly portrays the correct k^{-2} slope with a sharp cutoff at 1.78, and has the addition of a spike of energy at k=1.4 corresponding to the porpoising probe.

SUMMARY

These numerical experiments illustrate an analysis technique by which fine structure contamination can be eliminated. Depending on $Z_w/(c/\Delta\rho)$, it may require more than a straight horizontal tow to get enough independent data. The NAVOCEANO towed CTD is uniquely equipped to overcome this problem since it can easily accommodate vertically porpoising trajectories.

In principle, this technique can be used on density fields with nonuniform gradients or fields which are not fully "steppy," although details need to be worked out. Large scale matrix inversions are required, but these can be handled effectively by any modern computer. In a sense, this proposed analysis shifts at least part of the fine structure problem from the ship to the computer.

II. INTERPRETATION OF CLOSELY-SPACED XBT TEMPERATURE PROFILES

BACKGROUND

Expendable bathythermographs (XBTs) have been developed for obtaining

101

approximate temperature profiles of the water column with the advantages of ease of deployment, low cost, and high drop rate. The extent to which an accurate temperature and depth may be recorded will determine how useful the XBT will be for such additional applications as density and internal wave measurements. Further, because XBT drop rates are high, the problem of encountering phase changes in sampling the water column, as is the case with the more slowly dropping CTDs, is minimized.

An experiment was designed to evaluate the consistency of XBT data and the possibilities of distinguishing between probe/measurement irregularities and dynamics of the water column. It was carried out aboard the USNS KANE, during May 1981 on the NAVOCEANO Spring cruise to the Norwegian Sea.

EXPERIMENT

Fifteen Sippican T-7 XBTs were dropped from a single launch tube at five minute intervals with the ship stationary. The experiment was designed to sample the water column with XBTs in a time/distance short compared to the time/distance scales of most water column dynamics. All XBT casts are expected to look similar except perhaps for some slowly evolving features associated with ocean dynamics. Vertical offsets or uniform stretching between profiles were attributed to XBT entry and drop-rate anomalies. It is assumed that temperature tags the water so that any difference in vertical position of an isotherm is due to vertical displacement of that water. The series of XBT casts was analyzed in terms of the assumed relative vertical displacements.

For each of N XBT casts, there will be a vertical profile $\theta_i(z)$ for $Z \leq z \leq 0$ and $i = 1, N$. The maximum depth of interest is Z. If the water column were perfectly stationary, then $\theta_i(z) = \theta_j(z)$ for all i,j, regardless of probe trajectory differences. The case of interest is $\theta_i(z) \neq \theta_j(z)$. If the original assumption is correct, differences occur because the water column has been nonuniformly displaced, or stretched. A technique has been developed to estimate this stretching. Of the N casts, one is chosen as a reference cast, indicated by $*$, such that the reference profile will be $\theta_*(z)$ for $Z \leq z \leq 0$. A stretched vertical coordinate $\zeta_i(z)$ is identified such that, with respect to ζ_i all temperature profiles match the reference profile: $\theta_*(z) = \theta_i(\zeta_i)$. The relationship between z and ζ_i is to be determined as the stretching function S_i where $\zeta_i = S_i(z)$ such that $\theta_* = \theta_i(\zeta_i)$.

Suppose S_i is a polynomial so that vertical distortions can be expressed

$$\zeta_i(z) = a_i + b_i z + c_i z^2 + d_i z^3 \tag{6}$$

where this polynomial as written is limited to third order. Then S_i will be a polynomial with coefficients a_i, b_i, c_i, d_i. Since only four parameters are present, the criterion $\theta_*(z) = \theta_i(\zeta_i)$ cannot be satisfied for all z. The differences can, however, be minimized by maximizing the correlation C for all $i \neq *$ where

$$C(a_i, b_i, c_i, d_i) = \overline{\theta_*(z)\theta_i(a_i + b_i z + c_i z^2 + d_i z^3)} = \overline{\theta_*(z)\theta_i(\zeta_i)} \tag{7}$$

This entails for every i picking quadruples a_i, b_i, c_i, d_i to produce $\theta_i(\zeta_i(z))$ and then carrying out the correlation calculation. This is repeated until a set of values for a_i, b_i, c_i, d_i produces a maximum correlation.

Only a limited number of points are considered in the correlation calculation. The analysis procedure was as follows: A reference cast $i = *$ was chosen. In this case, cast 529 was selected since it was about in the middle of the sequence of casts. Next each

102

cast was characterized in terms of 35 nodal depths $z_{i,j}$, at which selected temperatures occur. Using ordinary least-squares analysis for $i = *$, coefficients a_i, b_i, c_i, d_i were calculated that would produce a minimum error and give the optimum stretched depth $\zeta_i(z)$ for each cast compared to the reference cast.

RESULTS

Results based on the original assumption that recorded temperatures are true temperatures were inconsistent. For example, nodal depths across casts were much more irregular than expected, and differences between actual stretched depths did not systematically change from one cast to the next. Such anomalies seem to violate the original assumption that temperature tags the fluid.

That the data are so poorly correlated indicates that the assumption of a true temperature measurement is incorrect. A temperature offset error associated with each XBT was estimated. This offset was based on the 7° nodal depths, and all temperatures were then adjusted by that offset. Offset values for the various casts are 0.06, -0.04, 0.08, -0.07, 0.02, 0.05, 0.17, -0.07, -0.09, 0.09, -0.21, and 0.06 $^\circ$C. Figures 4 and 5 show raw temperature profiles and first difference profiles, respectively, using adjusted data. Figure 6 shows the effect of a fourth order stretching function as determined from the procedure described previously.

In Figures 4 and 5 the nodal depths appear to be much more tied to the features of the cast profile and to vary much less erratically from cast to cast than if the recorded temperature were not adjusted. The stretching functions shown in Figure 6 also take on a much more coherent variation. The conclusion is that using the recorded temperature as a variable for estimating ocean dynamics or probe trajectory errors is not realistic.

FUTURE WORK

Casts will be compared by means of individual features throughout the water column, either with relative temperature data or first difference data. Data for each profile will be divided into segments by depth with each segment containing the temperature record for a fixed depth interval. For each segment a simplified stretching function will be defined and the correlation will be maximized. By considering only a small segment of the profile at a time, the simpler linear stretching function will probably adequately describe the changes between casts.

The purpose of these calculations is to determine the offset and stretching as a function of depth for each of the casts relative to the reference cast and to determine anomalies of recorded temperature associated with the same physical feature in the water column. By plotting each of these variables by depth and across casts it will be possible to address a variety of questions such as: How complicated a function is the error of the recorded temperature? How variable are the XBT trajectories in terms of fall rate? To what extent can vertical distortions in the water column be identified vis-a-vis XBT trajectory differences?

The present data set is sufficient to obtain preliminary answers to these questions. However, it is clear that a larger, more carefully calibrated experiment will be required to refine these answers. What is perhaps most evident is that only with closely spaced XBT casts can these questions even be asked.
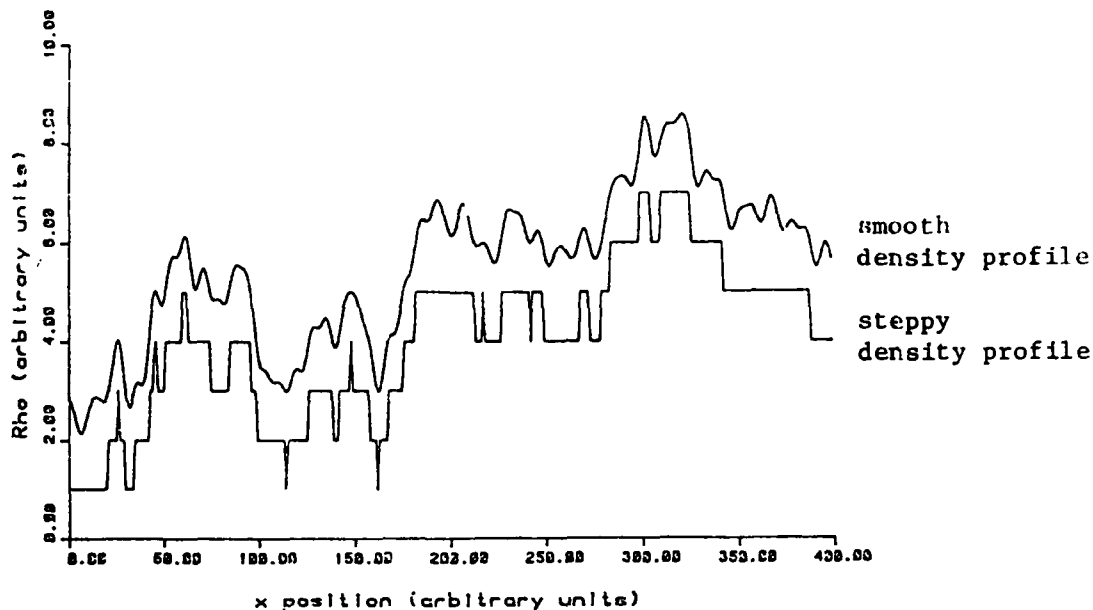
FIGURE 1. TWO HYPOTHETICAL DATA SETS FROM A PROBE SAMPLING DENSITY IN THE SAME INTERNAL WAVE FIELD, ONE HAVING A SMOOTH DENSITY PROFILE, AND THE OTHER HAVING A STEPPY DENSITY PROFILE. THE CURVES ARE VERTICALLY OFFSET FOR CLARITY.
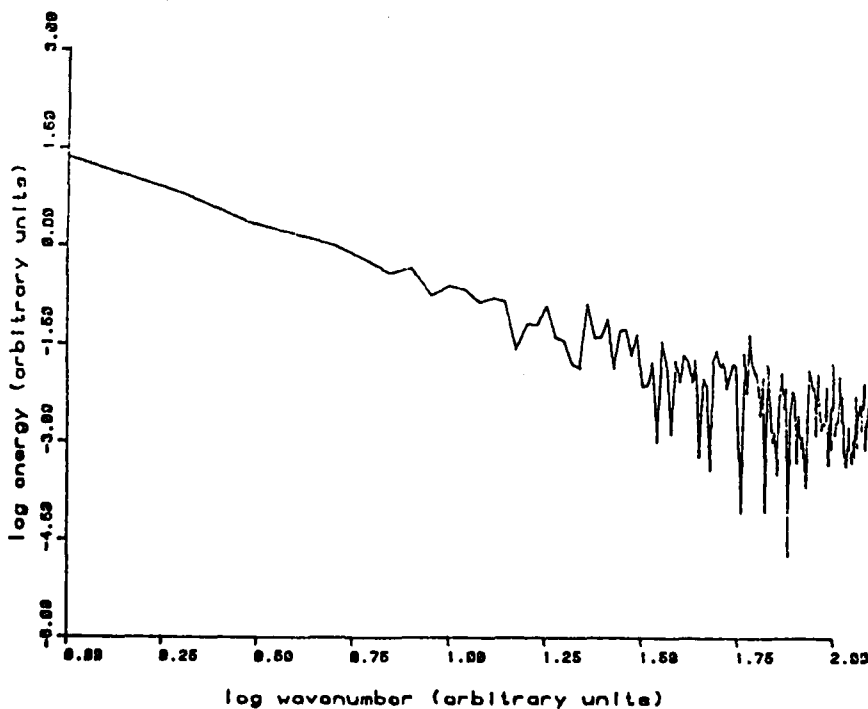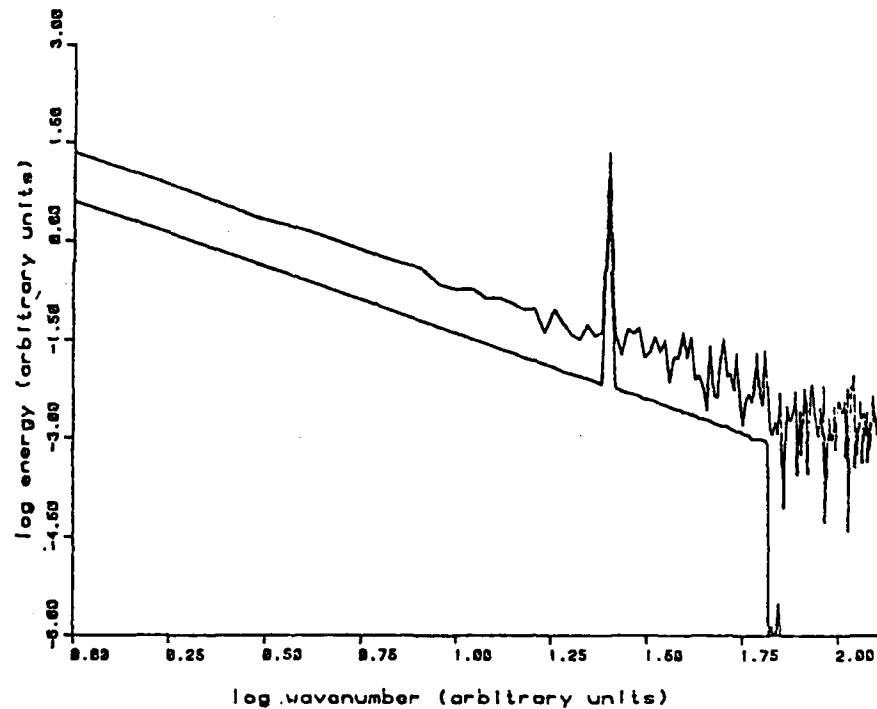

FIGURE 2. ENERGY SPECTRUM OF HYPOTHETICAL DATA FROM A HORIZONTALLY TOWED SENSOR IN A STEPPY DENSITY FIELD. INTERNAL WAVE SPECTRUM IS k^{-2} FOR $1 \leq k \leq 60$, AND ZERO ELSEWHERE. THE SHOWN SPECTRUM WAS CALCULATED USING THE ENTIRE TOW RECORD AND INDICATES ERRONEOUS SPECTRAL CONTRIBUTION BEYOND k=60 (LOG 60=1.78). THIS CONTRIBUTION IS PROPORTIONAL TO k^{-2} AND IS DUE TO THE STEPPY DENSITY FIELD.

FIGURE 3. ENERGY SPECTRA OF HYPOTHETICAL DATA FROM A PORPOISING TOWED SENSOR IN A STEPPY DENSITY FIELD. INTERNAL WAVE SPECTRUM IS k^{-2} FOR $1 \leq k \leq$ 60, AND ZERO ELSEWHERE. THE SPIKE IN BOTH SPECTRA CORRESPONDS TO $k_p=25$, THE PORPOISING WAVENUMBER OF THE SENSOR. BOTH SPECTRA ARE CALCULATED FROM THE SAME DATA SET. THE LOWER CURVE ACCURATELY REFLECTS THE CHARACTERISTICS OF THE HYPOTHETICAL INTERNAL WAVE FIELD; THE UPPER CURVE, EXTENDING BEYOND THE k=60 CUTOFF, DOES NOT. THE CURVES ARE VERTICALLY OFFSET FOR CLARITY.

2/2
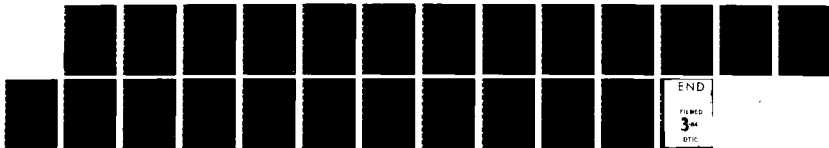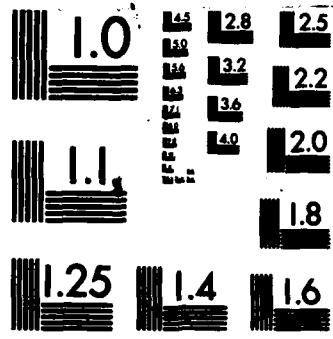
MICROCOPY RESOLUTION TEST CHART
NATIONAL BUREAU OF STANDARDS-1963-A
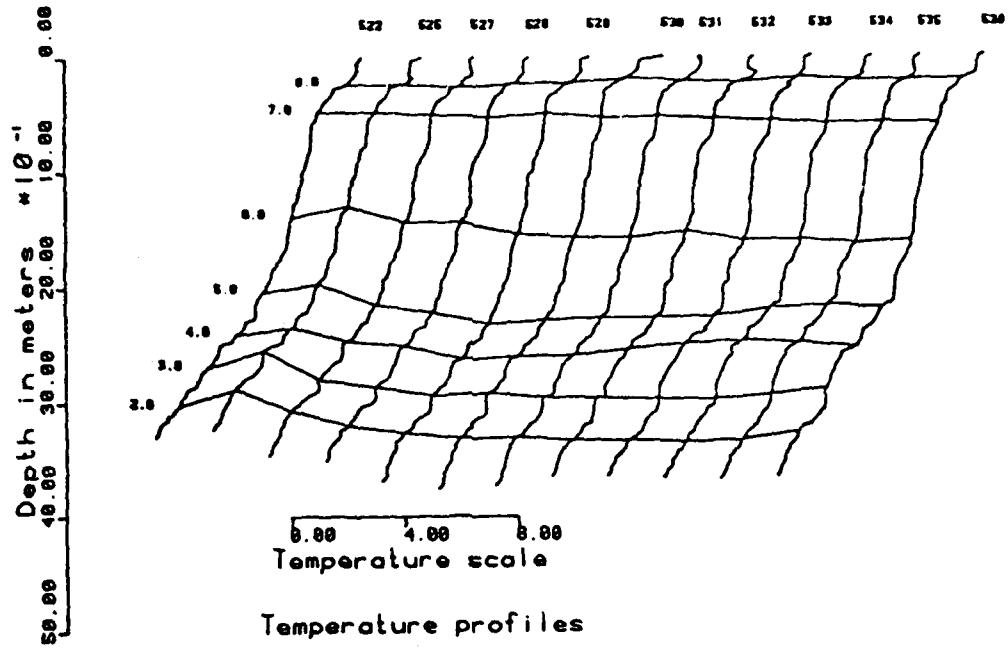
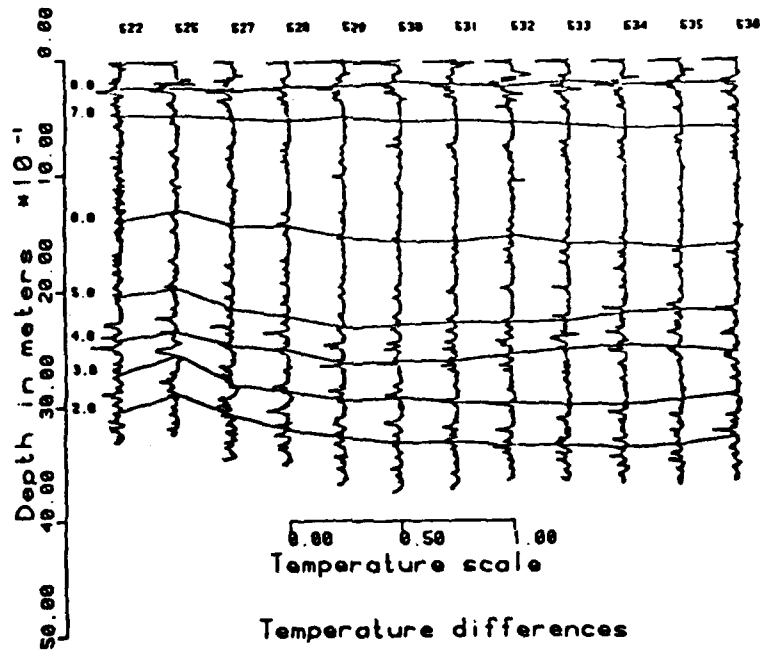FIGURE 4. ADJUSTED TEMPERATURE RAW PROFILES FROM XBT DROPS, WITH DEPTHS OF NODAL TEMPERATURES INDICATED.

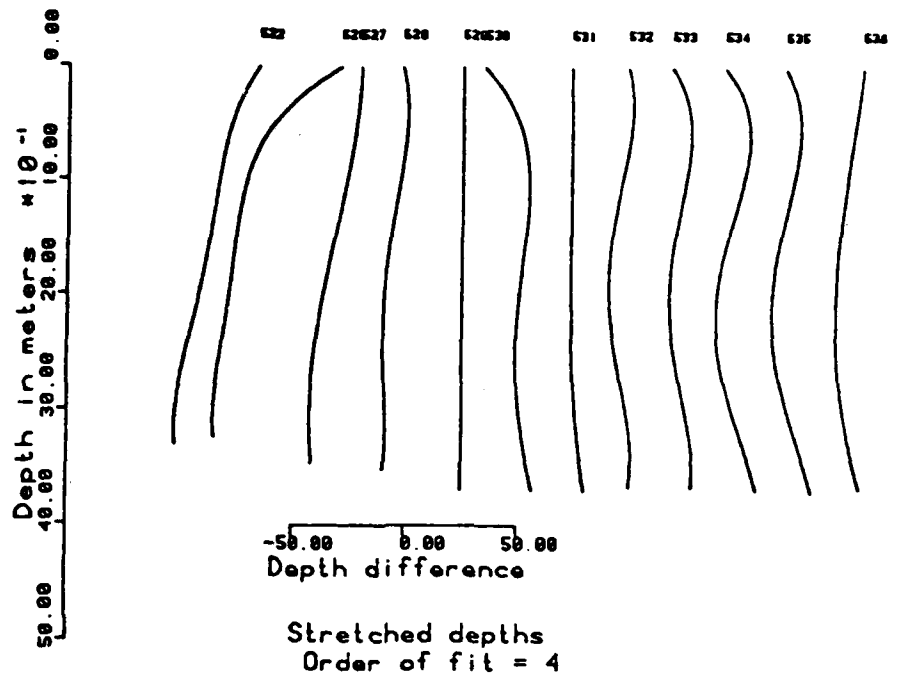FIGURE 5. ADJUSTED TEMPERATURE FIRST DIFFERENCE PROFILES FROM XBT DROPS WITH DEPTHS OF NODAL TEMPERATURES INDICATED.

106

FIGURE 6. DEPTH DIFFERENCES FOR A FOURTH ORDER STRETCHING FUNCTION USING ADJUSTED TEMPERATURE DATA.

LARGE SCALE SYNOPTIC SHEAR PREDICTION

S.A. Piacsek
J.M. Harding
Naval Ocean Research and Development Activity
NSTL Station, Mississippi 39529

R.H. Preller
JAYCOR
205 South Whiting Street
Alexandria, Virginia 22304

Abstract

The Thermodynamic Ocean Prediction System (TOPS) has provided the Fleet Numerical Oceanographic Center (FNOC) with operational capability to forecast vertical shear on a global basis. Examples of TOPS output for regions of the North Atlantic and North Pacific Oceans are provided and interpreted to illustrate the capability of TOPS. Future work will continue to address improvement of input data for TOPS, improvement of modeling techniques, and better verification of TOPS output.

BACKGROUND

The development and verification of the Thermodynamic Ocean Prediction System (TOPS) has led to an operational global ocean vertical shear forecasting capability at Fleet Numerical Oceanographic Center (FNOC). TOPS can routinely predict large scale synoptic changes in upper ocean thermal structure as well as Ekman and inertial current components, which account for a substantial fraction of the total upper ocean current.

Successful one-dimensional TOPS verification of sea surface temperature and mixed layer depth has been performed at ocean stations P and N in the North Pacific Ocean and for buoy data from the Gulf of Mexico. Large scale verifications have been performed for the TRANSPAC region of the northeast North Pacific Ocean. Computed vertical shear has been found to compare well with MILE data. This paper addresses the present shear prediction capability of FNOC.

EXPERIMENT

An important application of TOPS is upper ocean vertical shear prediction. Scalar shears, $S=((\Delta u/\Delta z)^2+(\Delta v/\Delta z)^2)^{1/2}$, and gradient Richardson numbers, $Ri=((-g/\rho)(\Delta\rho/\Delta z))/S^2$, were calculated from hourly TOPS output for regions of the North Pacific and North Atlantic Oceans. Ri gives an indication of stability of a given water parcel. Values less than 0 imply convective instability, values between 0 and 0.25 imply shear instability, and values greater than 0.25 imply stability. Predictions were made for November and December of 1976 and 1980. Results are presented as contour plots and frequency distributions of shear and Richardson number at various depths and as vertical cross-sections within each ocean region to investigate both horizontal and vertical distributions, as well as variability for different time scales. Figure 1 shows the two oceanic regions and indicates the cross-section transects. Three different time scales were expected to be differentiated as a result of these experiments, including a diurnal scale resulting from the diurnal heating cycle, a synoptic (3-7 day) scale resulting from synoptic meteorological patterns, and an annual scale resulting from annual meteorological patterns.

Contour and cross-sectional plots of North Pacific shear and Richardson number for a single day show a high degree of variability which probably results from a combination of diurnal and synoptic scale variations. One widespread feature shown in Figure 2 appears related to diurnal variation and occurs only south of 30°N. In this region shear decreases and instability increases with time, most likely as a result of night time cooling of surface layers and associated convective instability.

Averages of local noon and local midnight values of shear and Richardson number over 45 days indicate that synoptic scale forcing is of major importance compared to diurnal effects. On a synoptic scale, regions of shear instability appear to be directly correlated to frontal passage. Convective instability appears just after frontal passage and regions of stability occur with high pressure systems. Near surface and near mixed layer frequency distributions of Richardson number suggest frequent occurrence of shear instability. Figure 3 shows examples of near surface Richardson number frequency distributions (histograms).

Year to year variations in storm frequency, intensity, and tracks might cause shear variation on an annual scale. A comparison of shear cross sections and frequency distributions for 1976 and 1980, shown in Figure 4, demonstrates this annual variability.

In the North Atlantic Ocean the highest variability is also associated with synoptic rather than diurnal scale effects. An inter-ocean comparison of surface layer shear shows a slight bimodal surface shear distribution in the Pacific and a stronger bimodal surface shear distribution in the Atlantic, as illustrated in Figure 5. Increases and decreases of wind associated with weather systems may cause this shear bimodality as the model shifts between dominant Ekman and dominant inertial shear modes. Richardson numbers appear skewed toward convective instability in surface layers and toward shear instability at the base of the mixed layer in both oceans. Table 1 shows that higher shears occur in the surface layers than near the base of the mixed layers and that high day to day variability occurs in both oceans, although the North Pacific shows higher shear than does the North Atlantic for 1976.

SUMMARY

The ability of TOPS to forecast large scale vertical shears has been demonstrated. The quality of these forecasts remains questionable. Three problem areas in shear prediction that still need to be addressed are 1) the quality of forcing for the TOPS model; 2) model inadequacies; and 3) insufficient verification data. Experiment results tend to underpredict shear, especially at the base of the mixed layer, and to overpredict instability. TOPS input consists of FNOC analyses and atmospheric forecast fields. Winds and heat flux parameters have been found reliable, but further studies are required for areas where data input is less adequate. Improved Expanded Ocean Thermal Structure (EOTS) information should be available before runs in the Indian Ocean are performed. In addition, Naval Operational Global Atmospheric Prediction System (NOGAPS) and Naval Operational Regional Atmospheric Prediction System (NORAPS) products are required for further southern ocean and limited shear forecasts. The TOPS model itself has some inadequacies in that surface and internal wave effects are not presently included. The effects of the coarse horizontal resolution of the FNOC grid need to be investigated, as does vertical resolution which may nonuniformly affect results. Longer time series of shear combined with wind and heat flux measurements are required in both individual locations and over large geographic areas for verification of the model.

Future work will include further analyzing these results and relating them to forcing, calculating shear in different seasons and regions, performing further tests on the

effects of horizontal and vertical resolution, and comparing model results with available field data.
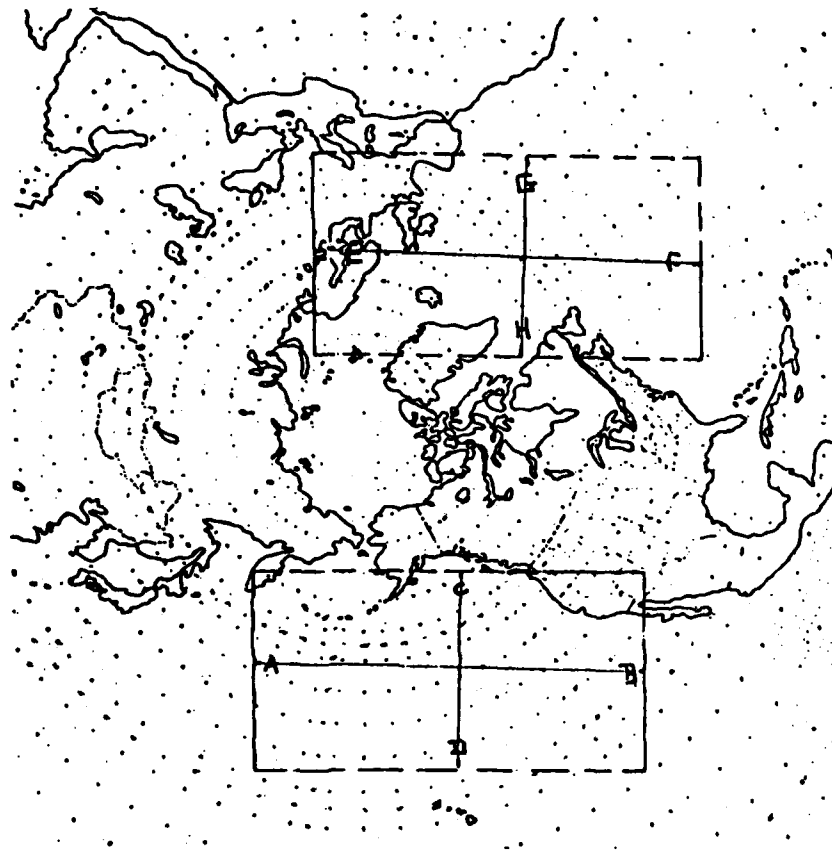
FIGURE 1. NORTH PACIFIC AND NORTH ATLANTIC REGIONS FOR TOPS UPPER OCEAN VERTICAL SHEAR EXPERIMENT. CONTOUR PLOTS COVER THE INDICATED REGIONS; CROSS-SECTION PLOTS INCLUDE TRANSECTS A-B AND C-D IN THE NORTH PACIFIC AND E-F AND G-H IN THE NORTH ATLANTIC.
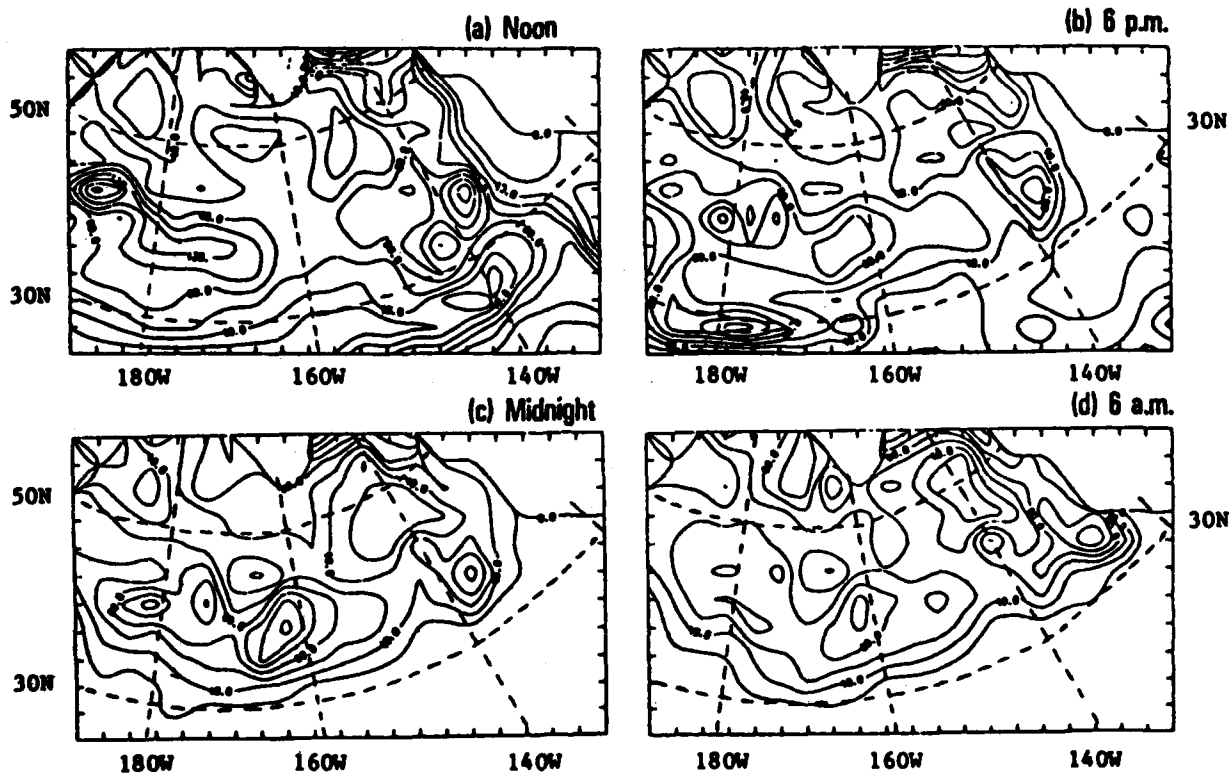
FIGURE 2. DIURNAL VARIATION OF SHEAR IN THE NORTH PACIFIC. CONTOUR PLOT OF SHEAR AT 7.5 m DEPTH FOR 13 NOV 1976 SHOWS DIURNAL SCALE VARIATIONS. THE REGION SOUTH OF 30°N SHOWS A DECREASE IN SHEAR WITH TIME. ASSOCIATED WITH THIS SHEAR DECREASE IS AN INCREASE IN INSTABILITY.
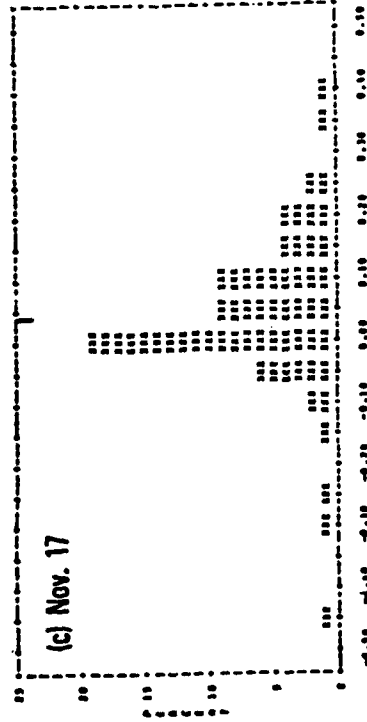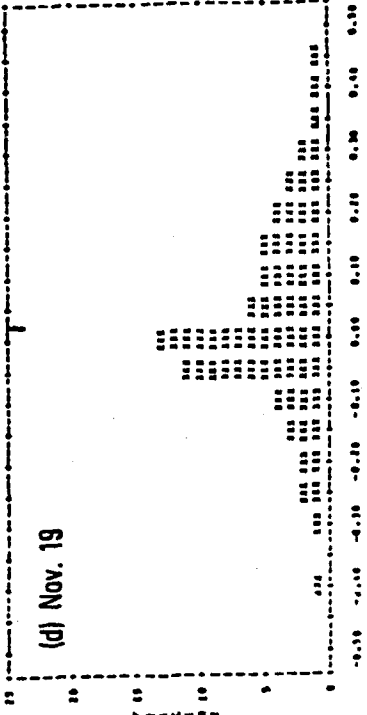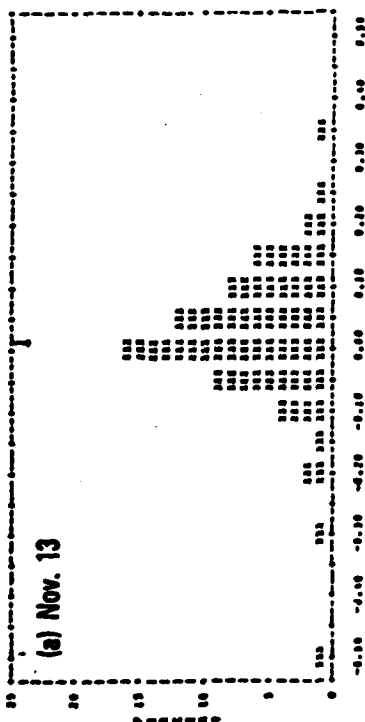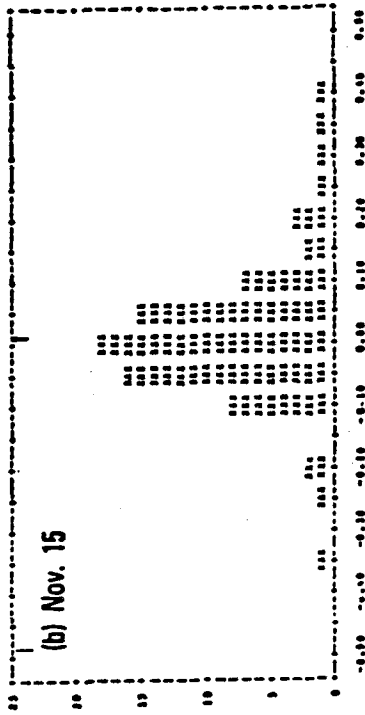
FIGURE 3. SYNOPTIC VARIATION OF RICHARDSON NUMBER IN THE NORTH PACIFIC. FREQUENCY DISTRIBUTIONS OF Ri CALCULATED IN THE SURFACE LAYER (10 m) SHOW SYNOPTIC SCALE VARIATIONS OVER A 6-DAY PERIOD IN NOVEMBER 1976.
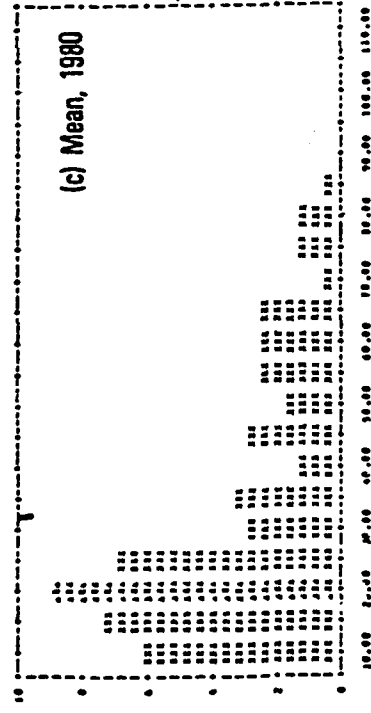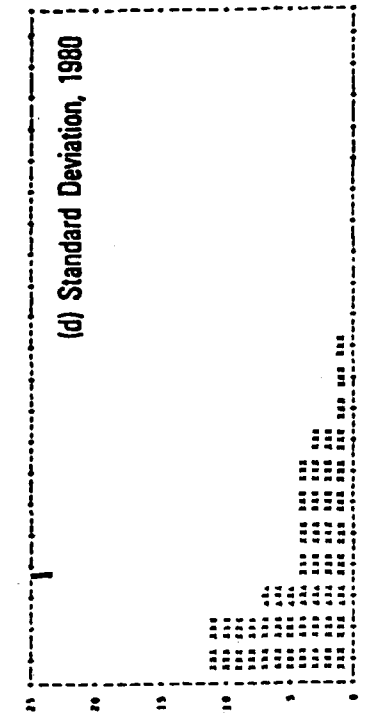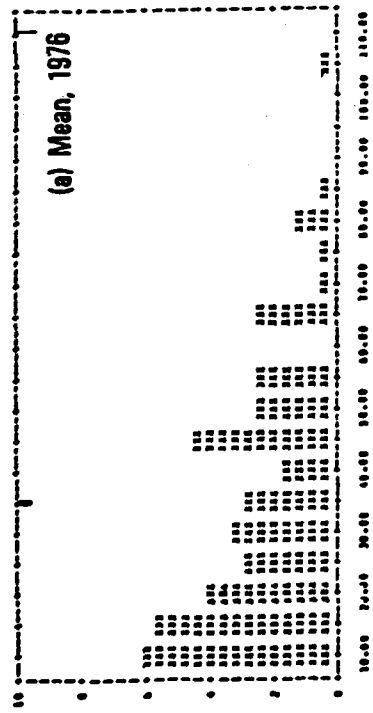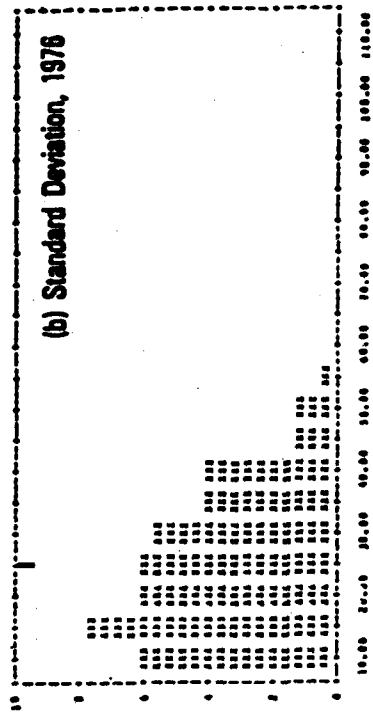
114

FIGURE 4. INTERANNUAL VARIATION OF SHEAR IN THE NORTH PACIFIC. PLOTS OF PROBABILITY DISTRIBUTIONS OF MEANS AND STANDARD DEVIATIONS OF HOURLY MEAN SURFACE SHEAR VALUES ACROSS TRANSECT C-D (SHOWN IN FIGURE 1) FOR 1976 AND 1980 SHOW DIFFERENCES BETWEEN THE TWO YEARS.
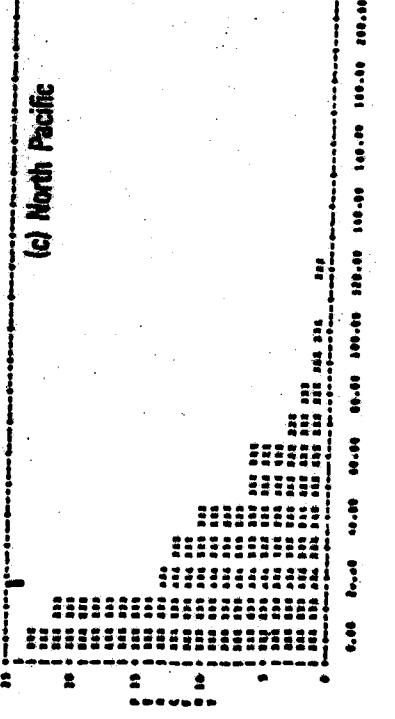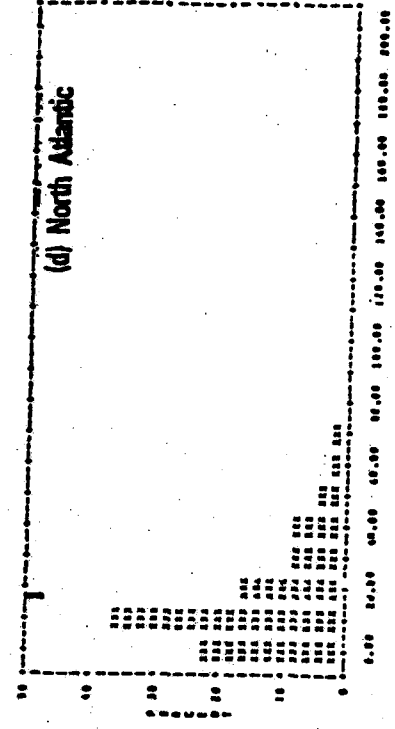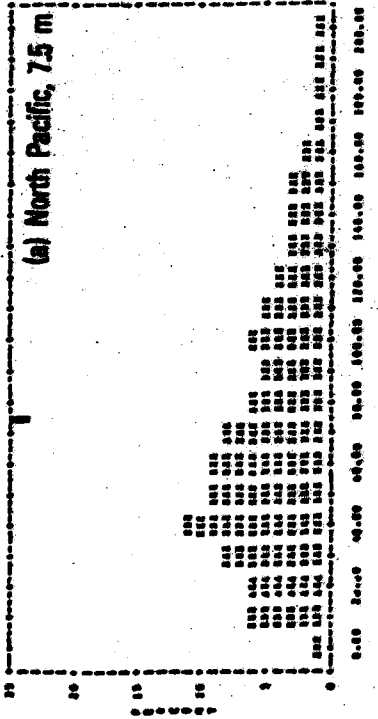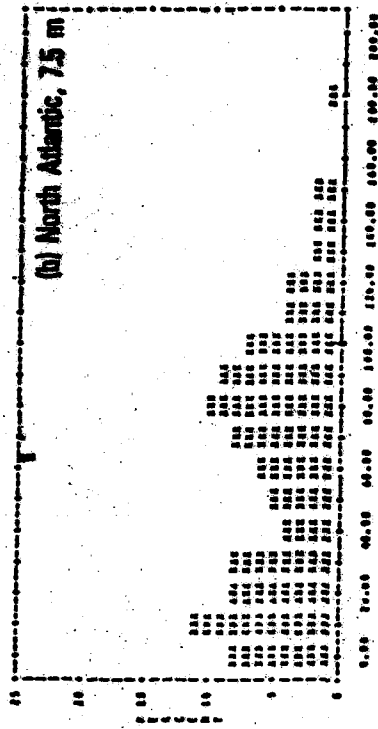
FIGURE 5. INTER-OCEAN COMPARISON OF SHEAR. PLOTS OF CUMULATIVE HOURLY SHEAR FOR 1976 SHOW A SLIGHT BIMODALITY IN THE NORTH PACIFIC SURFACE LAYER (a) AND A DEFINITE BIMODALITY IN THE NORTH ATLANTIC SURFACE LAYER (b). SHEAR NEAR THE BASE OF THE MIXED LAYER (c and d) IS LESS THAN THAT IN THE SURFACE LAYERS IN BOTH OCEANS AND DOES NOT EXHIBIT BIMODALITY.

116

N. Pacific 76	Depth (m)	12 Nov (12L)	14 Nov (12L)	16 Nov (12L)	18 Nov (12L)
% Shear $>10^{-3}$/s ,	7.5	87.5	93.5	85.3	88.8
	32.5	45.4	50.2	45.9	34.6
% Shear $>5 \times 10^{-3}$/s	7.5	60.6	61.9	60.6	42.9
	32.5	8.2	5.6	10.4	3.5

N. Atlantic 76	Depth (m)	12 Nov (12L)	14 Nov (12L)	16 Nov (12L)	18 Nov (12L)
% Shear $>10^{-3}$/s ,	7.5	57.2	75.4	70.3	71.8
	32.5	31.8	31.8	31.8	38.5
% Shear $>5 \times 10^{-3}$/s	7.5	29.7	29.7	22.6	42.0
	32.5	7.1	5.7	4.1	11.3

TABLE 1. SIGNIFICANT SYNOPTIC SHEAR IN THE NORTH PACIFIC AND NORTH ATLANTIC OCEANS. VALUES ARE FOR LOCAL NOON IN THE SURFACE LAYER (7.5 m) AND NEAR THE BASE OF THE MIXED LAYER (32.5 m).

117

MODELING OF INTERNAL WAVES IN THE UPPER OCEAN

S.A. Piacsek
Naval Ocean Research and Development Activity
NSTL Station, Mississippi 39529

P. Niiler
Oregon State University
School of Oceanography
Corvallis, Oregon 97331

R.H. Preller
JAYCOR
205 South Whiting Street
Alexandria, Virginia 22304

Abstract

Progress has continued on modeling the behavior of internal waves in the upper ocean, with emphasis on mixed layer interaction. Investigation of the generation of internal waves by tidal flows over seamounts has begun.   A non-hydrostatic model is being used for the internal wave-mixed layer interaction studies, while a hydrostatic model is being used for the seamount internal wave generation studies.

NON-HYDROSTATIC INTERNAL WAVES

Simulation of internal wave interaction with the mixed layer has involved computations of energy transformations between the mean flow and internal waves, and the evolution of spectral distributions from an initial distribution. It was found that energy transformations might be computed from finite difference moment equations derived from finite difference momentum equations. This technique may be an improvement over customary methods which may have greater truncation and round-off errors.

A simple spectral description composed of discrete bands related to the Garrett-Munk spectrum for moored measurements has been formulated for use in simulations. Parameters in the equations that describe initial internal wave velocity and temperature fields are calculated from the spectrum. The initial field of internal waves consists of ten internal modes with each mode represented by six frequency bands. Numerical simulation is based on a non-linear, two dimensional, finite difference model with equations as noted in the summary for the previous Oceanographic Measurements Program Review. Spectra become "gappy" as time goes by due to certain internal wave modes being extinguished by the developing mixed layer and dissipation region.

HYDROSTATIC INTERNAL WAVES

A two dimensional, two layer, semi-implicit ocean model is being used for simulations of internal wave generation due to tidal flow near seamounts. A time-dependent flow corresponding to tidal oscillations is specified at the model boundary which is near a topographic bump on the sea floor. During a "spin-up" time period a transient internal wave develops and travels down the channel away from the boundary. Figure 1 is an example for a simple case where the topographic bump is 75% of the depth of the lower layer, tidal flow is specified at the left boundary, and the model has simulated a ten day

time period from the onset of the boundary flow. Figure 2 shows the displacement of the interface between the layers after a twenty day time period from the onset of the boundary flow. The computer code for these calculations is actually a three dimensional code that is being tested in two dimensional simulations. After further testing, a three dimensional siumulation of tidal flow over seamounts in the JASIN region will be attempted.

FIGURE 1. SIMULATED INTERNAL WAVE DUE TO TIDAL FLOW NEAR A SEAMOUNT AFTER A 10 DAY TIME PERIOD. TOPOGRAPHIC BUMP IS 75% OF THE DEPTH OF THE LOWER LAYER.

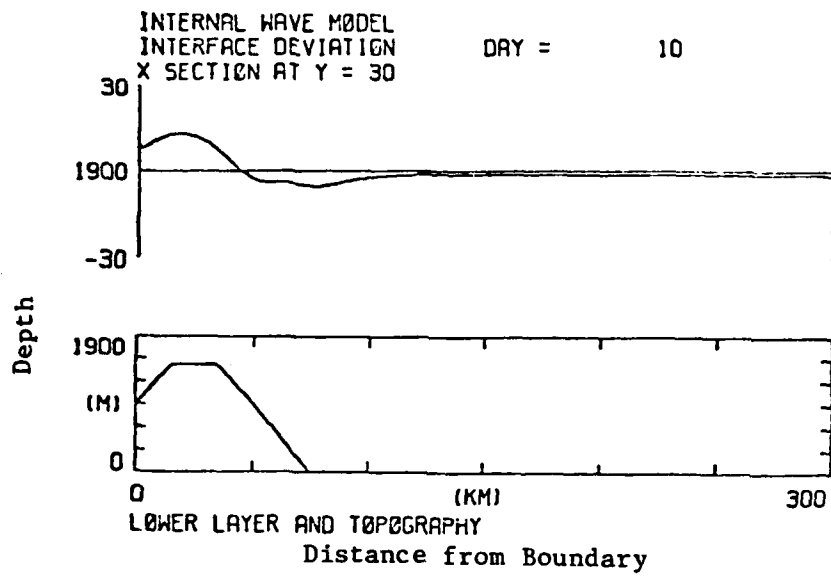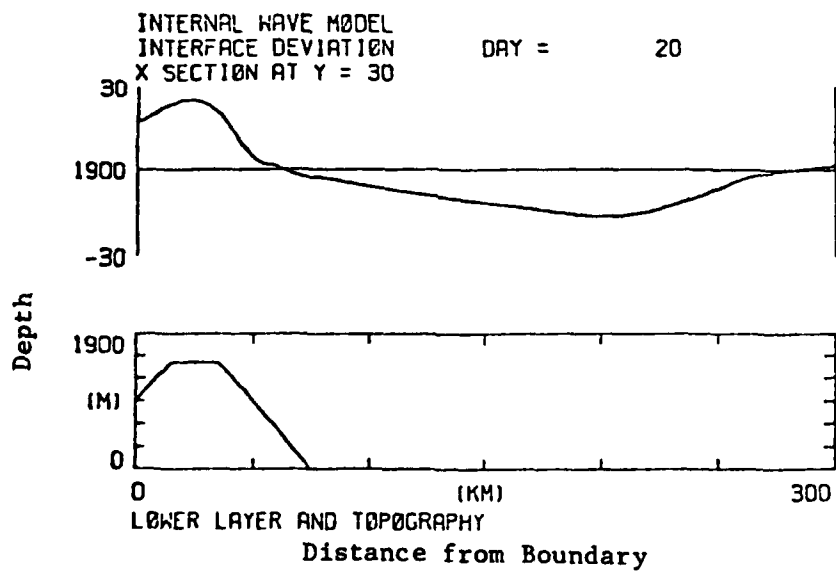FIGURE 2. SIMULATED INTERNAL WAVE DUE TO TIDAL FLOW NEAR A SEAMOUNT AFTER A 20 DAY TIME PERIOD. TOPOGRAPHIC BUMP IS 75% OF THE DEPTH OF THE LOWER LAYER.

121

TURBULENCE ASSESSMENT

A.D. Kirwan
Department of Marine Sciences
University of South Florida
St. Petersburg, Florida 33701

Abstract

A new study to be carried out during 1982 is described. The long range goal of this study is to investigate upper ocean turbulence, both naturally occurring and mechanically generated, in relation to specific needs of the OMP. Measurement or analysis techniques that may be useful to estimate turbulent effects for the various types of measurements developed for the OMP will be examined.

BACKGROUND

Turbulent fields in the mid-latitude upper ocean will be examined in order to determine which aspects of naturally occurring turbulence alter or are readily confused with mechanically generated oceanic turbulence. For purposes of this study mechanically generated turbulence is regarded as a signal embedded in a background noise of naturally occurring turbulence. This situation differs from the classical signal to noise problem in that there is strong interaction between signal and noise on the time and space scales of interest.

Naturally occurring turbulent density and velocity fields are delineated by time-space scales less than those of mechanically generated turbulent fields. Typically, naturally occurring turbulence has space scales in the millimeter to meter range and time scales in the seconds to minutes range. Turbulent flow fields have two characteristics, vorticity and randomness, which distinguish them from other naturally occurring flows.

OBJECTIVES AND APPROACH

The specific purpose of this study is to identify properties of naturally occurring turbulence that will enable a distinction to be made between naturally occurring and mechanically generated turbulence. The approach to be used involves identification and cross-comparison of basic scientific issues and turbulence measurement techniques. Scientific issues to be addressed include a description of turbulent phenomena, including identification of turbulent time and space scales; identification of turbulent processes; development of models and parameterizations of turbulence; and the relationship of these scientific issues to user needs. Special attention will be given to matching existing science and technology with present and projected OMP user needs.

This study will focus on naturally occurring turbulent phenomena found in the upper ocean between the sea surface and the seasonal thermocline and/or bottom of the mixed layer within a mid-latitude region of Naval interest. The program will involve continual intercomparisons of OMP user requirements and basic scientific and technological issues. For example, three scientific questions germane to the program are: 1. How does the small scale flow field interact with the fine and microstructure stratification? 2. What is the role of the vertical shear of the larger scale horizontal velocity in generating and dissipating fine and microstructure stratification? 3. How can upper ocean small scale variability parameterizations be related to dynamic processes?

Answers to these questions are important in responding to the following specific needs of OMP users: 1. How representative of a region is a single profile or towed cross-section? 2. Are there large scale features in XBT or towed vehicle data which can be related to phenomena on the centimeter to meter scale? If so, how? If not, identify what research and development is necessary. 3. What are criteria for determining how much data to collect in a survey?

FUTURE WORK

The turbulence assessment program will develop a more extensive and detailed comparison of science and technology issues with OMP user requirements. To the extent possible, likely technology developments will be projected and their impact on OMP users assessed. Phenomena resolvable with present operational technology need to be identified and the question of higher measurement resolution versus modeling and sampling options needs to be addressed. In addition, a basis for developing a user sampling strategy needs to be established.

ASSESSMENT OF SURFACE GRAVITY WAVE EFFECTS
ON UPPER OCEAN PARAMETERS

Marshall D. Earle
Marine Environments Corporation
10629 Crestwood Drive
Manassas, Virginia 22110

Abstract

To date, surface wave effects on measurements of interest to the OMP have not been considered. Direct generation of currents by surface waves, increased mixing and turbulence due to surface waves, and internal wave generation by surface waves will be examined by means of a literature review that considers OMP needs. Calculations of surface wave effects will be made using representative wave climatological information to evaluate the importance of these effects for the OMP. Special attention will be paid to the need to include surface wave effects in predictive upper ocean models.

BACKGROUND

The OMP is concerned with measurements of upper ocean physical oceanographic parameters such as current shear, temperature, and salinity. Of these parameters, current shear is most important. At the present time, surface wave effects on these measurements are not considered and the manner in which surface wave information should be used to interpret measurements is not known. The purpose of this planned work is to determine how surface waves affect OMP measurements or interpretation of these measurements.

APPROACH

Surface wave effects will be assessed in three general categories: direct effects on current and current shear primarily as a result of Stokes drift and interaction of Stokes drift with other currents; indirect effects due to increased mixing associated with wave motion, wave breaking and turbulence associated with Stoke's drift vertical shear; and effects on generation of internal waves by interaction between a spectrum of surface waves and internal waves with appropriate wave numbers. A major part of the work will be a critical review of available scientific literature. An evaluation of wave effects on upper ocean parameters such as current shear, temperature, and salinity will be based on estimates of relative changes between representative situations with and without waves. Measurement or computational techniques that may be operationally suitable to obtain wave information needed for estimating wave effects on upper ocean parameters will be identified but the work will not include development or evaluation of specific numerical wave models. While the work will describe physical principles and theory, it will not involve new theoretical work. In addition, wave effects on specific sensors will not be determined since examination of specific sensor effects is more appropriate after completion of the initial wave assessment.

PARTICULAR AREAS OF INTEREST

Wave-induced Stokes drift and interactions of Stokes drift with other currents are areas of major interest. Stokes drift is typically about one-half of the total near surface Lagrangian wind-driven current, which is here considered as a wind-driven Ekman-type current plus Stokes drift. The mass transport of Stokes drift typically ranges from

25% to 50% of the mass transport due to wind-driven Ekman-type currents. Previous work shows that Stokes drift, wind-driven Ekman-type currents, and Langmuir circulation are interrelated and that Stokes drift may contribute to wind generation of near surface inertial currents. Since Stokes drift may play a significant role in determining near surface vertical current shear of interest to the OMP, a careful review of Stokes drift is needed. The review will examine alternate conceptual methods for inclusion of Stokes drift in upper ocean current models.

The transfer of surface wave energy to internal waves and increased turbulence and mixing due to surface waves are processes that are not now included explicitly in upper ocean numerical models. The importance of these effects and the need to include such effects in predictive models will be assessed.

Oceanic mid-latitude storm belts in which severe extratropical storms often occur or intensify are of interest for naval applications. Wave climatological information will be examined to determine if there is a special need to consider wave effects in such severe wave regions.

III.   LIST OF PARTICIPANTS

Andrews, James
NORDA Code 110
NSTL Station, MS 39529

Ballard, Al
NORDA Code 543
NSTL Station, MS 39529

Beck, H.C.
NAVOCEANO
NSTL Station, MS 39529

Boyd, Janice
NORDA Code 331
NSTL Station, MS 39529

Bixby, Richard
Sippican Corporation
P.O. Box 139
Marion, MA 02738

Car, Martial
NAVOCEANO
NSTL Station, MS 39529

Carroll, Jerry
NAVOCEANO
NSTL Station, MS 39529

Cox, Claire
NAVOCEANO
NSTL Station, MS 39529

Earle, Marshall
Marine Environments Corp.
10629 Crestwood Drive
Manassas, VA 22110

Eppert, Herb
NORDA Code 111
NSTL Station, MS 39529

Ehrenberg, John
University of Washington
1013 Northeast 40th Street
Seattle, WA 98195

Ferer, Ken
NORDA Code 542
NSTL Station, MS 39529

Geiger, Mark
NAVOCEANO
NSTL Station, MS 39529

Goodman, Lou
Office of Naval Research
800 North Quincy Street
Arlington, VA 22217

Gough, Ed
Planning Systems, Inc.
1700 Old Spanish Trail
Slidell, LA 70458

Green, Albert
NORDA Code 330
NSTL Station, MS 39529

Gregg, Michael
University of Washington
Applied Physics Lab
1013 Northeast 40th Street
Seattle, WA 98195

Hallock, Z.R.
NORDA Code 331
NSTL Station, MS 39529

Hannon, James
Sippican Corporation
P.O. Box 139
Marion, MA 02738

Harlett, John
Chief of Naval Operations
Department of Navy
Washington, DC 20350

Harris, Mike
NORDA Code 543
NSTL Station, MS 39529

Hill, Robert
Naval Research Lab
4555 Overlook Ave., SW
Washington, DC 20375

Holland, Randy
NORDA Code 352
NSTL Station, MS 39529

Hollman, Rudolph
NORDA Code 541
NSTL Station, MS 39529

Kamminga, W.S.
NAVOCEANO
NSTL Station, MS 39529

Karweit, Michael
Johns Hopkins University
Dept. of Chemical Engineering
34th and Charles Streets
Baltimore, MD 21218

Kaulum, K.W.
ONR Detachment
NSTL Station, MS 39529

Keen, Jean
NORDA Code 115
NSTL Station, MS 39529

Kirwan, A.D.
University of South Florida
Dept. of Marine Sciences
140 7th Ave., S
St. Petersburg, FL 33701

Lambert, Richard
Science Applications, Inc.
1710 Goodridge Drive
P.O. Box 1303
McLean, VA 22102

Lorens, Robert
NAVOCEANO
NSTL Station, MS 39529

Losee, Jon
Naval Ocean Systems Center
Code 523
San Diego, CA 92152

McCaffrey, Joseph
NORDA Code 111
NSTL Station, MS 39529

Mied, Richard
Naval Research Lab, Code 4310
4555 Overlook Ave., SW
Washington, DC 20375

Miles, R.T.
NORDA Code 352
NSTL Station, MS 39529

Newman, Fred
Science Applications, Inc.
1710 Goodridge Drive
P.O. Box 1303
McLean, VA 22102

Osborn, T.R.
Department of Oceanography
University of British Columbia
Vancouver, BC, Canada, VGT TW5

Perkins, Hank
NORDA Code 331
NSTL Station, MS 39529

Phelps, G.T.
NORDA Code 100
NSTL Station, MS 39529

Piasek, Steve
NORDA Code 322
NSTL Station, MS 39529

Pinkel, Rob
Scripps Inst. of Oceanography
Marine Physical Lab
University of California, San Diego
La Jolla, CA 92037

Rubenstein, Dave
Science Applications, Inc.
1710 Goodridge Drive
P.O. Box 1303
McLean, VA 22102

Sanford, Thomas
University of Washington
Applied Physics Lab
1013 Northeast 40th St.
Seattle, WA 98195

Saunders, K.D.
NORDA Code 331
NSTL Station, MS 39529

Sharp, Jim
NAVOCEANO
NSTL Station, MS 39529

Smith, Gordon
Johns Hopkins University
Applied Physics Lab
Johns Hopkins Road
Laurel, MD 20810

Stanley, Mike
NORDA Code 540
NSTL Station, MS 39529

Teague, William
NAVOCEANO
NSTL Station, MS 39529

Trowel, Stephen
NORDA Code 543
NSTL Station, MS 39529

Von Zweck, Ortwin
NAVOCEANO
NSTL Station, MS 39529

Welsh, William
Project Manager, Trident Systems
Department of Navy
Washington, DC 20362

Wilems, Robert
Office of Naval Research
NSTL Station, MS 39529

REPORT DOCUMENTATION PAGE	READ INSTRUCTIONS BEFORE COMPLETING FORM

1. REPORT NUMBER	2. GOVT ACCESSION NO.	3. RECIPIENT'S CATALOG NUMBER
none	AD-A137674	

4. TITLE *(and Subtitle)*	5. TYPE OF REPORT & PERIOD COVERED
SUMMARY REPORT, OCEANOGRAPHIC MEASUREMENTS PROGRAM REVIEW, MARCH 1982	Technical Meeting Summary
	6. PERFORMING ORG. REPORT NUMBER

7. AUTHOR(s)	8. CONTRACT OR GRANT NUMBER(s)
editors: K.A. Bush, M.D. Earle, Marine Environments Corp. R. Hollman, NORDA	N00014-82-C-0237

9. PERFORMING ORGANIZATION NAME AND ADDRESS	10. PROGRAM ELEMENT, PROJECT, TASK AREA & WORK UNIT NUMBERS
Marine Environments Corporation 10629 Crestwood Drive Manassas, Virginia 22110	

11. CONTROLLING OFFICE NAME AND ADDRESS	12. REPORT DATE
Naval Ocean Research and Development Activity (NORDA), Code 540 NSTL Station, Mississippi 39529	March 1982
	13. NUMBER OF PAGES
	129

14. MONITORING AGENCY NAME & ADDRESS *(if different from Controlling Office)*	15. SECURITY CLASS. *(of this report)*
	UNCLASSIFIED
	15a. DECLASSIFICATION/DOWNGRADING SCHEDULE

16. DISTRIBUTION STATEMENT *(of this Report)*

UNLIMITED

DISTRIBUTION STATEMENT A

Approved for public release;
Distribution Unlimited

17. DISTRIBUTION STATEMENT *(of the abstract entered in Block 20, if different from Report)*

18. SUPPLEMENTARY NOTES

19. KEY WORDS *(Continue on reverse side if necessary and identify by block number)*

Oceanographic measurements, ocean instrumentation, ocean currents, fine structure, microstructure, shear, internal waves, stratification

20. ABSTRACT *(Continue on reverse side if necessary and identify by block number)*

See next page.

The Ocean Measurements Program (OMP) is part of the Ocean Programs Management Office of NORDA and has been in operation since 1978. Its purpose is to provide quantitative descriptions of the upper ocean non-acoustic environment and of phenomena which affect this environment. Such descriptions are increasingly important for naval requirements. The OMP is comprised of two complementary offices, Oceanographic Instrumentation Systems (OIS) and Oceanographic Techniques (OT), which work closely together. OIS is primarily concerned with the development of instrumentation to acquire the requisite ocean measurements, while OT is primarily concerned with design and verification of sampling and analysis techniques and with development of input to and verification of numerical models. The OMP emphasizes physical oceanographic upper ocean phenomena such as internal waves, vertical velocity shear, and upper ocean temperature, salinity, and density structure.

The annual OMP review was held on March 3 and 4, 1982, at the Naval Ocean Research and Development Activity (NORDA). The purpose of the review was to summarize past, present, and future work in a format that would facilitate communication among participants and provide an overview of the entire OMP and its applications. This report provides summaries of annual review presentations given by OMP principal investigators and contractors, with emphasis on progress and plans of projects supported by the OMP. These summaries briefly present work sponsored by the OMP.

FILM
3-8